

**NASA CONTRACTOR
REPORT**



NASA CR-2395

NASA CR-2395

**THE PASSAGE OF
AN INFINITE SWEEP AIRFOIL
THROUGH AN OBLIQUE GUST**

by John J. Adamczyk

Prepared by
UNITED AIRCRAFT RESEARCH LABORATORIES
East Hartford, Conn. 06108
for Langley Research Center

NATIONAL AERONAUTICS AND SPACE ADMINISTRATION • WASHINGTON, D. C. • MAY 1974

1. Report No. NASA CR- 2395		2. Government Accession No.		3. Recipient's Catalog No.	
4. Title and Subtitle THE PASSAGE OF AN INFINITE SWEEP AIRFOIL THROUGH AN OBLIQUE GUST				5. Report Date May 1974	
				6. Performing Organization Code	
7. Author(s) John J. Adamczyk				8. Performing Organization Report No.	
9. Performing Organization Name and Address United Aircraft Research Laboratories 400 Main Street East Hartford, CT 06108				10. Work Unit No.	
				11. Contract or Grant No. NAS 1-11557	
12. Sponsoring Agency Name and Address National Aeronautics and Space Administration Washington, D.C. 20546				13. Type of Report and Period Covered Contractor Report	
				14. Sponsoring Agency Code	
15. Supplementary Notes Final Report - The contract research effort which has lead to the results in this report was financially supported by USAAMRDL (Langley Directorate).					
16. Abstract An analysis is presented which yields an approximate solution for the unsteady aerodynamic response of an infinite swept wing encountering a vertical oblique gust in a compressible stream. The approximate expressions are of closed form and do not require excessive computer storage or computation time, and further, they are in good agreement with the results of exact theory. This analysis is used to predict the unsteady aerodynamic response of a helicopter rotor blade encountering the trailing vortex from a previous blade. Significant effects of three-dimensionality and compressibility are evident in the results obtained. In addition, an approximate solution for the unsteady aerodynamic forces associated with the pitching or plunging motion of a two-dimensional airfoil in a subsonic stream is presented. The mathematical form of this solution approaches the incompressible solution as the Mach number vanishes, the linear transonic solution as the Mach number approaches one, and the solution predicted by piston theory as the reduced frequency becomes large.					
17. Key Words (Suggested by Author(s)) Unsteady aerodynamics, Blade-vortex interaction, Analytical aerodynamics 2-D oscillating airfoil			18. Distribution Statement Unclassified - Unlimited STAR Category 01		
19. Security Classif. (of this report) Unclassified		20. Security Classif. (of this page) Unclassified		21. No. of Pages 96	22. Price* \$4.00

Page Intentionally Left Blank

TABLE OF CONTENTS

	<u>Page</u>
SUMMARY	1
INTRODUCTION	2
NOMENCLATURE	4
FORMULATION OF THE MATHEMATICAL PROBLEM	8
Governing Equation	8
Boundary Conditions	10
SOLUTION OF THE BOUNDARY PROBLEM	14
General Considerations	14
Solution for Small Values of $\gamma \geq 0$	14
Limiting Behavior as $\gamma \rightarrow 0^+$	16
Solution for Values of $\gamma^2 \leq 0$	16
Solution for Large Values of $ \gamma^2 $	18
Limiting Behavior as $ \gamma^2 \rightarrow \infty$	20
DISCUSSION OF THE APPROXIMATE SOLUTIONS	22
APPLICATION OF THE APPROXIMATE SOLUTIONS	24
RESULTS AND CONCLUSIONS	27
RECOMMENDATIONS	29
APPENDIXES	30
I. APPROXIMATE EXPRESSIONS FOR THE AERODYNAMIC RESPONSE FUNCTIONS FOR SMALL POSITIVE VALUES OF γ	30
II. APPROXIMATE EXPRESSIONS FOR THE AERODYNAMIC RESPONSE FUNCTIONS FOR NEGATIVE VALUES OF γ^2	38
III. SOLUTION FOR LARGE VALUES OF $ \gamma^2 $	42

IV. TWO-DIMENSIONAL PITCHING AND PLUNGING MOTION OF AN
AIRFOIL IN A COMPRESSIBLE STREAM 49

V. NONPERIODIC TIME DEPENDENT PROBLEMS 60

VI. COMPUTER FLOW DIAGRAM FOR COMPUTING THE AIRLOADS
GENERATED BY THE ENCOUNTER OF A HELICOPTER ROTOR
BLADE WITH A TIP VORTEX 66

REFERENCES 68

FIGURES 70

THE PASSAGE OF AN INFINITE SWEEP AIRFOIL

THROUGH AN OBLIQUE GUST

By John J. Adamczyk
United Aircraft Research Laboratories

SUMMARY

An analysis is presented which yields an approximate solution for the unsteady aerodynamic response of an infinite swept wing encountering a vertical oblique gust in a compressible stream. The approximate expressions are of closed form and do not require excessive computer storage or computation time, and further, they are in good agreement with the results of exact theory. This analysis is used to predict the unsteady aerodynamic response of a helicopter rotor blade encountering the trailing vortex from a previous blade. Significant effects of three-dimensionality and compressibility are evident in the results obtained. In addition, an approximate solution for the unsteady aerodynamic forces associated with the pitching or plunging motion of a two-dimensional airfoil in a subsonic stream is presented. The mathematical form of this solution approaches the incompressible solution as the Mach number vanishes, the linear transonic solution as the Mach number approaches one, and the solution predicted by piston theory as the reduced frequency becomes large.

INTRODUCTION

The prediction of the unsteady aerodynamic response of an airfoil to a vertical gust velocity field has long been of interest to aeroelasticians and acousticians. For the most part aeroelasticians have used the incompressible two-dimensional theories of Kussner (Ref. 1) and Sears (Ref. 2) to predict the unsteady response. In estimating the acoustic field generated by airfoil-gust interactions the acoustician typically uses the unsteady lift obtained from one of the previous theories to determine the strength of the acoustic dipole source which is then assumed to replace the airfoil in the flow field (e.g., Curle in Ref. 3).

Typical of the many unsteady aerodynamic problems in which these incompressible theories have been used in the past are: (1) rotor blades passing through the wakes of stator blades in turbomachinery, (2) an airfoil interacting with a turbulent gust, and (3) helicopter rotor blades encountering the tip vortices from preceding blades. In each of these problems some uncertainty arises as to the applicability of two-dimensional incompressible aerodynamics. It is not surprising, therefore, that several analytical studies have appeared recently which treat the complexities of three-dimensionality and compressibility in the unsteady problem. For example, Filotas (Ref. 4) obtained a closed form solution for an oblique sinusoidal gust encountering an infinite wing; however, this work is limited to a two-dimensional airfoil of zero sweep (i.e., the incoming flow is normal to the leading edge line of the wing) in an incompressible stream. Graham (Ref. 5) included the effects of compressibility and three-dimensionality but neglected the effects of sweep. His analysis is based on a numerical solution of the governing differential equations. Adamczyk (Refs. 6 and 7) also included the effects of compressibility and three-dimensionality, but the form of the solution was expressed in terms of an infinite series of Mathieu functions which are difficult to evaluate analytically. Another recent analysis by Johnson (Ref. 8) included the effects of compressibility and three-dimensionality; however, his approach is tailored towards analyzing the response of an airfoil to a free rectilinear vortex. Hence, the researcher has had no simple compressible three-dimensional analogue of the Sears solution available to him and was required to resort to the more restricted theories of Filotas or Sears for predicting the aerodynamic response of an airfoil to a vertical gust.

To overcome the deficiencies described above, an analysis has been developed which generates simple approximate expressions for the unsteady compressible lift and moment response functions for an infinite swept airfoil

encountering a three-dimensional oblique gust (see Fig. 1 and Fig. 2). The approximate expressions are of closed form and do not require excessive computer storage or computational time. This report describes the development of these approximate expressions, and presents a comparison of results with an exact theory and sample computations of the unsteady loading of a helicopter blade encountering a vortex.

NOMENCLATURE

a	speed of sound
A_n	coefficients in the series for $\Phi^{(1)}$, defined in Eq. (46)
b	semichord of the airfoil
B_n	coefficients in the series for $p^{(2)}$
C	cosine Fresnel Integral
ce_n	symmetric Mathieu functions
C_L, C_M	lift and moment coefficients per unit span
conj	complex conjugate operator
E	complex Fresnel Integral, defined by Eq. (85)
f	function defined by Eq. (96) or Eq. (151)
g_1, g_2	functions defined by Eqs. (135), (136), (138), and (139)
h	displacement of the airfoil from the x_2 plane, displacement of the vortex from the x_2 plane
h_o	amplitude of plunging motion
$H_0^{(1)}, H_1^{(1)}$	Hankel functions, first kind, orders 0 and 1
H	complex constant, defined by Eq. (31), modified acceleration potential, defined by Eq. (93)
I	integral defined by Eq. (99)
I_0, I_1	modified Bessel functions, first kind, order 0 and 1
J_0, J_1	Bessel functions, first kind, orders 0 and 1
J_n	Bessel function, first kind, order n
K	reduced frequency

\bar{K}	gust wave number
m	integer
M	Mach number of the free stream, U/a , function defined by Eq. (97)
M^*	Mach number of the gust relative to the oncoming flow, defined by Eq. (17)
$Me_n^{(2)}$	Mathieu-Hankel function, second kind, associated with ce_n
$Me_n^{(2)}$	$= \frac{d}{d\xi} Me_n^{(2)}(\xi, q)$
n	integer
$P(\gamma, \beta)_{INC}$	incompressible pressure distribution, defined by Eq. (70)
$p^{(1)}, p^{(2)}$	first and second terms of the solution for p^s for large γ^2
p	perturbation pressure
p_0	steady pressure, associated with the flow U
q	$= \gamma^2/4$
r	radial distance from the midchord line of the airfoil, distance measured in the plane of X_1, X_3 , defined by Eq. (147)
R	dimensionless radial distance
S	Sears function, or sine Fresnel Integral
sgn	sign operator
t	time
t'	non-dimensional time, defined by Eq. (43)
T_L	lift transfer function, defined in Eq. (22)
T_M	moment transfer function, defined in Eq. (23)

u	integration variable
U	free stream velocity
u_1	component of perturbation velocity
u_2	complex amplitude of u_2^I
x_1	Cartesian coordinates, Fig. 1
X_1	dimensionless coordinates, defined by Eqs. (11), (12), and (13)
z	variable
Z	complex constant, defined by Eq. (25)
α	angle of encounter, Fig. (1)
α^*	constant, defined by Eq. (43)
α_0	amplitude of pitching motion
β	frequency parameter, defined by Eq. (14)
γ	cutoff parameter, defined by Eq. (17)
Γ	circulation of free vortex
δ	constant defined by Eq. (79)
δ_1, δ_2	functions defined by Eqs. (137) and (140)
θ	angle of sweep, Fig. 1
ξ, η	elliptic-hyperbolic coordinates, defined by Eqs. (46) and (47)
ρ	density fluctuations
ρ_0	mean density
τ	integration variable
ϕ	perturbation velocity potential defined in Eq. (6)
Φ	complex amplitude of ϕ

Φ_{INC}	complex amplitude of Φ for an incompressible fluid
$\Phi^{(1)}$	noncirculatory component of Φ
$\Phi^{(2)}$	circulatory component of Φ
∇^2	Laplacian operator

Superscripts

I	incident disturbance
S	scattered field
^	Fourier transform of a variable

Subscript

1/4	quarter-chord
-----	---------------

FORMULATION OF THE MATHEMATICAL PROBLEM

Governing Equation

Figure 1 shows the geometry of the problem. An infinite swept airfoil of chord $2b$ is held rigidly in a compressible fluid which is flowing over it with uniform velocities $U \cos \theta$ in the x_1 direction, and $U \sin \theta$ in the x_3 direction. Superposed on U (see Fig. 2) is an unsteady three-dimensional disturbance u_i . The pressure and density are $p_0 + p$, and $\rho_0 + \rho$, respectively, where the subscripted part denotes the mean value, while the remaining part is associated with the disturbance. Far upstream of the airfoil, the perturbations u_i , p , and ρ are given functions, denoted by u_i^I , p^I , ρ^I .

The problem is described by the customary fluid dynamic equations for a compressible flow (see Ref. 9). The equations of conservation of mass and momentum are linearized by assuming that the perturbations are small compared to the mean values thereby allowing the squares and products of the perturbations (and their derivatives) to be neglected while first-order terms are retained. Hence,

$$\frac{\partial \rho}{\partial t} + U \cos \theta \frac{\partial \rho}{\partial x_1} + U \sin \theta \frac{\partial \rho}{\partial x_3} + \frac{\partial u_i}{\partial x_i} = 0 \quad (1)$$

$$\rho_0 \left(\frac{\partial u_i}{\partial t} + U \cos \theta \frac{\partial u_i}{\partial x_1} + U \sin \theta \frac{\partial u_i}{\partial x_3} \right) + \frac{\partial p}{\partial x_i} = 0 \quad (2)$$

For small fluctuations, the change in pressure is proportional to the change in density,

$$p = a^2 \rho \quad (3)$$

where a is the speed of sound.

Far from the airfoil the pressure, density, and velocity field must equal the incident disturbance. This condition

$$\{p, \rho, u_i\} = \{p^I, \rho^I, u_i^I\} \quad (4)$$

is most conveniently satisfied by taking

$$\{p, \rho, u_i\} = \{p^I + p^S, \rho^I + \rho^S, u_i^I + u_i^S\} \quad (5)$$

and imposing the condition that p^S , ρ^S and u_i^S vanish far from the airfoil.

The quantities p^I , ρ^I and u_i^I must satisfy Eqs. (1), (2) and (3) because far from the airfoil they constitute the entire disturbance. Hence, because the equations are linear, the quantities p^S , ρ^S , and u_i^S must also satisfy Eqs. (1), (2), and (3). Furthermore, since the fluid is inviscid, no change in vorticity can take place as the fluid passes over the airfoil. Hence, u_i^S must be an irrotational field, and may be represented by the derivative of a velocity potential

$$u_i^S = \frac{\partial \phi}{\partial x_i} \quad (6)$$

The momentum equation (2) provides a relation between the pressure and the potential, namely,

$$p^S = -\rho_0 \left(\frac{\partial \phi}{\partial t} + U \cos \theta \frac{\partial \phi}{\partial x_1} + U \sin \theta \frac{\partial \phi}{\partial x_3} \right) \quad (7)$$

and when this and the equation of state (3) are substituted into the continuity equation (1), one obtains the governing differential equation

for the problem

$$\begin{aligned}
 & a^2 \left(\nabla^2 \phi - M^2 \cos^2 \theta \frac{\partial^2 \phi}{\partial x_1^2} - M^2 \sin^2 \theta \frac{\partial^2 \phi}{\partial x_3^2} \right) \\
 & - 2a^2 \left(\frac{M \cos \theta}{a} \frac{\partial^2 \phi}{\partial x_1 \partial t} + \frac{M \sin \theta}{a} \frac{\partial^2 \phi}{\partial x_3 \partial t} \right. \\
 & \left. + M^2 \cos \theta \sin \theta \frac{\partial^2 \phi}{\partial x_1 \partial x_3} \right) - \frac{\partial^2 \phi}{\partial t^2} = 0
 \end{aligned} \tag{8}$$

Here $M = U/a$ is the Mach number of the mean flow.

Boundary Conditions

A solution of Eq. (8) is sought which describes outgoing waves which must decay as $r^{-\frac{1}{2}}$ for large distance, r , from the airfoil (cf. Ref. 7). On the surface of the airfoil the velocity normal to this surface must vanish. Hence,

$$\frac{\partial \phi}{\partial x_2} = -u_2^I \quad x_2 = 0 \quad -b \leq x_1 \leq b \tag{9}$$

u_2^I being a given function of space and time.

The present analysis assumes that the vertical velocity field induced by the incident disturbance on the airfoil is that of an oblique sinusoidal gust convected at the free stream velocity U . The mathematical form for this velocity field is

$$u_2^I = \bar{u}_2 \exp \left\{ i \left[\bar{K} \cos \alpha x_1 + \bar{K} \sin \alpha x_3 - \bar{K} U \cos (\theta - \alpha) t \right] \right\} \tag{10}$$

where the sweep angle θ and the encounter angle α are defined in Figs. 1 and 2. Since the gust is assumed to be convected with the mean flow velocity U , the pressure and density fluctuations associated with this velocity field

are zero (i.e., $p^I = \rho^I = 0$). Dimensionless coordinates X_1 , and a frequency parameter β are introduced for convenience in subsequent operations.

$$x_1 = x_1 / b \quad (11)$$

$$x_2 = x_2 (1 - M^2 \cos^2 \theta)^{\frac{1}{2}} / b \quad (12)$$

$$x_3 = x_3 (1 - M^2 \cos^2 \theta)^{\frac{1}{2}} / b \quad (13)$$

$$\beta = \frac{\bar{K} b \cos \alpha}{1 - M^2 \cos^2 \theta} \quad (14)$$

The solution for the velocity field u_1^B must have the same frequency and the same spanwise wave number as the incident gust. In addition it is found convenient to include an exponential factor in the x_1 direction of the potential. Thus the following form for ϕ is chosen:

$$\phi = \Phi(x_1, x_2) \exp \left(i \left[-\beta M^2 \cos^2 \theta x_1 - \bar{K} U \cos(\theta - \alpha) t + \frac{\bar{K} b \sin \alpha}{(1 - M^2 \cos^2 \theta)^{1/2}} x_3 \right] \right) \quad (15)$$

When the substitutions (11) through (15) are made in the governing equation, (8), one finds that Φ must satisfy

$$\frac{\partial^2 \Phi}{\partial x_1^2} + \frac{\partial^2 \Phi}{\partial x_2^2} + \gamma^2 \Phi = 0 \quad (16)$$

where γ is a compressible cutoff parameter defined as

$$\gamma = \frac{\bar{k} b \sin \alpha}{1 - M^2 \cos^2 \theta} \left[\left(\frac{M \cos \theta}{\sin \alpha} \right)^2 - 1 \right]^{1/2} = \frac{\bar{k} b \sin \alpha \sqrt{M^{*2} - 1}}{1 - M^2 \cos^2 \theta} \quad (17)$$

Note that the sign of γ^2 is dependent on whether the parameter $M^* = \frac{M \cos \theta}{\sin \alpha}$ is greater than or less than one. This parameter is proportional to the phase velocity of the disturbance along the span of the airfoil relative to the oncoming flow (see Fig. 3). When M^* is greater than one, the relative phase velocity of the disturbance is supersonic. However, if M^* is less than one, the relative phase velocity is subsonic. The behavior of the solution of Eq. (16) at large distances from the airfoil is critically dependent on the value of M^* . This dependence can be shown by examining the asymptotic limit of the solution of Eq. (16) for an isolated acoustical source (cf. Ref. 10). This solution has the form

$$\Phi \sim \frac{e^{i\gamma R}}{\sqrt{R}} \quad R = \sqrt{x_1^2 + x_2^2} \rightarrow \infty \quad (18)$$

Equation (18) requires Φ to decay exponentially with distance for imaginary γ which, from Eq. (17), is equivalent to $M^* < 1$. If the cutoff parameter γ is real (i.e., $M^* > 1$), Eq. (18) is the asymptotic form for a cylindrical acoustical wave propagating outward from the origin at $R = 0$.

The boundary conditions on Φ are

$$\frac{\partial \Phi}{\partial x_2} = - \frac{b}{\sqrt{1 - M^2 \cos^2 \theta}} \bar{u}_2 e^{i\beta x_1} \quad \text{for } -1 \leq x_1 \leq 1, x_2 = 0 \quad (19)$$

which was derived from Eq. (9) and

$$\Phi \sim R^{-\frac{1}{2}} \text{ as } R \rightarrow \infty \quad (20)$$

which is the asymptotic radiation condition of Eq. (18). In addition to the boundary conditions in Eq. (19) and (20) a Kutta-Joukowski condition must be imposed at the trailing edge of the airfoil. This condition requires that the pressure jump across the airfoil vanish at the trailing edge. This requirement can be mathematically expressed in terms of Φ and its derivatives by substituting Eq. (15) into Eq. (7) to yield

$$p^s = -\rho_0 \frac{U \cos \theta}{b} \left[\frac{\partial \Phi}{\partial x_1} - i\beta \Phi \right] \exp \quad (21)$$

$$\left[-i\beta M^2 \cos^2 \theta x_1 + \frac{i\bar{K} b \sin \alpha x_3}{\sqrt{1-M^2 \cos^2 \theta}} - i\bar{K} U \cos(\theta - \alpha) t \right]$$

which equals

$$p^s = 0 \quad \text{at } x_1 = 1, x_2 = 0 \quad (22)$$

The governing differential equation (16) and the boundary conditions, Eq. (19), (20) and (22), form a boundary value problem for Φ whose solution is dependent on only two variables, the cutoff parameter γ , and the frequency parameter β . The construction of the approximate solutions to this boundary value problem was divided into three parts: (1) a solution valid for small positive values of γ , (2) a solution valid for negative values of γ^2 , and (3) a solution valid for large values of γ^2 , each of which will be discussed below.

SOLUTION OF THE BOUNDARY PROBLEM

General Considerations

An important objective of this analysis is to determine the unsteady lift and moment coefficients (per unit span) resulting from the encounter of an infinite swept airfoil with a three-dimensional oblique sinusoidal gust in a compressible stream. This is accomplished by integrating the zero and first order moments of the pressure distribution over the chord of the airfoil; however, the pressure distribution is a highly specialized function of the cutoff parameter, and, as shown below, the solution changes its character for various regimes of γ . In general, the lift and moment coefficients can be written in the form

$$C_L = \left\{ \frac{2\pi \bar{U}_2 \cos \theta}{U \sqrt{1 - M^2 \cos^2 \theta}} \right\} T_L e^{i[\bar{K} \sin \alpha x_3 - U \bar{K} \cos(\theta - \alpha)t]} \quad (23)$$

$$C_M = \left\{ \frac{\pi \bar{U}_2 \cos \theta}{2U \sqrt{1 - M^2 \cos^2 \theta}} \right\} T_M e^{i[\bar{K} \sin \alpha x_3 - U \bar{K} \cos(\theta - \alpha)t]} \quad (24)$$

where T_L and T_M are the lift and moment transfer functions, and the expressions within the brackets $\{ \}$ represent the quasi-steady lift and moment response. The functions T_L and T_M will now be derived for the various values of γ^2 of interest here.

Solution for Small Values of $\gamma \geq 0$

The approximate solution of Eq. (16) for small positive values of γ was obtained by expanding the exact solution to this problem, taken from Ref. 7, in a power series of γ . The analysis presented in Ref. 7 was developed by linearly separating Φ into two components. The first component, $\Phi^{(1)}$, accounts for the noncirculatory flow field surrounding the airfoil. This solution for $\Phi^{(1)}$ satisfies Eq. (16) along with boundary conditions in Eqs. (19) and (20) and has the following properties: (i) the circulation around the airfoil is zero, and (ii) singularities in pressure and velocity occur at the leading and trailing edges of the airfoil. The desired solution for Φ is obtained by adding to $\Phi^{(1)}$ a second component, $\Phi^{(2)}$, which is the

circulatory solution. This new term cancels the trailing edge singularity of $\Phi^{(1)}$ (i.e., causes the solution for Φ to satisfy the Kutta-Joukowski condition, Eq. (22)), and has its normal gradient vanishing on the airfoil.

The details of the approximate solution for small positive values of γ will be found in Appendix I in which the final form for the pressure distribution on the surface of the airfoil is shown to be:

$$p^s = -\frac{\rho_0 U \bar{u}_2 \cos \theta}{(1-M^2 \cos^2 \theta)^{1/2}} \sqrt{\frac{1-X_1}{1+X_1}} \left[\frac{J_0(\beta) - iZ J_1(\beta)}{1+Z} \right] \exp \left[i \left[-\beta M^2 \cos^2 \theta x_1 + \frac{\bar{k} b \sin \alpha}{(1-M^2 \cos^2 \theta)^{1/2}} x_3 - \bar{k} U \cos(\theta - \alpha) t \right] \right] \quad (25)$$

$$-1 \leq x_1 \leq 1$$

where the variable

$$Z = -\frac{i H_0^{(1)}(\beta) + i(\gamma/\beta)^2 \left[H_0^{(1)}(\gamma/2) - H_0^{(1)}(\beta) \right]}{H_1^{(1)}(\beta)} \quad (26)$$

The equation for the lift and moment transfer functions T_L and T_M , respectively, can be obtained by integrating the zero and first order moments of the pressure distribution over the chord of the airfoil. The resulting expression for the lift transfer function T_L is:

$$T_L = \frac{J_0(\beta) - iZ J_1(\beta)}{1+Z} \left[J_0(\beta M^2 \cos^2 \theta) + i J_1(\beta M^2 \cos^2 \theta) \right] e^{i b \bar{k} \cos \alpha} \quad (27)$$

while that for the moment transfer function T_M about the quarter-chord is:

$$T_{M_{1/4}} = e^{i b \bar{k} \cos \alpha} \left[\frac{J_0(\beta) - iZ J_1(\beta)}{1+Z} \right] \left[-J_0(\beta M^2 \cos^2 \theta) + J_2(\beta M^2 \cos^2 \theta) - i 2 J_1(\beta M^2 \cos^2 \theta) \right] + T_L \quad (28)$$

Equations (25), (27), and (28) are used to determine the aerodynamic loading for small positive values of γ .

Limiting Behavior as $\gamma \rightarrow 0^+$

The influence of the cutoff parameter γ on the lift transfer function for small values of this parameter may be shown by examining the limiting form of Eq. (27) as $\gamma \rightarrow 0^+$. This limit is given by the equation

$$\tau_L = \left[\text{conj} \{ S(\beta) \} - \frac{i\gamma^2}{\beta} \ln \frac{\gamma}{4\beta} \right] \left[J_0(\beta M^2 \cos^2 \theta) + i J_1(\beta M^2 \cos^2 \theta) \right] e^{i\bar{k}b \cos \alpha} \quad (29)$$

where $\text{conj} \{ \}$ denotes the complex conjugate of the enclosed quantity, and where

$$\frac{\gamma^2}{\beta} \ln \frac{\gamma}{4\beta} = \frac{b\bar{k} [(M \cos \theta)^2 - \sin^2 \alpha]}{(1 - M^2 \cos^2 \theta) \cos \alpha} \ln \left[\frac{\sqrt{(M \cos \theta)^2 - \sin^2 \alpha}}{4 \cos \alpha} \right] \quad (30)$$

can be obtained by manipulating Eq. (17). Note that $S(\beta)$ is the two-dimensional gust response function derived by Sears (Ref. 2). The influence of γ is shown by Eq. (30) to be of first order in \bar{k} and $(M \cos \theta)^2 - \sin^2 \alpha$, and its effect on the moment transfer function is of secondary importance compared with the parameter $\beta M^2 \cos^2 \theta$. An expansion of Eq. (28) for small values of $\beta M^2 \cos^2 \theta$ yields the result that the moment transfer function is a linear function of this parameter. This result implies that the moment transfer function about the quarter chord vanishes as (1) the gust wave number \bar{k} approaches its steady-state limit of zero, or (2) the speed of sound of the fluid medium approaches infinity.

Solution for Values of $\gamma^2 \leq 0$

A power series expansion of the result presented in Ref. 7 for the circulatory pressure distribution on the surface of the airfoil for negative values of γ^2 was derived. It is shown above that this approach leads to

very simple expressions for the aerodynamic response functions (i.e., Eqs. (25), (27), and (28)) for small positive values of γ . However, when the expansion technique was applied to the problem for $\gamma^2 \leq 0$, it yielded solutions which contained definite integrals whose values had to be determined numerically. This form of a solution is not satisfactory because it does not lead to a simplified analytical procedure. Hence, an alternative approach was developed based on Graham's similarity rules (Ref. 5) and the analysis developed by Filotas (Ref. 4) for an oblique sinusoidal gust encountering an infinite airfoil in an incompressible stream. This alternative approach led to an approximate expression for the pressure distribution on the surface of the airfoil which can be applied over the entire range of $\gamma^2 \leq 0$.

The details of the approximate solution for negative values of γ^2 will be found in Appendix II in which the final form of the pressure distribution is shown to be

$$p_s = \frac{\rho_0 U \bar{u}_2 \cos \theta}{\sqrt{1-M^2 \cos^2 \theta}} \frac{H(\gamma, \beta)}{I_0(\gamma) + I_1(\gamma)} \sqrt{\frac{1-x_1'}{1+x_1'}} \exp \quad (31)$$

$$\left[-(\gamma + i\beta M^2 \cos^2 \theta) x_1 + \frac{i b \bar{K} \sin \alpha}{(1-M^2 \cos^2 \theta)^{1/2} x_3} - i U \bar{K} \cos(\theta - \alpha) \right]$$

$$-1 \leq x_1 \leq 1$$

where

$$H(\gamma, \beta) = \exp \left\{ -i \sqrt{\gamma^2 + \beta^2} \left[\cos \delta - \pi (\pi/2 - \delta) \left(1 + \frac{\sin \delta}{2} \right) \right] / \left(1 + 2\pi \sqrt{\gamma^2 + \beta^2} \left(1 + \frac{\sin \delta}{2} \right) \right) \right\} \quad (32)$$

$$\frac{\exp \left\{ -i \sqrt{\gamma^2 + \beta^2} \left[\cos \delta - \pi (\pi/2 - \delta) \left(1 + \frac{\sin \delta}{2} \right) \right] / \left(1 + 2\pi \sqrt{\gamma^2 + \beta^2} \left(1 + \frac{\sin \delta}{2} \right) \right) \right\}}{\left\{ 1 + \pi \sqrt{\gamma^2 + \beta^2} \left[1 + \cos^2 \delta + \pi \sqrt{\gamma^2 + \beta^2} \sin \delta \right] \right\}}$$

and

$$\delta = \tan^{-1} \gamma / \beta \quad (33)$$

The lift transfer function T_L is computed by integrating the pressure distribution, Eq. (31), over the chord of the airfoil, yielding

$$T_L = e^{i\bar{k}b \cos \theta} \frac{I_0(\gamma + i\beta M^2 \cos^2 \theta) + I_1(\gamma + i\beta M^2 \cos^2 \theta)}{I_0(\gamma) + I_1(\gamma)} H(\gamma, \beta) \quad (34)$$

The corresponding expression for the moment transfer function T_M about the quarter-chord is

$$T_{M,1/4} = -\frac{2 e^{i\bar{k}b \cos \alpha}}{I_0(\gamma) + I_1(\gamma)} \left[I_0(\gamma + i\beta M^2 \cos^2 \theta) + I_1(\gamma + i\beta M^2 \cos^2 \theta) \left(1 - \frac{1}{\gamma + i\beta M^2 \cos^2 \theta} \right) \right] H(\gamma, \beta) + T_L \quad (35)$$

Equations (31), (34), and (35) can be used to compute the aerodynamic response functions over the entire range of negative γ^2 .

Solution for Large Values of $|\gamma^2|$

The results predicted by the analysis of Ref. 7 for the pressure distribution on the surface of an airfoil encountering a two-dimensional sinusoidal gust indicate that for large values of $|\gamma^2|$ the pressure distribution appears to be composed of acoustical waves whose points of origin are the leading and trailing edges of the airfoil. The spatial influence of the acoustical wave emitted from the leading edge of the airfoil increases as γ increases, while the influence of the wave emitted from the trailing edge decreases. This is indicated by the behavior of the pressure phase angle (both theoretical and experimental) in Fig. 11 of Ref. 11 and is further corroborated by computations performed during the development of the basic theory (Ref. 6). This behavior implies that for large values of $|\gamma^2|$ a good approximation to the pressure field in the neighborhood of the leading edge (i.e., far upstream of the trailing edge) can be obtained by considering the interaction of a gust with a semi-infinite plate. For values of $\gamma^2 \neq 0$ the pressure distribution $p^{(1)}$ on the surface of the plate possesses a leading edge singularity, and decays with distance aft of the leading edge. Thus the pressure distribution is a monotonically decreasing function which vanishes only at an infinite distance downstream of the leading edge, and therefore the pressure

distribution $p^{(1)}$ does not satisfy the Kutta-Joukowski condition. This error can be corrected by adding to $p^{(1)}$ a pressure field $p^{(2)}$ which is equal and opposite to $p^{(1)}$ downstream of the airfoil (i.e., $X_1 \geq 1$, $X_2 = 0$) and has its normal gradient vanishing everywhere on the airfoil.

The details of the approximate solution for large values of γ^2 will be found in Appendix III in which the final form for the pressure distribution on the surface of the airfoil is shown to be

$$p^S = p^{(1)} + p^{(2)} \quad (36)$$

where

$$p^{(1)} = \left\{ \frac{\rho_0 U \bar{U}_2 \cos \theta}{\sqrt{1 - M^2 \cos^2 \theta}} \frac{(1+i)}{\sqrt{2 X_1' \pi (\beta + \gamma)}} \exp \left[i(\gamma - \beta M^2 \cos^2 \theta) X_1' + i \bar{K} \sin \alpha x_3 - i U \bar{K} \cos(\theta - \alpha) t \right] \right\} \quad (37)$$

and

$$p^{(2)} = \left\{ \frac{\rho_0 U \bar{U}_2 \cos \theta}{\sqrt{1 - M^2 \cos^2 \theta}} \left[\frac{1+i}{2} - \epsilon \left(\sqrt{2\gamma(2 - X_1')} \right) \right] \frac{1}{\sqrt{\pi (\beta + \gamma)}} \right\} \exp \left[i(\gamma - \beta M^2 \cos^2 \theta) X_1' + i \bar{K} \sin \alpha x_3 - i U \bar{K} \cos(\theta - \alpha) t \right] \quad (38)$$

$$X_1' = X_1 + 1, \quad -1 \leq X_1 \leq 1$$

The mathematical form of the two-dimensional limit of Eq. (37) is that of an outward propagating acoustical wave whose point of origin is the leading edge, while the equivalent limit of Eq. (38) yields a form which represents an outward propagating wave whose apparent origin is the trailing edge. Once again the lift and moment transfer functions are obtained by integrating the zero and first order moments of the pressure distribution, Eq. (36), over

the chord of the airfoil. The result for the lift transfer function T_L is

$$\begin{aligned}
 T_L = & \frac{1}{\sqrt{\pi(\beta+\gamma)}} \left\{ (1+i) \sqrt{\frac{\pi}{\gamma-\beta M^2 \cos^2 \theta}} \times \right. \\
 & E \left[\sqrt{2(\gamma-\beta M^2 \cos^2 \theta)} \right] + \left[1 - e^{2i(\gamma-\beta M^2 \cos^2 \theta)} \right] \times \\
 & \frac{1-i}{2(\gamma-\beta M^2 \cos^2 \theta)} + \frac{iE[\sqrt{4\gamma}]}{(\gamma-\beta M^2 \cos^2 \theta)} - \frac{i\sqrt{2\gamma}}{\gamma-\beta M^2 \cos^2 \theta} \times \\
 & \left. \frac{e^{2i(\gamma-\beta M^2 \cos^2 \theta)}}{\sqrt{\gamma+\beta M^2 \cos^2 \theta}} E \left[\sqrt{2(\gamma+\beta M^2 \cos^2 \theta)} \right] \right\} \quad (39)
 \end{aligned}$$

while that for the moment transfer function about the quarter-chord is

$$\begin{aligned}
 T_{M_{1/4}} = & -\frac{(1-i)\sqrt{\pi}}{(\gamma-\beta M^2 \cos^2 \theta)^{3/2}} E \left[\sqrt{\frac{4}{\pi}(\gamma-\beta M^2 \cos^2 \theta)} \right] + \\
 & \frac{1+i}{(\gamma-\beta M^2 \cos^2 \theta)^2} \left[1 - e^{2i(\gamma-\beta M^2 \cos^2 \theta)} \right] - \frac{2E[2\sqrt{\gamma}]}{(\gamma-\beta M^2 \cos^2 \theta)^2} - \\
 & \frac{i2\sqrt{2\gamma}}{(\gamma-\beta M^2 \cos^2 \theta)} \frac{e^{2i(\gamma-\beta M^2 \cos^2 \theta)}}{\sqrt{\gamma+\beta M^2 \cos^2 \theta}} E \left[\sqrt{2(\gamma+\beta M^2 \cos^2 \theta)} \right] \left\| 2 - \frac{2}{2(\gamma+\beta M^2 \cos^2 \theta)} \right\| \\
 & + 2\sqrt{\frac{2\gamma}{\pi}} \frac{e^{4i\gamma}}{\gamma^2 \beta^2 M^4 \cos^4 \theta} + \frac{2\sqrt{2\gamma} e^{2i(\gamma-\beta M^2 \cos^2 \theta)}}{(\gamma-\beta M^2 \cos^2 \theta)^2 \sqrt{\gamma+\beta M^2 \cos^2 \theta}} E \left[\sqrt{2(\gamma+\beta M^2 \cos^2 \theta)} \right] + T_L \quad (40)
 \end{aligned}$$

Equations (36), (39), and (40) can be used to determine the aerodynamic response function for large values of γ^2 .

Limiting Behavior as $|\gamma^2| \rightarrow \infty$

The limiting form attained by Eq. (39) for very large values of $|\gamma^2|$ can be derived by expanding Eq. (39) in powers of $1/\gamma^2$. The result is

$$T_L = \frac{i}{\pi} \frac{1}{\sqrt{(\beta+\gamma)(\gamma-\beta M^2 \cos^2 \theta)}} \quad (41)$$

provided $\gamma - \beta M^2 \cos^2 \theta \neq 0$. Equation (41) shows that T_L is proportional to \bar{K}^{-1} since both γ and β are linear functions of \bar{K} . However, if $\gamma - \beta M^2 \cos^2 \theta = 0$ Eq. (39) will approach

$$T_L = \frac{2(1+i)}{\pi \sqrt{\pi(\beta+\gamma)}} \quad (42)$$

for large values of γ . This result is proportional to $\bar{K}^{-\frac{1}{2}}$ and occurs when the gust phase velocity along the span is sonic relative to the mean span flow velocity $U \sin \theta$. This phenomenon will occur when the wave front encounter angle is equal to

$$\alpha = \alpha^* \equiv \cos^{-1} \sqrt{\frac{1}{1+M^2 \cos^2 \theta}} \quad 0 \leq M \leq 1 \quad (43)$$

A comparable expansion of Eq. (40) for very large values of $|\gamma^2|$ yields an expression for $T_{M^{\frac{1}{2}}}$ which is proportional to $\bar{K}^{-3/2}$, provided $\gamma - \beta M^2 \cos^2 \theta \neq 0$. However if $\gamma - \beta M^2 \cos^2 \theta = 0$, the limiting form attained by the expansion of Eq. (40) is proportional to \bar{K}^{-2} . This large variation in the asymptotic limit of the moment transfer function can, for example, have an effect on the unsteady aerodynamic response of a helicopter rotor blade encountering the tip vortex shed by a previous blade.

DISCUSSION OF THE APPROXIMATE SOLUTIONS

The objective of this section is to demonstrate the validity of the approximate solutions that were developed in the previous sections for the aerodynamic response functions. First, consider the equations for the lift transfer function, T_L , for both small and large positive values of γ (i.e., Eqs. (27) and (39), respectively) and compare the two-dimensional limits of these equations to the exact results of Refs. 5 and 6. This comparison is presented in Figs. 4 and 5 in which the complex function T_L is plotted in the phase plane at specific values of nondimensional wave number, $b\bar{K}$, for Mach numbers of 0.3 and 0.6, respectively. The solid curve appearing in both figures corresponds to the exact results presented in Refs. 5 and 6, while the dashed curves represent values computed from Eqs. (27) and (39) and a linear curve fit procedure to join the upper limit of validity of Eq. (27) (i.e., $\gamma = 0.2$) to the lower limit of validity of Eq. (39) (i.e., $\gamma = 0.7$). Figures 4 and 5 show that the present approximate solutions for the lift transfer functions are in good agreement with the exact result over a wide range of $b\bar{K}$. The accuracy of Eqs. (28) and (40) in predicting the two-dimensional moment transfer function is shown in Figs. 6 and 7 for Mach numbers of 0.3 and 0.6. The values of the moment transfer function for the region between the upper limit of Eq. (28) (i.e., $\gamma = 0.1$) and the lower limit of Eq. (40) (i.e., $\gamma = 0.7$) were determined by employing the same linear curve fitting procedure that was used for the lift transfer function. The agreement between the approximate solutions and the exact solutions for the moment transfer functions is seen to be comparable to that attained for the lift transfer functions.

The accuracy of the approximate expression for the lift and moment transfer functions governing the region $\gamma^2 \leq 0$ and zero angle of sweep is first demonstrated at $\gamma^2 = 0$ by comparing the results predicted by Eqs. (34) and (35) at this limit with those predicted by Eqs. (27) and (28). In Eqs. (27) and (28) the limit as $\gamma \rightarrow 0^+$ yields exact results while the limit of Eqs. (34) and (35) is approximate. A comparison for $\gamma^2 = 0$ is shown in Figs. 8 through 11 in which the complex functions T_L and T_M are plotted in the phase plane for specific values of nondimensional gust wave number, $b\bar{K}$. Once again the agreement between the exact solutions and the approximate solutions is good. To establish the accuracy of Eqs. (34) and (35) for values of $\gamma^2 < 0$ a comparison was made with the results obtained from an analysis based on the theory of Ref. 7. This comparison is presented for the real part of T_L and T_M in Figs. 12 through 15 for an encounter angle of 90 deg, zero angle of sweep and for Mach numbers of 0.3 and 0.6. (The imaginary part of T_L and T_M predicted by Eqs. (34) and (35) is zero, which is the correct solution for this particular encounter.) The solid curves appearing in these figures correspond to the exact results while the dashed

curves were predicted by Eqs. (34) and (35). In addition, the results predicted by Eqs. (39) and (40) are included as the dot-dash curves. The agreement between the approximate solutions and the exact solution is very good for values of $\bar{K}b > 1.0$. For values of $\bar{K}b \leq 1.0$ the agreement between Eqs. (34) and (35) and the exact results has deteriorated somewhat but is more than adequate for computational purposes.

The validity of these approximate solutions is clearly demonstrated by the good agreement with exact theory, and the closed form structure of the solutions facilitates their use. The latter is particularly important when these results are applied to specific problems of unsteady aerodynamic response where computer time and core storage may be limiting factors. Furthermore, the mathematical procedure that was employed to develop the approximate expressions for the unsteady response functions is sufficiently general to be applied to additional unsteady aerodynamic problems. In particular the current procedure can be used to predict the unsteady forces generated by the pitching or plunging motion of a two-dimensional airfoil in a subsonic stream. The derivation and discussion of these transfer functions is presented in Appendix IV.

APPLICATION OF THE APPROXIMATE SOLUTIONS

The theory of the preceding sections has been applied to the study of the lift and moment response of a helicopter rotor blade encountering the trailing vortex from a previous blade. The model that has been developed to simulate this aerodynamic interaction problem assumes the rotor blade to be an infinite swept airfoil. The trailing vortex is modeled as a rectilinear vortex translating at a velocity equal to the mean stream velocity.

The lift and moment coefficients per unit span generated by the encounter are obtained by the Fourier superposition of the lift and moment responses to an infinite series of oblique gusts which constitute the Fourier decomposition of the rectilinear vortex. The mathematical details of this procedure are discussed in Appendix V, while the computer program used to compute the example cases is described in Appendix VI. A series of computations were performed to determine the effects of encounter angle, Mach number, and vertical vortex displacement on the lift and moment response and these results are presented in Figs. 16 through 23. In all cases examined, the airfoil sweep angle was fixed at zero (i.e., the incoming flow was normal to the leading edge line of the wing). The lift and moment coefficients per unit span appearing in these figures are normalized with respect to the parameter Γ/Ub where Γ is the circulation of the free vortex, U is the free stream velocity, and b is the semichord of the airfoil. A typical range of this parameter for a helicopter blade is $0.2 \leq \Gamma/Ub \leq 2$. Figure 16 shows the lift coefficient per unit span generated by a parallel encounter of a vortex with a two-dimensional wing as a function of free stream Mach number and nondimensional time, $t' = Ut/b$. At $t' = 0$ the position of the vortex is one semichord below the airfoil leading edge, while at $t' = 2$ it is located one semichord below the trailing edge. The lift coefficient calculated on the basis of quasi-steady lifting line theory is also shown as a dashed line in Fig. 16. This result is presented to illustrate the effects of unsteadiness. It is seen from the figure that lifting line theory overestimates the maximum values of the lift coefficient when the vortex is directly beneath ($0 \leq t' \leq 2$) or slightly downstream ($t' > 2$) of the airfoil. This behavior can be attributed to rapid time variations in downwash that occur during the time the vortex is beneath the airfoil. In Fig. 17 the moment coefficient about the quarter-chord produced by a parallel encounter is shown as a function of Mach number and nondimensional time t' . A non-zero moment coefficient about the quarter-chord for a parallel encounter can be directly attributed to compressibility, since the moment is zero for an incompressible fluid. (This is shown on page 287 of Ref. 9. In addition, it should be noted that lifting line theory does not predict pitching moment.) It is seen from Fig. 17 that significant values of $C_{M1/4}/(\Gamma/Ub)$ can be obtained, which increase with increasing Mach number.

The results appearing in Figs. 18 and 19 illustrate the effects of three-dimensionality at a free stream approach Mach number of 0.6. These figures represent the lift and moment coefficients, respectively, produced by a vortex encountering an airfoil at an oblique angle as shown in the sketch in Fig. 18. Both results are presented as a function of nondimensional time t' , which is more generally defined as

$$t' = \frac{U t}{b} \cos(\theta - \alpha) - \frac{x_3}{b} \sin \alpha \quad (44)$$

In this equation α is the angle between the vortex and the leading edge of the wing, and x_3 is the spanwise coordinate. The spanwise position of the vortex at time $t = 0$ is $x_3 = 0$, while its vertical position is one semichord below the wing. The lift response shown in Fig. 18 appears to be a weak function of the encounter angle, while the corresponding moment response, shown in Fig. 19, appears to be very sensitive to variations in the encounter angle. This effect can be directly related to the asymptotic behavior of the Fourier transform of the moment response. Over most of the range of encounter angle, α , from parallel to normal encounter, this asymptotic limit is inversely proportional to $K^{3/2}$ (details can be found in the section entitled Limiting Behavior as $|\gamma^2| \rightarrow \infty$). However, if the value of the encounter angle is such that $\alpha = \alpha^*$ (cf. Eq. (43)) the asymptotic limit is proportional to K^{-2} . This was the case for $\alpha \cong 30$ deg. It appears from Fig. 19 that there is a definite transition in the character of the moment response at $\alpha = \alpha^*$.

A number of computations were performed to determine the effect of the vertical position of the free vortex beneath the airfoil on the unsteady lift and moment response generated by an encounter. The results for the normalized lift and moment coefficients per unit span generated by a parallel encounter at a Mach number 0.6 are shown in Figs. 20 and 21 as functions of nondimensional time t' and nondimensional vertical distance $h' = h/b$ (where h is the vertical height of the free vortex beneath the wing). The geometry of the encounter at time $t = 0$ is shown in the sketch of Fig. 20. These results indicate that the effect of increasing the vertical distance between the airfoil and the free vortex is to reduce the lift and moment response. Figures 22 and 23 show the maximum positive and negative values of the response curves as functions of vertical displacement and encounter angle. These results were obtained for an approach Mach number 0.6. Decreasing the vertical displacement between the free vortex and the wing causes the lift and moment response to increase for all encounter angles examined to date.

These results also show that the maximum positive values of the lift and moment response curves appear to be relatively insensitive to the encounter angle. However, the maximum negative values are strongly dependent on the encounter angle.

The final set of results that are presented is for a UH/1D rotor in forward flight at 90 Kts where the advancing blade in the second quadrant encounters the tip vortex shed by the preceding blade. Data for an experimentally measured wake geometry (Ref. 12) has been used to predict the spanwise distribution of the aerodynamic loads when the vortex-rotor blade intersection point is at 0.85, 0.753, and 0.674 of the rotor radius. The vertical displacement of the vortex beneath the plane of the rotor is 0.874 semichords while the azimuth position of the intersection at 0.85 of the rotor radius is 92 deg, at 0.753 of the rotor radius is 104 deg, and at 0.674 of the rotor radius is 115 deg. The resulting normalized lift and pitching moment coefficients are presented in Figs. 24 and 25 for the three blade radial locations. The results indicate the lift and moment coefficients to be relatively insensitive to radial location. This result can be attributed to the small variation of the geometry of the encounter with radial position. A variety of blade/vortex intersections can occur in a rotor depending upon advance ratio, azimuth position, lift and propulsive forces, and maneuvering condition; however, an evaluation of such intersections is beyond the scope of this study.

RESULTS AND CONCLUSIONS

A primary objective in developing the present analysis was to significantly reduce the computational time required by the theory of Ref. 7 to predict the aerodynamic response resulting from the encounter of a two-dimensional swept airfoil with a three-dimensional oblique sinusoidal gust in a compressible stream. This general objective was achieved, and the following are specific results obtained and conclusions reached in the development of this analysis:

1. A simple set of approximate expressions was derived to model the airfoil unsteady pressure, lift, and moment response.
2. In predicting the airfoil aerodynamic response, use of these approximate expressions significantly reduced the computation time (by a factor of 10 or more) over that required by the theory of Ref. 7.
3. The validity of these expressions was demonstrated by the close agreement with the exact results (i.e., based on the theories of Refs. 5 and 7) over a wide range of values of the governing parameters.
4. The approximate expressions clearly show the influence of compressibility and three-dimensionality on the response functions, and they show that a major effect is to generally increase the asymptotic decay rate of the response functions relative to their incompressible two-dimensional counterparts.

The approximate expressions were used to predict the aerodynamic loading on a helicopter rotor blade encountering the tip vortex shed by a previous blade. The major conclusion reached in this application of the analysis is that compressibility, unsteadiness, and three-dimensionality are important terms which must be included to correctly predict the aerodynamic response, particularly if the vortex is located within two chord lengths of the airfoil. Some of the specific results that were obtained in this application are:

1. The influence of unsteadiness is to reduce the magnitude of the lift response compared with that predicted by lifting line theory.
2. The influence of compressibility and three-dimensionality is to cause the generation of a moment about the quarter-chord which would be zero if the flow field were incompressible and two-dimensional.

3. The lift and moment response amplitudes increase as the Mach number of the flow increases.

4. The maximum value of the lift and moment response decreases rapidly as the distance between the center of the vortex and the plane of the airfoil increases.

RECOMMENDATIONS

The tasks described in the following recommendations will provide a framework for future studies of the vortex encounter problem:

1. An experimental program should be undertaken to measure the aerodynamic forces and moments generated during the encounter of a rotor blade and a vortex. These measurements should be made over a wide range of flow conditions and specifically should include the region of vortex-induced stalled flow on the suction surface of the rotor blade.
2. The present analytical model does not account for the influence of a tip region on the forces and moments generated during an encounter. Work should be undertaken to introduce this effect into the present analysis.
3. The results predicted by the present analysis indicate that lifting-line theory is inadequate for predicting the aerodynamic forces and moments generated during an encounter. It is therefore suggested that rotor blade dynamic response analyses which rely on lifting-line models to determine the aerodynamic forces be modified to incorporate the present analysis to yield a more realistic prediction of the forces and moments generated during an encounter.
4. Finally, the present analysis should be combined with an acoustic analysis to predict the acoustic field generated by a vortex encounter.

APPENDIX I

APPROXIMATE EXPRESSIONS FOR THE AERODYNAMIC

RESPONSE FUNCTIONS FOR SMALL POSITIVE VALUES OF γ

In this Appendix approximate expressions for both the circulatory and noncirculatory solutions of Eq. (16) are derived for small positive values of γ . Consider first the variable $\Phi^{(1)}$ associated with the noncirculatory flow field which is obtained by solving Eq. (16) subject to the boundary conditions, Eqs. (19) and (20). From the results presented in Ref. 7 it can be shown that a solution for the noncirculatory flow field of order γ (i.e., a series which neglects all terms of order γ^n for $n > 1$) is given by an expression which satisfies Laplace's equation:

$$\nabla^2 \Phi^{(1)} = 0 \quad (45)$$

and the boundary condition, Eq. (19). The solution of Eq. (45) is given in Ref. 7 as

$$\Phi^{(1)} = \sum_{n=1}^{\infty} A_n \sin n\eta e^{-n\xi} \quad (46)$$

where the elliptical cylindrical coordinates η and ξ are defined by the equations

$$x_1 = \cosh \xi \cos \eta \quad (47)$$

and

$$x_2 = \sinh \xi \sin \eta \quad (48)$$

The surfaces $\xi = \text{constant}$ and $\eta = \text{constant}$ are elliptic and hyperbolic cylinders, respectively, and the degenerate ellipse $\xi = 0$ corresponds to the portion of the X_1, X_3 plane occupied by the airfoil; that is, $-1 \leq X_1 \leq 1$.

The constants A_n in Eq. (46) are determined by requiring $\Phi^{(1)}$ to satisfy the boundary conditions in Eq. (19).

$$\left. \frac{\partial \Phi^{(1)}}{\partial X_2} \right|_{X_2=0} = \left. \frac{\partial \Phi^{(1)}}{\partial \xi} \right|_{\xi=0} \frac{1}{\sin \eta} = - \sum_{n=1}^{\infty} \frac{A_n n \sin n \eta}{\sin \eta} \quad (49)$$

Eqs. (19) and (49) may be rearranged to yield

$$\sum_{n=1}^{\infty} A_n n \sin n \eta = \frac{b}{\sqrt{1 - M^2 \cos^2 \theta}} \sin \eta \bar{u}_2 e^{i\beta \cos \eta} \quad (50)$$

If both sides of this equation are multiplied by $\sin m \eta$ and integrated over the interval $0 \leq \eta \leq \pi$ the result is

$$\begin{aligned} A_m &= \frac{2}{\pi} \frac{b \bar{u}_2}{\sqrt{1 - M^2 \cos^2 \theta}} \int_0^{\pi} \sin \eta \sin m \eta e^{i\beta \cos \eta} d\eta \\ &= \frac{1}{\pi} \frac{b \bar{u}_2}{\sqrt{1 - M^2 \cos^2 \theta}} \int_0^{\pi} [\cos(m+1)\eta + \cos(m-1)\eta] e^{i\beta \cos \eta} d\eta \end{aligned} \quad (51)$$

$$m \geq 1$$

Upon introducing the integral relationship

$$J_n(\beta) = \frac{i^{-n}}{\pi} \int_0^{\pi} e^{i\beta \cos \eta} \cos n \eta d\eta \quad (52)$$

and the Bessel Function recurrence formula

$$J_{n+1}(Z) + J_{n-1}(Z) = \frac{2n}{Z} J_n(Z) \quad (53)$$

into Eq. (51), one obtains

$$A_m = \frac{2b\bar{u}_2}{\sqrt{1-M^2\cos^2\theta}} \frac{i^{n-1}}{\beta} \frac{J_m(\beta)}{M} \quad m \geq 1 \quad (54)$$

which when combined with Eq. (46), transforms Eq. (46) to

$$\Phi^{(1)} = \frac{2b\bar{u}_2}{(1-M^2\cos^2\theta)^{1/2}} \frac{1}{\beta} \sum_{n=1}^{\infty} i^{n-1} J_n(\beta) \sin n\eta e^{-n\xi} \quad (55)$$

An expression for the noncirculatory pressure field on the surface of the airfoil is obtained by combining Eqs. (21) and (55) yielding

$$p^{s(1)} = \frac{\rho_0 U \bar{u}_2 \cos \theta}{(1-M^2\cos^2\theta)^{1/2}} \frac{1}{\sin \eta} \left[J_0(\beta) \cos \eta + i J_1(\beta) \right] \times \quad (56)$$

$$e^{i \left[-\beta M^2 \cos^2 \theta \cos \eta + \frac{\bar{k} b \sin \alpha}{1-M^2\cos^2\theta} X_3 - \bar{K} U \cos(\theta-\alpha)t \right]}$$

Since $\sin \eta = 0$ at the leading and trailing edges of the airfoil, the pressure distribution given by Eq. (56) is singular at these points.

The trailing edge singularity is removed by adding a circulatory field. The approximate expression for the circulatory flow field pressure distribution on the surface of the airfoil for small positive values of γ is obtained by expanding the exact solution for the circulatory pressure distribution presented in Ref. 7 in a power series of γ . This pressure distribution is equal to

$$p^{s(2)} = \bar{p}^{(2)} e^{i \left[-\beta M^2 \cos^2 \theta \cos \eta + \frac{\bar{k} b \sin \alpha}{1-M^2\cos^2\theta} X_3 - \bar{K} U \cos(\theta-\alpha)t \right]} \quad (57)$$

where $\bar{p}^{(2)}$ is defined by Eq. (62) of Ref. 7 as

$$\bar{p}^{(2)}(0, \eta) = -\frac{\rho_0 U \cos \theta}{b} \text{conj} \left\{ \sum_{n=0}^{\infty} B_n \text{ce}_n(n, q) \text{Me}_n^{(2)'}(0, q) \right\} \quad q = \gamma^2/4 \quad (58)$$

and the symbol conj denotes the complex conjugate operator. The coefficients B_n which appear in Eq. (58) are defined by Eq. (54) of Ref. 7. For small positive values of γ , an expression for $\bar{p}^{(2)}$, correct to first order in γ , can be obtained by retaining the first two terms of the series in Eq. (58), namely

$$\bar{p}^{(2)}(0, \eta) \approx -\frac{\rho_0 U \cos \theta}{b \sin \eta} \text{conj} \left\{ \frac{B_0 \text{Me}_0^{(2)'}(0, q)}{\sqrt{2}} \times \left[\sqrt{2} \text{ce}_0(\eta, q) + \frac{\sqrt{2} B_1}{B_0} \frac{\text{Me}_1^{(2)'}(0, q)}{\text{Me}_0^{(2)'}(0, q)} \text{ce}(\eta, q) \right] \right\} \quad (59)$$

When $\text{ce}_0(\eta, q)$ and $\text{ce}_1(\eta, q)$ are expanded in a power series, the following results are obtained to first order in γ :

$$\text{ce}_0(\eta, q) = \frac{1}{\sqrt{2}} \quad (60)$$

$$\text{ce}_1(\eta, q) = \cos \eta \quad (61)$$

Similarly, if the quantity $\frac{\sqrt{2} B_1}{B_0} \frac{\text{Me}_1^{(2)'}}{\text{Me}_0^{(2)'}}$ is expanded (i.e., by employing the results presented on pages 146 and 147 of Ref. 7 with γ and β replacing μ and

ν , respectively) the result will be

$$\frac{\sqrt{2} B_1 Me_1'^{(2)}}{B_0 Me_0'^{(2)}} = \frac{\gamma^2 e^{-i\beta} [1+i\beta] \frac{Me_0^{(2)}(0,q)}{Me_0'^{(2)}(0,q)} + (\gamma^2 - \beta^2) \int_0^\infty \frac{Me_0'^{(2)}(\xi,q)}{Me_0'^{(2)}(0,q)} e^{-i\beta \cosh \xi} d\xi}{e^{i\beta} \left[\gamma^2 - i\beta \left(1 - \frac{\gamma^2}{2} \right) \right] \frac{Me_1^{(2)}(0,q)}{Me_1'^{(2)}(0,q)} + (\gamma^2 - \beta^2) \int_0^\infty \frac{Me_1'^{(2)}(\xi,q)}{Me_1'^{(2)}(0,q)} e^{-i\beta \cosh \xi} d\xi} \quad (62)$$

The first order expansions of the remaining Mathieu function are:

$$\frac{Me_0^{(2)}(0,q)}{Me_0'^{(2)}(0,q)} \cong \frac{\pi i}{2} H_0^{(2)}(\gamma/2) \quad (63)$$

$$\frac{Me_1^{(2)}(0,q)}{Me_1'^{(2)}(0,q)} \cong -1 \quad (64)$$

$$\int_0^\infty \frac{Me_0'^{(2)}(\xi,q)}{Me_0'^{(2)}(0,q)} e^{-i\beta \cosh \xi} d\xi \cong \int_0^\infty e^{-i\beta \cosh \xi} d\xi = -\frac{i\pi}{2} H_0^{(2)}(\beta) \quad (65)$$

$$\begin{aligned} \int_0^\infty \frac{Me_1'^{(2)}(\xi,q)}{Me_1'^{(2)}(0,q)} e^{-i\beta \cosh \xi} d\xi &\cong \int_0^\infty e^{-\xi} e^{-i\beta \cosh \xi} d\xi \\ &= -\frac{\pi}{2} H_1^{(2)}(\beta) - \frac{e^{-i\beta}}{i\beta} \end{aligned} \quad (66)$$

Upon substituting Eq. (63) through (66) into Eq. (62) and neglecting terms of higher order than γ which appear in the denominator of Eq. (62) the result is

$$\frac{\sqrt{2} B_1 Me_1^{(2)}}{B_0 Me_0^{(2)}} \cong \frac{i\gamma^2 e^{-i\beta} (1+i\beta) H_0^{(2)}(\gamma/2) - i(\gamma^2 - \beta^2) H_0^{(2)}(\beta)}{\beta^2 H_1^{(2)}(\beta)} \quad (67)$$

Equation (67) is reduced to its final form by interpreting $1 + i\beta$ as the leading terms in the expansion of $e^{i\beta}$. With this replacement, Eq. (67) becomes

$$\frac{\sqrt{2} B_1 Me_1^{(2)}}{B_0 Me_0^{(2)}} \cong \frac{iH_0^{(2)}(\beta) + i\gamma^2/\beta^2 [H_0^{(2)}(\gamma/2) - H_0^{(2)}(\beta)]}{H_1^{(2)}(\beta)} \quad (68)$$

The substitution of $e^{i\beta}$ for $(1 + i\beta)$ causes Eq. (68) to approach zero as $\beta \rightarrow \infty$. This substitution improves the accuracy of the approximate expressions for the lift and moment transfer function for large values of β .

Equation (68) contains an expression of apparent second order in γ . However, if this term is neglected, a term of first order in \bar{K} would be lost. This first order term results from a combination of the expressions within the brackets and the Hankel function $H_1^{(2)}(\beta)$. Thus if γ^2 is neglected in Eq. (62) the validity of the approximation is reduced to zero order in \bar{K} . When Eqs. (60), (61), and (68) are introduced into Eq. (59) an approximate expression for $\bar{p}^{(2)}$ is obtained.

$$\bar{p}^{(2)}(0, \eta) \cong - \frac{\rho_0 U \cos \theta}{b \sin \eta} c \text{ conj} \quad (69)$$

$$\left[1 + \left\{ \frac{iH_0^{(2)}(\beta) + i(\gamma/2)^2 [H_0^{(2)}(\gamma/2) - H_0^{(2)}(\beta)]}{H_1^{(2)}(\beta)} \right\} \cos \eta \right]$$

where the constant C must be assigned a value which will cause $p^s(2)$ at the trailing edge to be equal in magnitude but opposite in sign to $p^s(1)$ evaluated at the trailing edge.

The final form for the pressure distribution on the surface of the airfoil for small positive values of γ is obtained by substituting Eq. (69) into Eq. (57) and adding the result to Eq. (56) to yield

$$p^s = - \frac{\rho_0 U \bar{U}_2 \cos \theta}{(1 - M^2 \cos^2 \theta)^{1/2}} \sqrt{\frac{1 - x_1}{1 + x_1}} \left[\frac{J_0(\beta) - iZ J_1(\beta)}{1 + Z} \right] \times \quad (70)$$

$$e^{i[-\beta M^2 \cos^2 \theta x_1 + \bar{k} \sin \alpha x_3 - [R U \cos(\theta - \alpha) t]]}$$

where the variable

$$Z = - \frac{i H_0^{(1)}(\beta) + (\gamma/\beta)^2 i [H_0^{(1)}(\gamma/2) - H_0^{(1)}(\beta)]}{H_1^{(1)}(\beta)} \quad (71)$$

The equations for the lift and moment transfer functions T_L and T_M , respectively, can be obtained by integrating the zero and first order moments of the pressure distribution over the chord of the airfoil. The resulting expression for the lift transfer function T_L is:

$$T_L = e^{ib\bar{k}\cos\alpha} \left[\frac{J_0(\beta) - iZ J_1(\beta)}{1 + Z} \right] [J_0(M^2\beta \cos^2\theta) + iJ_1(M^2\beta \cos^2\theta)] \quad (72)$$

while that for the moment transfer function T_M about the quarter-chord is:

$$T_{M_{1/4}} = e^{ib\bar{k}\cos\alpha} \left[\frac{J_0(\beta) - iZJ_1(\beta)}{1+Z} \right] \times \quad (73)$$

$$\left[-J_0(M^2\beta\cos^2\theta) + J_2(M^2\beta\cos^2\theta) - 2iJ_1(M^2\beta\cos^2\theta) \right] + T_L$$

The factor $e^{ib\bar{k}\cos\alpha}$ which appears in Eqs. (72) and (73) has been added to shift the phase of the lift and moment response relative to the gust field to the leading edge of the airfoil.

APPENDIX II

APPROXIMATE EXPRESSIONS FOR THE AERODYNAMIC RESPONSE FUNCTIONS FOR NEGATIVE VALUES OF γ^2

The objective of this Appendix is to present the derivation of the approximate expressions for the aerodynamic response functions for the region $\gamma^2 \leq 0$. This derivation was accomplished by employing an extended version of the similarity rules developed by Graham (Ref. 5), which were modified to include the effect of airfoil sweep angle. Graham shows that the solution for the modified velocity potential Φ (cf. Eq. (15)) for the region $\gamma^2 \leq 0$ and for zero sweep angle is directly related to the solution for Φ associated with the problem of an unswept two-dimensional airfoil encountering a three-dimensional oblique sinusoidal gust in an incompressible stream. This correspondence also exists for swept infinite airfoils and is expressed by the equation:

$$\Phi(\gamma, \beta) = \frac{\Phi(\gamma, \beta)_{INC}}{\sqrt{1 - M^2 \cos^2 \theta}} \quad (74)$$

which is derivable from Eq. (16). Here $\Phi(\gamma, \beta)_{INC}$ is the solution to the three-dimensional incompressible problem expressed in terms of γ and β . The substitution of Eqs. (74) and (13) into Eq. (21) yields the expression for the compressible pressure field

$$p^s = \frac{-\rho_0 U \cos \theta}{b \sqrt{1 - M^2 \cos^2 \theta}} \left[\frac{\partial \Phi_{INC}}{\partial x_1} - i\beta \Phi_{INC} \right] \times \exp \left[-i\beta^2 M^2 \cos^2 \theta x_1 + i\bar{k} \sin \alpha x_3 - i\bar{k} U \cos(\theta - \alpha) t \right] \quad (75)$$

The equation for the corresponding incompressible pressure field is obtained by letting $M \rightarrow 0$ in Eq. (75)

$$p(\gamma, \beta)_{INC} = -\frac{\rho_0 U \cos \theta}{b} \left[\frac{\partial \Phi_{INC}}{\partial x_1} - i\beta \Phi_{INC} \right] \times \exp \left[i\bar{k} \sin \alpha x_3 - i\bar{k} U \cos(\theta - \alpha) t \right] \quad (76)$$

and it is seen that Eqs. (75) and (76) are related by the equation

$$p^s = \frac{p(\gamma, \beta)_{INC} e^{-i(\beta M^2 \cos^2 \theta x_1)}}{\sqrt{1 - M^2 \cos^2 \theta}} \quad (77)$$

which is a pressure similarity rule comparable to Eq. (74) for the modified potential.

A formula for the pressure field $p(\gamma, \beta)_{INC}$ can be derived from the approximate expression developed by Filotas (Ref. 4) for the pressure distribution on the surface of an unswept airfoil encountering a three-dimensional gust in an incompressible stream,

$$p = \left\{ \rho_0 U \bar{u}_2 \right\} \left\{ \frac{e^{-K_F \cos \beta_F H}}{I_0(K_F \cos \beta_F) + I_1(K_F \cos \beta_F)} \right\} \sqrt{\frac{1 - X_1}{1 + X_1}} \times \left\{ \exp(i K_F \cos \beta_F x_3) \right\} \times \left\{ \exp(-i U K_F \sin \beta_F t) \right\} \quad (78)$$

$$-1 \leq X_1 \leq 1$$

where

$$H(K_F, \beta_F) = \frac{e^{-i K_F \left\{ \sin \beta_F - \pi \beta_F \left(1 + \cos \frac{\beta_F}{2} \right) \right\} / \left[1 + 2\pi K_F \left(1 + \cos \frac{\beta_F}{2} \right) \right]}}{\sqrt{1 + \pi K_F (1 + \sin^2 \beta_F + \pi K_F \cos \beta_F)}} \quad (79)$$

The subscript F which appears in these equations refers to the variables defined in Ref. 4. The transformation of Eq. (78) to p_{INC} is accomplished by letting the terms in brackets (1), (3), and (4) become

bracket (1)

$$\left\{ \rho_0 U \bar{u}_2 \right\} \rightarrow \left\{ \rho_0 U \cos \theta \bar{u}_2 \right\} \quad (80)$$

bracket (3)

$$\left\{ \exp \left[i K_F \cos \beta_F x_3 \right] \right\} \rightarrow \left\{ \exp \left[i \bar{K} \sin \alpha x_3 \right] \right\} \quad (81)$$

bracket (4)

$$\left\{ \exp \left[-i K_F \sin \beta_F t \right] \right\} \rightarrow \left\{ \exp \left[-i \bar{K} U \cos (\theta - \alpha) t \right] \right\} \quad (82)$$

while the remaining terms which appear in bracket (2) are transformed by replacing the variables K_F and β_F by the expressions

$$K_F = \sqrt{\gamma^2 + \beta^2} \quad (83)$$

$$\beta_F = \pi/2 - \delta \quad (84)$$

where

$$\delta = \tan^{-1} \gamma/\beta \quad (85)$$

Introducing these transformations into Eq. (78) and combining the result with Eq. (77) yields an expression for p^s

$$p^s = \frac{\rho_0 U \bar{u}_2 \cos \theta}{\sqrt{1 - M^2 \cos^2 \theta}} \left[\frac{e^{-\gamma x_1}}{I_0(\gamma) + I_1(\gamma)} H(\gamma, \beta) \right] \sqrt{\frac{1 - x_1}{1 + x_1}} \times \exp \left[-i \bar{K} \sin \alpha x_3 - i \bar{K} U \cos (\theta - \alpha) t \right] e^{-i \beta M^2 \cos^2 \theta x_1} \quad (86)$$

where

$$H(\gamma, \beta) = \frac{e^{-i \sqrt{\gamma^2 + \beta^2} x_1} \left\{ \cos \delta - \frac{\pi [\pi/2 - \delta] [1 + \sin \delta/2]}{1 + 2\pi \sqrt{\gamma^2 + \beta^2} [1 + \sin \delta/2]} \right\}}{\sqrt{1 + \pi \sqrt{\gamma^2 + \beta^2} [1 + \cos \delta + \pi \sqrt{\gamma^2 + \beta^2} \sin \delta]}} \quad (87)$$

The lift and moment transfer functions per unit span are obtained by integrating the appropriate moments of the pressure distribution, Eq. (86), over the chord of the airfoil. The expression for the lift transfer function T_L is

$$T_L = \frac{I_0(\gamma + i\beta M^2 \cos^2 \theta) + I_1(\gamma + i\beta M^2 \cos^2 \theta)}{I_0(\gamma) + I_1(\gamma)} H(\gamma, \beta) e^{i\bar{K}b \cos \alpha} \quad (88)$$

while the corresponding expression for the moment transfer function about the quarter-chord is

$$T_{M_{1/4}} = -2 e^{i\bar{K}b \cos \alpha} \frac{H(\gamma, \beta)}{I_0(\gamma) + I_1(\gamma)} I_0(\gamma + i\beta M^2 \cos^2 \theta) + I_1(\gamma + i\beta M^2 \cos^2 \theta) \left[\left(1 - \frac{1}{\gamma + i\beta M^2 \cos^2 \theta} \right) \right] + T_L \quad (89)$$

The factor $e^{i\bar{K}b \cos \alpha}$ has been introduced to refer the phase of the lift and moment response functions to the gust downwash at the leading edge.

APPENDIX III

SOLUTION FOR LARGE VALUES OF $|\gamma^2|$

In the main body of the text it is suggested that for large positive values of γ^2 the pressure distribution on the surface of the airfoil is composed of two cylindrical acoustical waves whose origins are the leading and trailing edges of the airfoil. Furthermore, it is suggested that the solution for the pressure field whose origin is the leading edge could be approximated by the solution for the pressure field resulting from the encounter of a three-dimensional gust with a semi-infinite plate. The solution for the modified velocity potential Φ associated with this pressure field satisfies Eq. (16) and the boundary condition of Eq. (19) on the surface of the plate. The solution for Φ can be obtained from an analysis based on the Weiner-Hopf technique, the details of which can be found on pages 48 to 98 of Ref. 13. This solution is

$$\Phi(x_1, 0) = \frac{E(1+i)e^{i\beta x_1'}}{\sqrt{\beta^2 + \gamma^2}} \left[-\frac{b\bar{u}_2}{\sqrt{1-M^2\cos^2\theta}} \right] \quad x_1' \geq 0 \quad (90)$$

where

$$E = C \left[\sqrt{(\beta - \gamma)x_1} \right] - iS \left[\sqrt{(\beta - \gamma)x_1} \right] \quad (91)$$

and C and S are cosine and sine Fresnel Integrals, respectively. The pressure distribution is obtained by substituting Eq. (90) into Eq. (21) yielding the result

$$p^{(1)} = \frac{\rho U \bar{u}_2 \cos \theta}{\sqrt{1-M^2\cos^2\theta}} \frac{(1+i) \exp}{\sqrt{2\pi x_1'(\beta + \gamma)}} \times \quad (92)$$

$$\left[i(\gamma - M^2\beta \cos^2\theta)x_1' + i\bar{K} \sin \alpha x_3 - i\bar{K}U \cos(\theta - \alpha)t \right]$$

where $x_1' = x_1 + 1$ and the superscript (1) denotes that Eq. (92) is an approximate expression for p^S in a region removed from the trailing edge of the airfoil. The magnitude of the pressure distribution as given by Eq. (92) monotonically approaches zero as the distance from the leading edge of the airfoil becomes large without bound. However, the value for the pressure distribution predicted by the exact theory of Ref. 7 for the region downstream of the airfoil (i.e., $X_1 \geq 1, X_2 = 0$) is zero. Hence, the pressure distribution, Eq. (92), is incorrect in a region surrounding the trailing edge of the airfoil, the magnitude of the error being proportional to $\gamma^{-1/2}$. This error may be corrected by adding to $p^{(1)}$ a pressure field $p^{(2)}$ which is equal and opposite to $p^{(1)}$ downstream of the airfoil (i.e., $X_1 \geq 1, X_2 = 0$) and has its normal gradient vanishing everywhere on the airfoil. An approximate expression for this pressure field can be developed for $\gamma^2 > 0$ by considering the problem of an oblique cylindrical acoustical wave impinging on an infinitely compliant, semi-infinite surface (i.e., a surface on which the pressure vanishes) in a uniform compressible stream. (For $\gamma^2 < 0$ the problem of an oblique cylindrical cut-off wave impinging on a compliant surface can be considered.) The solution for the scattered pressure field $p^{(2)}$ is developed by again employing the Weiner-Hopf technique (Ref. 13). The construction of the solution for the pressure field $p^{(2)}$ is accomplished by introducing a modified acceleration potential H which is defined in terms of $p^{(2)}$ by the equation

$$p^{(2)} = \rho H e^{i[-\beta M^2 \cos^2 \theta \bar{X}_1' + \bar{K} \sin \alpha x_3 - \bar{K} U \cos(\theta - \alpha) t]} \quad (93)$$

where the variable transformation $\bar{X}_1' = X_1' - 2$ now places the local origin at the trailing edge. Substitution yields the result that H satisfies Eq. (16) everywhere in the flow field.

Downstream of the airfoil (i.e., $\bar{X}_1' \geq 0, X_2 = 0$) $p^{(2)}$ is equal in magnitude but opposite in sign to $p^{(1)}$. Hence from Eqs. (92) and (93) H must equal

$$H = - \frac{U \bar{u}_2 \cos \theta}{\sqrt{1 - M^2 \cos^2 \theta}} \frac{(1+i) e^{i\gamma(\bar{X}_1'+2)}}{\sqrt{2\pi(\bar{X}_1'+2)(\beta+\gamma)}} e^{-2i\beta M^2 \cos^2 \theta} \quad (94)$$

$$\bar{X}_1' \geq 0, \quad X_2 = 0$$

downstream of the trailing edge. Upstream of the trailing edge (i.e., $\bar{X}_1' \leq 0, X_2 = 0$) the normal gradient of $p^{(2)}$ must vanish, hence

$$\frac{\partial H}{\partial X_2} = 0 \quad \bar{X}_1' \leq 0, \quad X_2 = 0 \quad (95)$$

The solution for the pressure field $p^{(2)}$ may be derived from the solution of the mixed boundary value problem for H_2 , which can be found on pg. 79 of Ref. 13. The value of H on the boundary $X_1' \leq 0, X_2 = 0$ is given by the expression

$$\begin{aligned} H &= \frac{1}{2} \pi^{-3/2} e^{\frac{3i\pi}{4}} \left\{ \int_0^\infty M(U, \bar{X}_1', 0) e^{-i\gamma U} dU \left[\frac{d}{dU} \int_0^\infty \xi^{-1/2} e^{i\gamma(U+\xi)} f(U+\xi) d\xi \right] \right\} \\ &= \frac{1}{2} \pi^{-3/2} e^{\frac{3i\pi}{4}} \left\{ \int_0^\infty M e^{-i\gamma U} \frac{d}{dU} I(U) dU \right\} \end{aligned} \quad (96)$$

$$\bar{X}_1' \leq 0, \quad X_2 = 0$$

where

$$M(U, \bar{X}_1', 0) = \begin{cases} 2\pi^{1/2} e^{i\pi/4} (U - \bar{X}_1')^{-1/2} e^{i\gamma(U - \bar{X}_1')} & (U - \bar{X}_1') > 0 \\ 0 & (U - \bar{X}_1') < 0 \end{cases} \quad (97)$$

and the variable f is equal to H evaluated on the boundary $\bar{X}_1' \geq 0, X_2 = 0$

$$f(\bar{X}_1') = H(\bar{X}_1') \quad (98)$$

$$\bar{X}_1' \geq 0, \quad X_2 = 0$$

The evaluation of the inner integral in Eq. (96) is accomplished by first introducing Eq. (98) into Eq. (96) and replacing $H(U + \xi)$ with Eq. (94). These manipulations yield

$$I(U) = - \frac{U\bar{u}_2 \cos \theta}{\sqrt{1-M^2 \cos^2 \theta}} \frac{(1+i)e^{2i(\gamma - \beta M^2 \cos^2 \theta)}}{\sqrt{2\pi(\beta + \gamma)}} \int_0^\infty \frac{e^{2i\gamma(U+\xi)}}{\sqrt{U+\xi+2} \sqrt{\xi}} d\xi \quad (99)$$

This result may be reduced to

$$I(U) = - \frac{U\bar{u}_2 \cos \theta}{\sqrt{1-M^2 \cos^2 \theta}} \frac{ie^{2i(\gamma - \beta M^2 \cos^2 \theta)}}{\sqrt{2\gamma(\beta + \gamma)}} \frac{e^{2i\gamma U}}{\sqrt{U+2}} \quad (100)$$

by employing the method of stationary phase (i.e., Ref. 14) in evaluating the integral over ξ . Substituting Eq. (100) into Eq. (96) and performing the differentiation with respect to U yields

$$H = \frac{U\bar{u}_2 \cos \theta}{\sqrt{1-M^2 \cos^2 \theta}} \frac{ie^{2i(\gamma - \beta M^2 \cos^2 \theta)}}{\pi \sqrt{2\gamma(\beta + \gamma)}} \times \quad (101)$$

$$e^{-i\gamma \bar{x}'_1} \int_0^\infty \frac{e^{2i\gamma U}}{\sqrt{(U-\bar{x}'_1)(U+2)}} \left[2i\gamma - \frac{1}{2(U+2)} \right] dU \quad \bar{x}'_1 \leq 0$$

The evaluation of the remaining integral in Eq. (101) is accomplished by employing the variable transformation $\tau^2 = U - \bar{x}'_1$ to obtain

$$H = \frac{2U\bar{u}_2 \cos \theta}{\pi \sqrt{1-M^2 \cos^2 \theta}} \frac{ie^{2i(\gamma - \beta M^2 \cos^2 \theta)}}{\sqrt{2\gamma(\beta + \gamma)}} \times \quad (102)$$

$$e^{i\gamma \bar{x}'_1} \int_{\sqrt{-\bar{x}'_1}}^\infty \frac{e^{2i\gamma \tau^2}}{[\tau^2 + \bar{x}'_1 + 2]^{1/2}} \left[2i\gamma - \frac{1}{2(\tau^2 + \bar{x}'_1 + 2)} \right] d\tau$$

An approximate value of the integral is obtained by noting that for large values of γ the major contribution of the integrand to the integral comes from the region surrounding the lower limit. Thus, Eq. (102) may be approximated as

$$H \approx \frac{U\bar{u}_2 \cos \theta}{\pi \sqrt{1-M^2 \cos^2 \theta}} \frac{e^{2i(\gamma-M^2\beta \cos^2 \theta)}}{\sqrt{\gamma(\beta+\gamma)}} e^{i\gamma\bar{x}'_1} \left[2i\gamma - \frac{1}{4} \right] \int_{\sqrt{-\bar{x}'_1}}^{\infty} e^{2i\gamma\tau^2} d\tau \quad (103)$$

$$\approx \frac{U\bar{u}_2 \cos \theta}{\sqrt{1-M^2 \cos^2 \theta}} \frac{e^{i\gamma(2+\bar{x}'_1)}}{\sqrt{\pi(\beta+\gamma)}} e^{-2iM^2\beta \cos^2 \theta} \left[\frac{1+i}{2} - E\left(\sqrt{-2\gamma\bar{x}'_1}\right) \right]$$

The pressure distribution $p^{(2)}$ on the boundary $\bar{x}'_1 \leq 0$, $X_2 = 0$ is obtained by combining Eqs. (93) and (103) which yields

$$p^{(2)} = \frac{-\rho U\bar{u}_2 \cos \theta}{\sqrt{1-M^2 \cos^2 \theta}} \frac{e^{i\left\{\left[\gamma-\beta M^2 \cos^2 \theta\right]x'_1 + \bar{K}b \sin \alpha X_3 - U\bar{K} \cos(\theta-\alpha)t\right\}}}{\sqrt{\pi(\beta+\gamma)}} \times \quad (104)$$

$$\left[\frac{1+i}{2} - E\left(\sqrt{2\gamma(2-x'_1)}\right) \right] \quad 0 \leq x'_1 \leq 2$$

An approximate expression for the pressure field p^S is obtained by combining the expressions for $p^{(1)}$, Eq. (92) and $p^{(2)}$, Eq. (104). The result is

$$p^S = \frac{\rho U\bar{u}_2 \cos \theta}{\sqrt{1-M^2 \cos^2 \theta}} \frac{1}{\sqrt{\pi(\beta+\gamma)}} \left\{ \frac{1+i}{\sqrt{2x'_1}} - \frac{1+i}{2} + E\left[\sqrt{2\gamma(2-x'_1)}\right] \right\} \times \quad (105)$$

$$\exp i\left\{\left[\gamma-\beta M^2 \cos^2 \theta\right]x'_1 + \bar{K}b \sin \alpha X_3 - U\bar{K} \cos(\theta-\alpha)t\right\}$$

In Ref. 7 it is shown that upstream of the airfoil the solution for p^S must vanish. However, the approximate expression given by Eq. (105) equals $p^S = p^{(2)}$ upstream of the airfoil since the pressure distribution $p^{(1)}$ vanishes on the boundary $X_1 \leq 0, X_2 = 0$. It is seen from Eq. (104) for $p^{(2)}$ that the magnitude of this expression for large values of $|\gamma^2|$ is proportional to γ^{-1} . Hence, although the pressure distribution, Eq. (105) is correct near the trailing edge, the result $p^S = p^{(2)}$ shows that it is now incorrect in the region upstream of the airfoil leading edge, (i.e., $X_1 < -1$), the error being proportional to γ^{-1} . This error could be removed by employing an analytical procedure which is identical to the one used earlier to remove the error associated with the pressure distribution $p^{(1)}$. The result would be an estimate for the pressure distribution p^S which would now be in error in the region surrounding the trailing edge, the magnitude of the error being proportional to $\gamma^{-3/2}$. This could be further corrected at the expense of the leading edge solution, and if desired the analytical procedure could be employed as many times as necessary to achieve the desired degree of accuracy. The final form for the pressure distribution p^S on the surface of the airfoil would then be an asymptotic series involving powers of $\gamma^{-1/2}$. In the present analysis the series is terminated after the second term, $p^{(2)}$, which yields the result given by Eq. (105).

The approximate expressions for the lift and moment transfer functions are obtained by integrating the appropriate moments of the pressure distribution, Eq. (105), over the chord of the airfoil. The resulting integration yields an expression for the lift transfer function T_L which is

$$\begin{aligned}
 T_L = \frac{1}{\sqrt{\pi(\beta+\gamma)}} & \left\{ (1+i) \sqrt{\frac{\pi}{\gamma-\beta M^2 \cos^2 \theta}} E \left[\sqrt{2(\gamma-\beta M^2 \cos^2 \theta)} \right] \right. \\
 & + \left[1 - e^{2i(\gamma-\beta M^2 \cos^2 \theta)} \right] \frac{1-i}{2(\gamma-\beta M^2 \cos^2 \theta)} \\
 & + \frac{i E \left[\sqrt{4\gamma} \right]}{(\gamma-\beta M^2 \cos^2 \theta)} - \frac{i \sqrt{2\gamma}}{\gamma-\beta M^2 \cos^2 \theta} \times \\
 & \left. \frac{e^{2i(\gamma-\beta M^2 \cos^2 \theta)}}{\sqrt{\gamma+\beta M^2 \cos^2 \theta}} E \left[\sqrt{2(\gamma+\beta M^2 \cos^2 \theta)} \right] \right\} \quad (106)
 \end{aligned}$$

while the corresponding expression for the moment transfer function about the quarter-chord is

$$\begin{aligned}
 T_{M_{1/4}} &= \frac{(1-i)\sqrt{\pi}}{(\gamma - \beta M^2 \cos^2 \theta)^{3/2}} E \left[\sqrt{\frac{4}{\pi} (\gamma - \beta M^2 \cos^2 \theta)} \right] + \frac{1+i}{(\gamma - \beta M^2 \cos^2 \theta)^2} \times \\
 &\left[1 - e^{2i(\gamma - \beta M^2 \cos^2 \theta)} \right] - \frac{2E \left[2\sqrt{\gamma} \right]}{(\gamma - \beta M^2 \cos^2 \theta)^2} - \frac{i2\sqrt{2\gamma}}{(\gamma - \beta M^2 \cos^2 \theta)} \frac{e^{2i(\gamma - \beta M^2 \cos^2 \theta)}}{\sqrt{\gamma + \beta M^2 \cos^2 \theta}} \times \\
 &E \left[\sqrt{2(\gamma + \beta M^2 \cos^2 \theta)} \right] \left[2 - \frac{2}{2(\gamma + \beta M^2 \cos^2 \theta)} \right] + 2\sqrt{\frac{2\gamma}{\pi}} \times \\
 &\frac{e^{4i\gamma}}{\gamma^2 \beta^2 M^4 \cos^4 \theta} + \frac{2\sqrt{2\gamma} e^{2i(\gamma - \beta M^2 \cos^2 \theta)}}{(\gamma - \beta M^2 \cos^2 \theta)^2 \sqrt{\gamma + \beta M^2 \cos^2 \theta}} \left[E \sqrt{2(\gamma + \beta M^2 \cos^2 \theta)} \right] + T_L.
 \end{aligned} \tag{107}$$

The corresponding expressions for the lift and moment transfer functions for $\gamma^2 < 0$ are obtained by replacing γ by $i\gamma$ in Eqs. (106) and (107).

APPENDIX IV.

TWO-DIMENSIONAL PITCHING AND PLUNGING MOTION OF

AN AIRFOIL IN A COMPRESSIBLE STREAM

The mathematical procedure developed in the previous sections was shown to be capable of generating simple approximate expressions for the aerodynamic response functions associated with the gust encounter problem. This result might lead one to attempt to apply the same procedure to develop aerodynamic response functions for arbitrary motion of a finite lifting surface. This general three-dimensional problem cannot be analyzed exactly by the present theory because tip effects are not included. However, the present analysis can be used to examine the two-dimensional problem, and in particular, the sinusoidal pitching and plunging motion of an airfoil. The objective of this Appendix is to develop the equations for the unsteady pressure distribution associated with these motions. The resulting aerodynamic forces and moments can be computed from the zero and first order moments of the pressure distribution.

The format for the analysis to be presented in this Appendix will parallel that of the main text. First a solution valid for small values of γ (i.e., $\gamma = KM/(1-M^2)$, where $K = \omega b/U = Kb$ is the reduced frequency and ω is the circular frequency of the motion) will be derived by following the procedure developed in Appendix I. This will be followed by an analysis based on the theory in Appendix III which will be valid for large values of γ .

Solution for Small Positive Values of γ

The analysis presented in Appendix I showed that a solution for the noncirculatory flow field of order γ is given in terms of a modified velocity potential $\Phi^{(1)}$ which is a solution of Laplace's equation. This solution is given by Eq. (46) as

$$\Phi^{(1)} = \sum_{n=1}^{\infty} A_n \sin n\eta e^{-n\xi} \quad (108)$$

where the coefficients A_n are dependent on the blade motion (i.e., the A_n 's are functions of the downwash distribution). The value of these coefficients must be such that the fluid velocity normal to the surface of the airfoil is

equal to the velocity induced by the airfoil motion. The mathematical form of this boundary condition is

$$\frac{\partial \phi}{\partial x_2} = \frac{\partial h}{\partial t} + U \frac{\partial h}{\partial x} \quad -b \leq x_1 \leq b, \quad x_2 = 0 \quad (109)$$

where h is the displacement of the airfoil from the x_2 plane. The form of h for pitching motion about mid-chord is

$$h = \alpha_0 x_1 e^{-i\omega t} \quad (110)$$

while for plunging motion

$$h = h_0 e^{-i\omega t} \quad (111)$$

where the parameters α_0 and h_0 are the amplitudes of motion.

The value of the normal derivative of ϕ on the surface of the airfoil is given in terms of $\Phi^{(1)}$ by

$$\frac{\partial \phi}{\partial x_2} = \frac{\sqrt{1-M^2}}{b} \frac{1}{\sin \eta} e^{-i\beta M^2 \cos \eta} e^{-i\omega t} \left. \frac{\partial \Phi^{(1)}}{\partial \xi} \right|_{\xi=0} \quad (112)$$

where $\beta = K/1-M^2$. This result is derived from Eq. (15), by letting $\alpha = \theta = 0$ and $K U = \omega$. Thus from Eqs. (108) and (112)

$$\frac{\partial \phi}{\partial x_2} = -\frac{\sqrt{1-M^2}}{b \sin \eta} e^{-i\omega t} e^{-i\beta M^2 \cos \eta} \left\{ \sum_{n=1}^{\infty} A_n n \sin \eta \right\} \quad (113)$$

which from Eqs. (109) and (110) must be equal to $(i\omega \alpha_0 b x_1 + U \alpha_0) e^{-i\omega t}$ for pitching motion and from Eqs. (109) and (111) must be equal to $(-i\omega h_0) e^{-i\omega t}$ for

plunging motion. The coefficients A_n are evaluated by employing the orthogonality relationship described in Eq. (51) of Appendix I. The result for pitching motion can be shown to be

$$A_n^{(a)} = \frac{\alpha_0 b}{n(1-M^2)^{1/2}} \frac{i\omega b}{2} i^{n-2} \left[J_{n-2}(\beta M^2) - J_{n+2}(\beta M^2) \right] \\ + \frac{2\alpha_0 b}{(1-M^2)^{1/2}} \frac{U}{\beta M^2} i^{n-1} J_n(\beta M^2) \quad n \geq 1 \quad (114)$$

and for plunging motion the result is

$$A_n^{(h)} = \frac{2i\omega h_0 b}{(1-M^2)^{1/2}} \frac{i^{n-1}}{\beta M^2} J_n(\beta M^2) \quad n \geq 1 \quad (115)$$

The noncirculatory pressure distribution on the surface of the airfoil is derived by letting $\alpha = \theta = 0$ and $K U = \omega$ in Eq. (21) and combining the resulting expression with Eq. (108). The result is

$$p^{s(1)} = \frac{\rho_0 U}{b} \left[\frac{1}{\sin \eta} \sum_{n=1}^{\infty} A_n n \cos n \eta + i \beta \sum_{n=1}^{\infty} A_n \sin n \eta \right] e^{-i\beta M^2 \cos \eta} e^{-i\omega t} \quad (116)$$

where the coefficients A_n are defined by Eq. (114) or (115). This noncirculatory pressure distribution is unbounded at the airfoil leading and trailing edges. Only the trailing edge singularity must be removed. This is accomplished by the addition of a circulatory flow field. In Appendix I an analysis is presented which yields an expression for the circulatory pressure distribution on a swept airfoil encountering an oblique gust. The two-dimensional circulatory pressure distribution on the surface of the airfoil, obtained from the two-dimensional limit of that analysis, is

$$p^{s(2)} = \bar{p}^{(2)} e^{-i\beta M^2 \cos \eta} e^{-i\omega t} \quad (117)$$

where

$$\bar{p}^{(2)} = -\frac{\rho_0 U}{b} \frac{C}{\sin \eta} [1 + Z \cos \eta] \quad (118)$$

and where the parameter Z is defined by Eq. (71). The constant C is assigned a value which will cause $p^s(2)$ at the trailing edge to be equal in magnitude but opposite in sign to $p^s(1)$ evaluated at the trailing edge. For plunging motion the value of C can be shown to be

$$C = \frac{i\omega h_0 b}{(1-M^2)^{1/2}} [J_0(\beta M^2) + iJ_1(\beta M^2)] / (1+Z) \quad (119)$$

while for pitching motion about mid-chord

$$C = \left\{ \frac{\alpha_0 b^2 i\omega}{2(1-M)^2} [J_0(\beta M^2) - J_2(\beta M^2) + Z_0 J_1(\beta M^2)] \right. \\ \left. + \frac{\alpha_0 b U}{1-M^2} [J_0(\beta M^2) + iJ_1(\beta M^2)] \right\} / (1+Z) \quad (120)$$

The pressure distribution on the surface of the airfoil for small values of γ is obtained by combining Eqs. (116) and (117). The result is

$$p^s = \frac{\rho_0 U}{b} \left[\frac{1}{\sin \eta} \sum_{n=1}^{\infty} A_n n \cos n\eta + i\beta \sum_{n=1}^{\infty} A_n \sin n\eta \right] e^{-i\beta M^2 x_1} e^{-i\omega t} \\ - \frac{\rho_0 U}{b} \frac{C}{\sin \eta} [1 + Z \cos \eta] e^{-i\beta M^2 x_1} e^{-i\omega t} \quad (121)$$

The transfer functions associated with the unsteady motion of the airfoil are obtained by integrating the product of the pressure distribution and the appropriate weighting functions over the chord of the airfoil. For example,

the lift transfer function associated with plunging motion is dependent on the integral of the pressure distribution over the chord, and is given by the equation

$$T_L = C_L \frac{U \sqrt{1-M^2}}{2\pi \bar{U}_2} e^{i\omega t} \quad (122)$$

where

$$C_L = \int_0^\pi \frac{p^{(s)}}{\frac{1}{2} \rho_0 U^2} \sin \eta \, d\eta \quad (123)$$

and $\bar{U}_2 = -i\omega h_0$. Substituting Eq. (121) into Eq. (123) and performing the chordwise integration yields

$$\begin{aligned} C_L = & \frac{2}{U_b} \sum_{n=1}^{\infty} A_n^{(h)} n^i \pi (-i)^n J_n(\beta M^2) \\ & + \frac{2}{U_b} i\beta \sum_{n=1}^{\infty} A_n^{(h)} i^{n-1} n (-i)^n J_n(\beta M^2) \left(-\frac{\pi}{\beta M^2} \right) \\ & - \frac{2C}{U_b} \pi J_0(\beta M^2) + \frac{2C}{U_b} Z \pi i J_1(\beta M^2) \end{aligned} \quad (124)$$

which reduces to

$$\begin{aligned} C_L = & \frac{2\pi}{\sqrt{1-M^2}} \frac{(-i\omega h_0)}{U} \frac{2(-i)}{\beta M^2} \frac{1-M^2}{M^2} \sum_{n=1}^{\infty} n J_n^2(\beta M^2) e^{-i\omega t} \\ & + \frac{2\pi}{\sqrt{1-M^2}} \frac{(-i\omega h_0)}{U} \left[J_0(\beta M^2) + iZ J_1(\beta M^2) \right] \frac{[J_0(\beta M^2) + iJ_1(\beta M^2)]}{1+Z} e^{-i\omega t} \end{aligned} \quad (125)$$

when Eqs. (115) and (119) are introduced. Thus the lift transfer function for plunging motion is equal to

$$T_L = -\frac{2i}{\beta M^2} \frac{1-M^2}{M^2} \sum_{n=1}^{\infty} n J_n^2(\beta M^2) + \frac{[J_0(\beta M^2) + iZJ_1(\beta M^2)]}{1+Z} [J_0(\beta M^2) + iJ_1(\beta M^2)] \quad (126)$$

The remaining transfer functions can be derived by a similar procedure.

Solution for Large Values of γ

The analytical procedure presented in Appendix III can be used to develop the asymptotic form of the pressure distribution on a two-dimensional airfoil undergoing sinusoidal pitching or plunging motion. These expressions will approach the exact results as γ become large.

The asymptotic analysis will begin by considering the pressure field generated by a semi-infinite plate oscillating sinusoidally in a pitching or plunging motion. The solution for the modified velocity potential associated with this pressure satisfies the two-dimensional limit of Eq. (16) and the boundary condition

$$\frac{\partial \Phi}{\partial X_2} = \frac{b}{\sqrt{1-M^2}} e^{-i\beta M^2 X_1} e^{i\omega t} \left[\frac{\partial h}{\partial t} + \frac{U}{b} \frac{\partial h}{\partial X_1} \right] \quad (127)$$

on the surface of the plate. Equation (127) which is derived from Eqs. (15) and (109) is a consequence of the boundary condition requiring the fluid velocity normal to the surface of the plate to be equal to the velocity induced by the plate motion. The desired solution to the boundary value problem for Φ can be obtained from an analysis based on the Weiner-Hopf technique, the essence of which can be found on pages 48 to 98 of Ref. 13.

The pressure distribution on the surface of the plate is obtained by substituting the resulting solution for the modified potential Φ into the two-dimensional limit of Eq. (21). This procedure will yield

$$\begin{aligned}
 p^{(1)} = & \rho_0 U i \omega \alpha_0 b \left\{ -\frac{e^{i\frac{\pi}{4}}}{\sqrt{\pi}} \frac{\sqrt{1+M}}{(KM)^{3/2}} \left[\frac{iK\sqrt{X'_1}}{1+M} + \frac{1}{2\sqrt{X'_1}} \right] e^{i\frac{KM}{1+M}X'_1} \right. \\
 & - \frac{e^{i\frac{\pi}{4}}\sqrt{2}}{KM} \left[E \left[\sqrt{\frac{KM}{1+M}X'_1} \right] + \sqrt{\frac{X'_1 KM}{2\pi(1+M)}} e^{i\frac{KM}{1+M}X'_1} - iKX'_1 E \left[\sqrt{\frac{KM}{1+M}X'_1} \right] \right] \\
 & + \frac{\sqrt{2} e^{i\frac{3\pi}{4}}}{K^2 M} \left[\sqrt{\frac{KM}{2\pi(1+M)}} \frac{e^{i\frac{KM}{1+M}X'_1}}{\sqrt{X'_1}} - iK E \left[\sqrt{\frac{KM}{1+M}X'_1} \right] \right] \left. \right\} e^{-i\omega t} \quad (128) \\
 & + \rho_0 U^2 \alpha_0 \left\{ \frac{(1-i)E \left[\sqrt{\frac{KM}{1+M}X'_1} \right]}{M} + \frac{(1+i)}{\sqrt{KM(1+M)}} \frac{e^{i\frac{MK}{1+M}X'_1}}{\sqrt{2\pi X'_1}} \right\} e^{-i\omega t} \\
 & \qquad \qquad \qquad X'_1 \geq 0
 \end{aligned}$$

for pitching motion about the leading edge (i.e., $h = \alpha_0 b X'_1 e^{-i\omega t}$ $X'_1 \geq 0$) and

$$p^{(1)} = \rho_0 U (-i\omega h_0) \left\{ \frac{(1-i)E \left[\sqrt{\frac{KM}{1+M}X'_1} \right]}{M} + \frac{(1+i)}{\sqrt{KM(1+M)}} \frac{e^{i\frac{KM}{1+M}X'_1}}{\sqrt{2\pi X'_1}} \right\} e^{-i\omega t} \quad (129)$$

for plunging motion (i.e., $h = h_0 e^{-i\omega t}$). As was shown in Appendix III the unsteady pressure distribution on a semi-infinite plate approximates the pressure distribution in the neighborhood of the leading edge of an airfoil at high frequencies. These approximations (i.e., Eqs. (128) and (129)) may be extended to include the trailing edge region of an airfoil by combining the pressure field $p^{(1)}$ with a field $p^{(2)}$ which is equal in magnitude but opposite in sign to $p^{(1)}$ downstream of the trailing edge (i.e., $X_1 \geq 2$, $X_2 = 0$) and has its normal gradient vanishing upstream of the trailing edge (i.e., $X_2 \leq 2$, $X_2 = 0$). The solution for such a pressure field can be obtained by following the procedure used in Appendix III. In that analysis an acceleration potential H is defined which is related to $p^{(2)}$ by the two-dimensional limit of Eq. (93)

$$p^{(2)} = \rho_0 H e^{-i[\beta M^2 \bar{X}'_1 + \omega t]} \quad (130)$$

where $\bar{X}_1' = X_1' - 2$. Downstream of the trailing edge of the airfoil (i.e., $X_1' \geq 0, X_2' = 0$) the value of $p^{(2)}$ is specified to be equal to the negative of $p^{(1)}$. Thus H must equal

$$H = -\frac{p^{(1)}}{\rho_0} e^{i[\beta M^2 \bar{X}_1' + \omega t]} \quad (131)$$

on the boundary $\bar{X}_1' \geq 0, X_2' = 0$. The value of H on the upstream boundary $\bar{X}_1' \leq 0, X_2' = 0$ is given by Eq. (96) as

$$H = \frac{\pi^{-3/2}}{2} e^{\frac{3i\pi}{4}} \left\{ \int_0^\infty M(u, \bar{X}_1', 0) e^{i\gamma u} du \times \frac{d}{dU} \int_0^\infty \xi^{-1/2} e^{i\gamma(U+\xi)} f(U+\xi) d\xi \right\} \quad (132)$$

$$\bar{X}_1' \leq 0, X_2' = 0$$

where the function $M(u, \bar{X}_1', 0)$ is defined by Eq. (97) and

$$f(\bar{X}_1') = H \quad \bar{X}_1' \geq 0, X_2' = 0 \quad (133)$$

For large values of γ the function f may be approximated by the asymptotic form of H. This asymptotic expression is obtained by combining Eq. (131) with the asymptotic form of Eqs. (128) or (129). The result will be of the form

$$H \approx g_1(\bar{X}_1') e^{i\delta_1 \bar{X}_1'} + g_2(\bar{X}_1') e^{i\delta_2 \bar{X}_1'} \quad (134)$$

where

$$g_1(\bar{X}_1') = -\frac{U i \omega a_0 b}{M} (\bar{X}_1' + 2) + \frac{U^2 a_0}{M} \quad (135)$$

$$g_2(\bar{X}'_1) = \left[U i \omega a_0 b \left\{ \frac{(1-i)(1-M)}{(KM)^{3/2} 2\sqrt{1+M}} \frac{1}{\sqrt{2\pi(2+\bar{X}'_1)}} + \frac{2(1+i)\sqrt{2+\bar{X}'_1}}{M\sqrt{2\pi KM(1+M)}} \right\} - U^2 a_0 \left\{ \frac{1+i}{M\sqrt{2\pi KM(1+M)}} \frac{1}{\sqrt{2+\bar{X}'_1}} \right\} \right] e^{\frac{2iKM}{1+M}} \quad (136)$$

and

$$\delta_1 = \frac{KM^2}{1-M^2}, \quad \delta_2 = \frac{KM}{1-M^2} \quad (137)$$

for pitching motion about the leading edge. For plunging motion Eqs. (135) through (137) are replaced by

$$g_1(\bar{X}'_1) = -\frac{U i \omega h_0}{M} \quad (138)$$

$$g_2(\bar{X}'_1) = -\frac{U(1-i)\omega h_0}{\sqrt{2\pi KM}} \frac{e^{\frac{2iKM}{1+M}}}{\sqrt{2+\bar{X}'_1}} \frac{1}{M\sqrt{1+M}} \quad (139)$$

$$\delta_1 = \frac{KM^2}{1-M^2}, \quad \delta_2 = \frac{KM}{1-M^2} \quad (140)$$

Substituting Eq. (134) into Eq. (133) and combining the result with Eq. (132) yields

$$H \approx \frac{1}{2} \pi^{-3/2} e^{3i\pi/4} \left\{ \int_0^\infty M(U, X'_1, 0) e^{-i\gamma U} dU \times \frac{d}{dU} \int_0^\infty \xi^{-1/2} e^{-i\gamma(U+\xi)} [g_1(U+\xi) e^{i\delta_1(U+\xi)} + g_2(U+\xi) e^{i\delta_2(U+\xi)}] d\xi \right\} \quad (141)$$

The evaluation of the integrals in Eq. (141) can again be performed by the method of stationary phase (Ref. 14), which yields

$$H \approx (1-i) \left\{ e^{i\delta_1 \bar{x}_1'} g_1(0) \left[\frac{1+i}{2} - E \left[\sqrt{-(\gamma + \delta_1) \bar{x}_1'} \right] \right] + e^{i\delta_2 \bar{x}_1'} g_2(0) \left[\frac{1+i}{2} - E \left[\sqrt{-(\gamma + \delta_2) \bar{x}_1'} \right] \right] \right\} \quad (142)$$

$$\bar{x}_1' \leq 0, \quad x_2 = 0$$

Thus from Eq. (130) the pressure distribution upstream of the trailing edge (i.e., $\bar{x}_1' \leq 0, x_2 = 0$) is equal to

$$p^{(2)} = \rho_0 \left\{ e^{i\delta_1 \bar{x}_1'} g_1(0) \left[\frac{1+i}{2} - E \left[\sqrt{-(\gamma + \delta_1) \bar{x}_1'} \right] \right] + e^{i\delta_2 \bar{x}_1'} g_2(0) \left[\frac{1+i}{2} - E \left[\sqrt{-(\gamma + \delta_2) \bar{x}_1'} \right] \right] \right\} e^{-i[\beta M^2 \bar{x}_1' + \omega t]} \quad (143)$$

where the functions g_1 and g_2 are defined by Eqs. (135) and (136) for pitching motion and by Eqs. (138) and (139) for plunging motion. The parameters δ_1 and δ_2 are defined by Eqs. (137) or (140).

The addition of the pressure field $p^{(2)}$ to $p^{(1)}$ yields the asymptotic form of the pressure distribution p^s on an oscillating two-dimensional airfoil in a compressible stream. The integral of the zero and the first order moment of this pressure distribution over the chord of the airfoil will yield the asymptotic forms of the unsteady lift and moment.

Limiting Behavior as $K \rightarrow \infty, M \neq 0$

The limiting form attained by the pressure distribution p^s as the reduced frequency approaches infinity can be obtained by expanding the pressure distributions $p^{(1)}$ and $p^{(2)}$ in a power series of $K^{-1/2}$. The result can be

shown to be dependent on the limiting form of $p^{(1)}$, which is

$$p^s \approx p^{(1)} \approx \rho_0 a [-i\omega\alpha_0 b x'_1 + U\alpha_0] e^{-i\omega t} \quad 0 < x'_1 < 2 \quad (144)$$

for pitching motion about the leading edge and

$$p^s \approx p^{(1)} \approx \rho_0 a [-i\omega h_0] e^{-i\omega t} \quad 0 < x'_1 < 2 \quad (145)$$

for plunging motion. Equations (144) and (145) are precisely the results predicted by piston theory (cf. Ref. 9) for pitching and plunging motion. This result is to be expected, since piston theory may be used to predict the pressure distribution on an oscillating airfoil in a subsonic stream if the product of reduced frequency and Mach number is large. The agreement between the limiting form of Eq. (142) or (143) and the results predicted by piston theory for pitching or plunging motion appears to be in conflict with the poor correlation between the two-dimensional limit of Eq. (36) and the result predicted by piston theory for the gust encounter problem. This apparent discrepancy can easily be resolved by recalling that piston theory is only applicable to problems in which the local acceleration of the downwash distribution is much greater than the convected acceleration which is the case for the airfoil motion described above at high reduced frequency. For the gust encounter problem the local acceleration and the convected acceleration of the downwash distribution are equal.

APPENDIX V

NONPERIODIC TIME DEPENDENT PROBLEMS

The objective of this analysis is to discuss the mathematical procedure by which the analysis presented in the main text can be extended to predict the unsteady airloads on an infinite swept airfoil encountering a nonperiodic gust. The downwash distribution resulting from the encounter of an infinite swept airfoil with a one-dimensional oblique gust is of the general form

$$U_2^I = f[r - U \cos(\theta - \alpha)t] \quad x_2 = 0, \quad -b \leq x_1 \leq b \quad (146)$$

where

$$r = x_1 \cos \alpha + x_3 \sin \alpha \quad (147)$$

This velocity field is convected at a speed of $U \cos(\theta - \alpha)$ in the r direction. The analysis in this Appendix assumes the existence of the Fourier transform in time of Eq. (146). This transform is defined as

$$\hat{U}_2^I = \frac{1}{\sqrt{2\pi}} \int_{-\infty}^{\infty} U_2^I e^{i\omega t} dt \quad (148)$$

while its inverse is defined to be

$$U_2^I = \frac{1}{\sqrt{2\pi}} \int_{-\infty}^{\infty} \hat{U}_2^I e^{-i\omega t} \alpha \omega \quad (149)$$

The explicit form of the Fourier transform of Eq. (146) is obtained by substituting Eq. (147) into Eq. (148). The resulting integral may be evaluated by replacing the integration variable t with τ^* where $\tau^* = t - \frac{r}{U \cos(\theta - \alpha)}$,

yielding

$$\hat{U}_2^I = e^{\frac{i\omega r}{U \cos(\theta-\alpha)}} \hat{f}(\omega) \quad -b \leq x_1 \leq b, \quad x_2 = 0 \quad (150)$$

where

$$\hat{f}(\omega) = \frac{1}{\sqrt{2\pi}} \int_{-\infty}^{\infty} f(\tau) e^{i\omega\tau^*} d\tau^* \quad (151)$$

The spatial dependence of Eq. (150) is identical to that for a one-dimensional sinusoidal gust (i.e., Eq. (10)). The remaining equations to be transformed are Eq. (7) for the pressure field and Eq. (8) for velocity potential. These equations are transformed by multiplying each term by $\frac{1}{\sqrt{2\pi}} e^{i\omega t}$ and integrating the result with respect to time from minus to plus infinity. This procedure leads to the result

$$\hat{p}^S = -\rho_0 \left[-i\omega \hat{\phi} + U \cos \theta \frac{\partial \hat{\phi}}{\partial x_1} + U \sin \theta \frac{\partial \hat{\phi}}{\partial x_3} \right] \quad (152)$$

for the Fourier transform of Eq. (7) and

$$\begin{aligned} & a^2 \left(\nabla^2 \hat{\phi} - M^2 \cos^2 \theta \frac{\partial^2 \hat{\phi}}{\partial x_1^2} - M^2 \sin^2 \theta \frac{\partial^2 \hat{\phi}}{\partial x_3^2} \right) \\ & - 2a^2 \left(-\frac{M \cos \theta}{a} i\omega \frac{\partial \hat{\phi}}{\partial x_1} - \frac{M \sin \theta}{a} i\omega \frac{\partial \hat{\phi}}{\partial x_3} + M^2 \cos \theta \sin \theta \frac{\partial^2 \hat{\phi}}{\partial x_1 \partial x_3} \right) + \frac{\omega^2}{a^2} \hat{\phi} = 0 \end{aligned} \quad (153)$$

for the Fourier transform of Eq. (8). Equation (153) can be reduced to the Helmholtz equation (i.e., Eq. (16)) for a modified velocity potential Φ . This transformation is accomplished by introducing dimensionless coordinates

(i.e., Eqs. (11), (12), and (13)) and the following form for $\hat{\phi}$

$$\hat{\phi} = \hat{\Phi}(X_1, X_2) e^{i \left[-\beta M^2 \cos \theta X_1 + \frac{\bar{K} b \sin \alpha X_3}{(1 - M^2 \cos^2 \theta)^{1/2}} \right]} \quad (154)$$

into Eq. (153) which yields

$$\frac{\partial^2 \hat{\Phi}}{\partial X_1^2} + \frac{\partial^2 \hat{\Phi}}{\partial X_2^2} + \gamma^2 \hat{\Phi} = 0 \quad (155)$$

The variables β and γ which appear in Eqs. (154) and (155) are defined by Eqs. (14) and (17) of the main text while the variable \bar{K} is related to ω by the equation

$$\bar{K} = \frac{\omega}{U \cos(\theta - \alpha)} \quad (156)$$

The boundary conditions for $\hat{\phi}$ can be explicitly expressed in terms of $\hat{\Phi}$ and its spatial derivatives. The transformation of the downwash boundary condition, Eq. (9), is

$$\frac{\partial \hat{\phi}}{\partial X_2} = -\hat{U}_2^i \quad X_2 = 0, \quad -b \leq X_1 \leq b \quad (157)$$

which, when combined with Eqs. (149) and (152), yields

$$\frac{\partial \hat{\Phi}}{\partial X_2} = -\frac{b}{\sqrt{1 - M^2 \cos^2 \theta}} \hat{f}(\omega) e^{i\beta X_1} \quad -1 \leq X_1 \leq 1, \quad X_2 = 0 \quad (158)$$

The transformation of the Kutta-Joukowski condition requires \hat{p}^s to vanish downstream of the trailing edge of the airfoil. The mathematical form of

this condition is obtained by combining Eqs. (152) and (154), yielding

$$\hat{p}^S = -\rho_0 \frac{U \cos \theta}{b} \left[\frac{\partial \hat{\Phi}}{\partial x_1} - i\beta \hat{\Phi} \right] e^{-i\beta M^2 \cos^2 \theta x_1 + \frac{i\bar{k} b \sin \alpha x_3}{(1-M^2 \cos^2 \theta)^{1/2}}} = 0 \quad (159)$$

$$x_1 = 1, \quad x_2 = 0$$

The field equation (155) and the boundary conditions in Eqs. (158) and (159) form a boundary value problem for $\hat{\Phi}$ which is identical to that for the sinusoidal gust discussed in the main body of text. Thus, the solution for the modified velocity potential associated with the sinusoidal gust problem can be used in conjunction with Eqs. (152) and (154) to predict the Fourier transform of the pressure distribution p^S on the surface of the airfoil. The integrals of the zero and first order moments of the Fourier transform of the pressure coefficient induced by the gust are equal to

$$\hat{C}_L = \left\{ \frac{2\pi \hat{f} \cos \theta}{U \sqrt{1-M^2 \cos^2 \theta}} \right\} T_L e^{i[\bar{k} \sin \alpha x_3]} \quad (160)$$

and

$$\hat{C}_M = \left\{ \frac{\pi \hat{f} \cos \theta}{2U \sqrt{1-M^2 \cos^2 \theta}} \right\} T_M e^{i[\bar{k} \sin \alpha x_3]} \quad (161)$$

which are the Fourier transforms of the lift and moment coefficients. The functional forms for the variables T_L and T_M are defined in the main text. Finally the lift and moment coefficients resulting from the encounter of the airfoil with the gust are obtained by inverting the Fourier transforms, Eqs. (160) and (161), yielding the results

(162)

$$C_L [x_3 \sin \alpha - U \cos(\theta - \alpha)t] = \frac{\sqrt{2\pi} \cos \theta \cos(\theta - \alpha)}{\sqrt{1-M^2 \cos^2 \theta}} \int_{-\infty}^{\infty} \hat{f} T_L e^{i\bar{k} [x_3 \sin \alpha - U \cos(\theta - \alpha)t]} d\bar{k}$$

and

(163)

$$C_M [X_3 \sin \alpha - U \cos(\theta - \alpha)t] = \frac{\sqrt{2\pi}}{4} \frac{\cos \theta \cos(\theta - \alpha)}{\sqrt{1 - M^2 \cos^2 \theta}} \int_{-\infty}^{\infty} \hat{f}_M e^{i\bar{k} [X_3 \sin \alpha - U \cos(\theta - \alpha)t]} d\bar{k}$$

A typical application of the analysis in this Appendix is to the problem of predicting the unsteady air loads generated by a helicopter rotor blade encountering a tip vortex from a previous blade. This problem can be analyzed by considering the interaction between an infinite swept airfoil and a two-dimensional rectilinear vortex which has an induced downwash field given by

$$U_2^I = - \frac{\Gamma [r - U \cos(\theta - \alpha)t]}{2\pi \left\{ [r - U \cos(\theta - \alpha)t]^2 + h^2 \right\}} \quad (164)$$

where h is the vertical position of the vortex beneath the X_1, X_2 plane and Γ is the strength of the vortex. The Fourier transform of Eq. (164) is

$$\hat{U}_2^I = \text{sgn}(\bar{k}) \sqrt{\frac{\pi}{2}} \frac{i\Gamma/2\pi e^{i\bar{k}r}}{U \cos(\theta - \alpha)} e^{-|\bar{k}|h} \quad (165)$$

Thus from Eq. (150)

$$\hat{f}(k) = \text{sgn}(\bar{k}) \sqrt{\frac{\pi}{2}} \frac{i\Gamma/2\pi e^{-|\bar{k}|h}}{U \cos(\theta - \alpha)} \quad (166)$$

Introducing Eq. (166) into Eqs. (162) and (163) yields

$$C_L = \frac{\Gamma \cos \theta i}{2U \sqrt{1 - M^2 \cos^2 \theta}} \int_{-\infty}^{\infty} \text{sgn}(\bar{k}) e^{-|\bar{k}|h} \frac{i\bar{k} [X_3 \sin \alpha - U \cos(\theta - \alpha)t]}{T_M e} d\bar{k} \quad (167)$$

for the lift coefficient and

$$C_M = \frac{\Gamma \cos \theta i}{8U \sqrt{1 - M^2 \cos^2 \theta}} \int_{-\infty}^{\infty} \text{sgn}(\bar{k}) e^{-|\bar{k}|h} T_M e^{i\bar{k} [x_3 \sin \alpha - U \cos(\theta - \alpha)t]} d\bar{k} \quad (168)$$

for the moment coefficient. Numerical results for the lift or moment coefficient can be obtained by introducing the appropriate transfer function into these equations and integrating the resulting expression numerically. This procedure has been used to obtain the results presented in the main text.

APPENDIX VI

COMPUTER FLOW DIAGRAM FOR COMPUTING THE AIRLOADS GENERATED

BY THE ENCOUNTER OF A HELICOPTER ROTOR BLADE WITH A TIP VORTEX

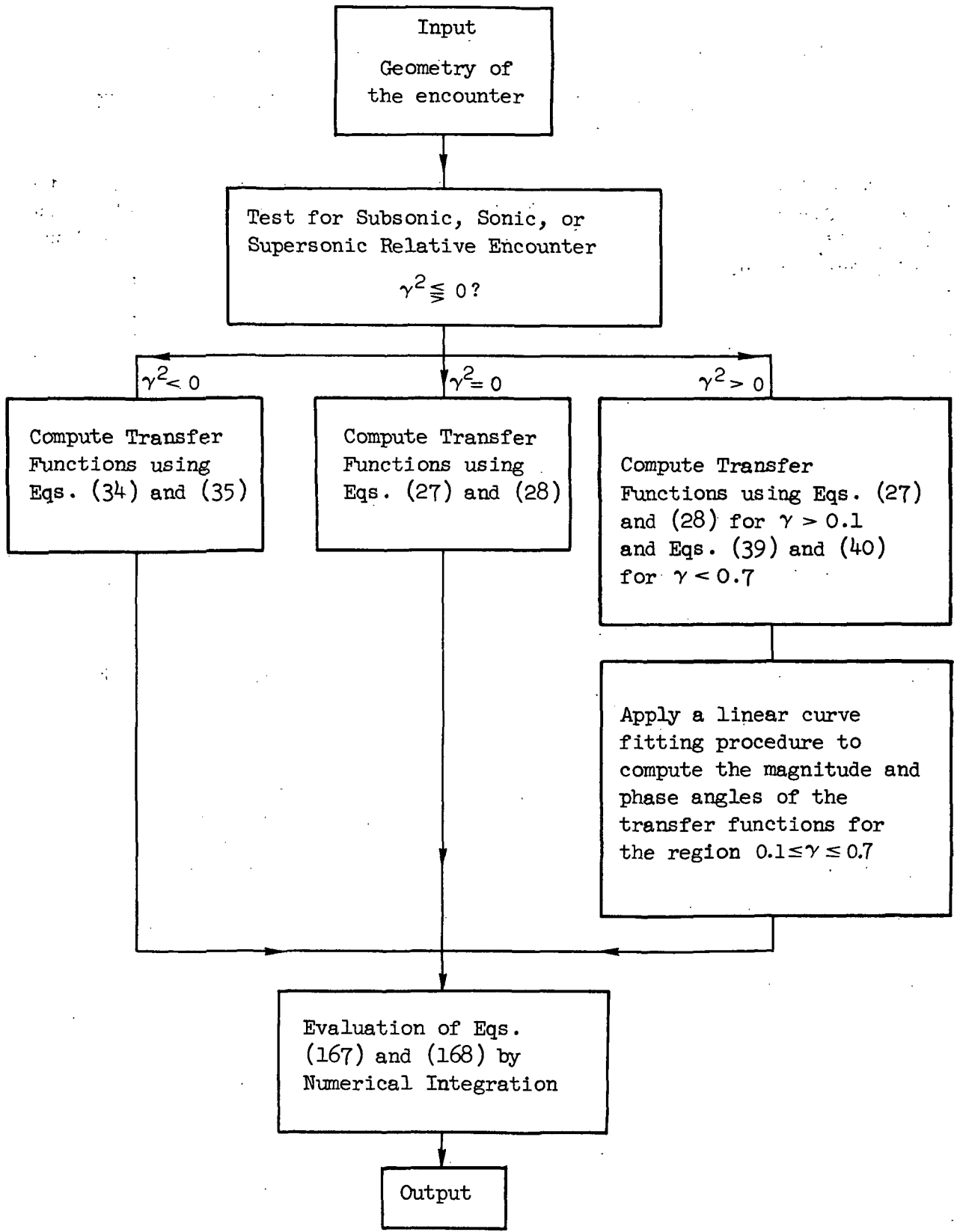
The flow diagram for the computer program that was developed to predict the aerodynamic loads generated by the encounter of a helicopter rotor blade with a tip vortex is presented in this Appendix, along with a list of input and output variables.

Input Variables

1. Azimuth position at which the encounter occurs.
2. Advance ratio.
3. Rotational tip Mach number.
4. Angle of encounter.
5. Rotor blade semi-chord.
6. Vertical displacement of the vortex beneath the plane of the rotor.
7. Radial position at which the encounter occurs.

Output Variables

1. Mach number at the position at which the encounter occurs.
2. Sweep angle.
3. Time history of the normalized lift coefficient.
4. Time history of the normalized moment coefficient.



REFERENCES

1. Küssner, H. G.: "Zusammenfassender Bericht über den 1stationären Augtrieb von Flügeln" Luftfahrtforsch., Bd. 13, Nr. 12, December 1936.
2. Sears, W. R.: "Some Aspects of Non-Stationary Airfoil Theory and Its Practical Application" J. Aero. Sci., 8, pp.104-108, 1941.
3. Curle, N.: "The Influence of Solid Boundaries Upon Aerodynamic Sound." Proc. Roy. Soc. A, 231, pg. 505, 1955.
4. Filotas, L. T.: "Response of an Infinite Wing to an Oblique Sinusoidal Gust." Basic Aerodynamic Noise Research, NASA SP-207, pp. 231-246, 1969.
5. Graham, J. M. R.: "Similarity Rules for Thin Aerofoils in Non-Stationary Subsonic Flows." J. of Fluid Mechs., Vol. 43, 1970, pg. 753.
6. Adamczyk, J. J.: "Passage of an Isolated Airfoil Through a Three-Dimensional Disturbance." Ph.D. Thesis, U. of Conn., May 1971.
7. Adamczyk, J. J. and R. S. Brand: "Scattering of Sound by an Aerofoil of Finite Span in a Compressible Stream." J. of Sound and Vib., Vol. 25, 1972, pp. 139-156.
8. Johnson, W.: "A Lifting Surface Solution for Vortex Induced Airloads and Its Application to Rotor Wing Airloads Calculations." Sc. D. Thesis, M.I.T., May 1970.
9. Bisplinghoff, R. L., H. Ashley and R. L. Halfman: "Aeroelasticity." Addison-Wesley Publishing Company, Inc., Reading, Mass., 1955.
10. Morse, P. M. and K. U. Ingard: "Theoretical Acoustics." McGraw-Hill Book Company, New York, 1968.
11. Commerford, G. L. and F. O. Carta: "An Exploratory Investigation of the Unsteady Aerodynamic Response of a Two-Dimensional Airfoil at High Reduced Frequency." Presented at the A.I.A.A. Dynamics Specialists Conference, Williamsburg, Virginia, March 19-20, 1973, A.I.A.A. Paper No. 73-309.
12. Landgrebe, A. J. and E. D. Bellinger: "An Investigation of the Quantitative Applicability of Model Helicopter Rotor Wake Patterns Obtained from a Water Tunnel." U. S. Army Air Mobility Research and Development Laboratory, Fort Eustis, Virginia. USAAMRDL Tech. Report 71-69, Dec. 1971.

13. Noble, B.: "Methods Based on the Weiner-Hopf Technique for the Solution of Partial Differential Equations." Pergamon Press, Inc., New York, 1958.
14. Carrier, G. F., M. Krook and C. E. Pearson: "Functions of a Complex Variable." McGraw-Hill Book Company, New York, 1966.

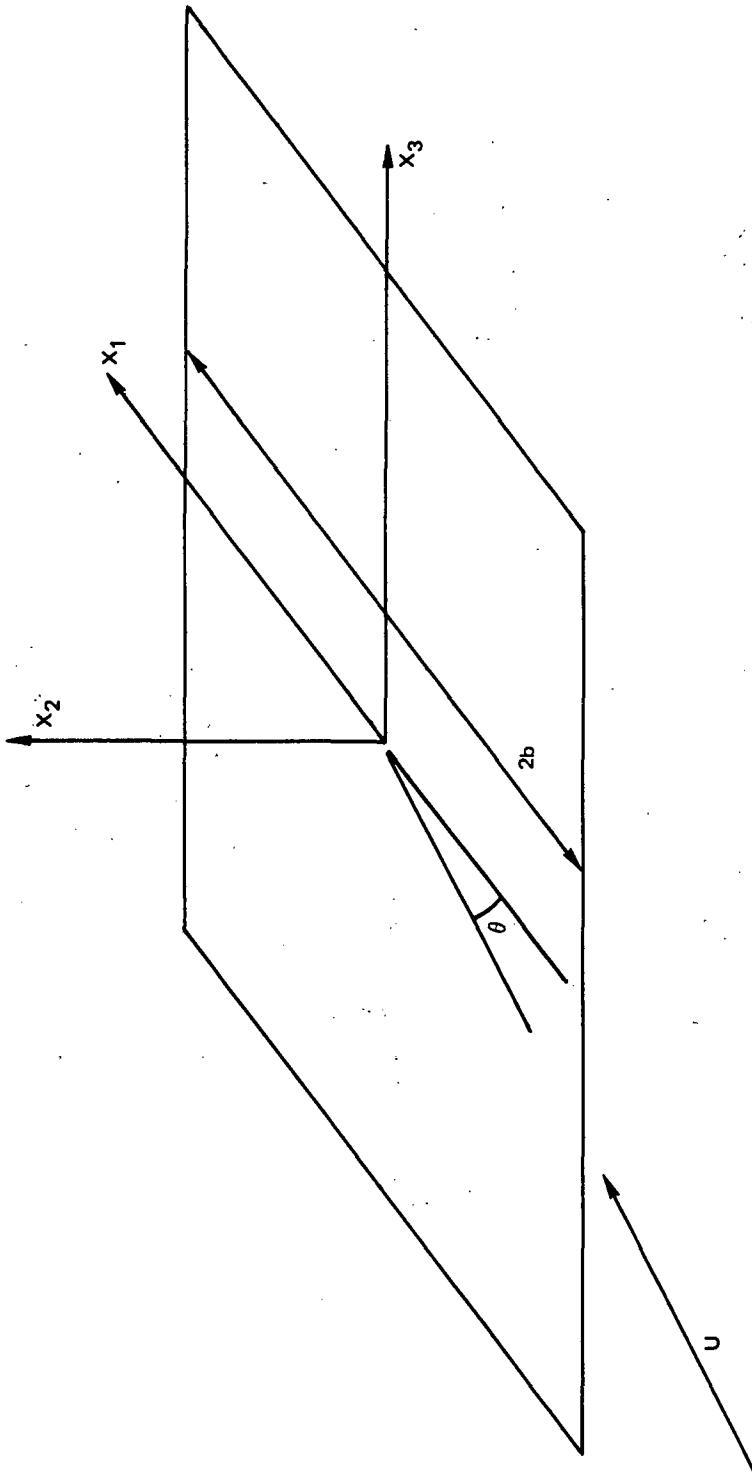


FIGURE 1. COORDINATE SYSTEM GEOMETRY

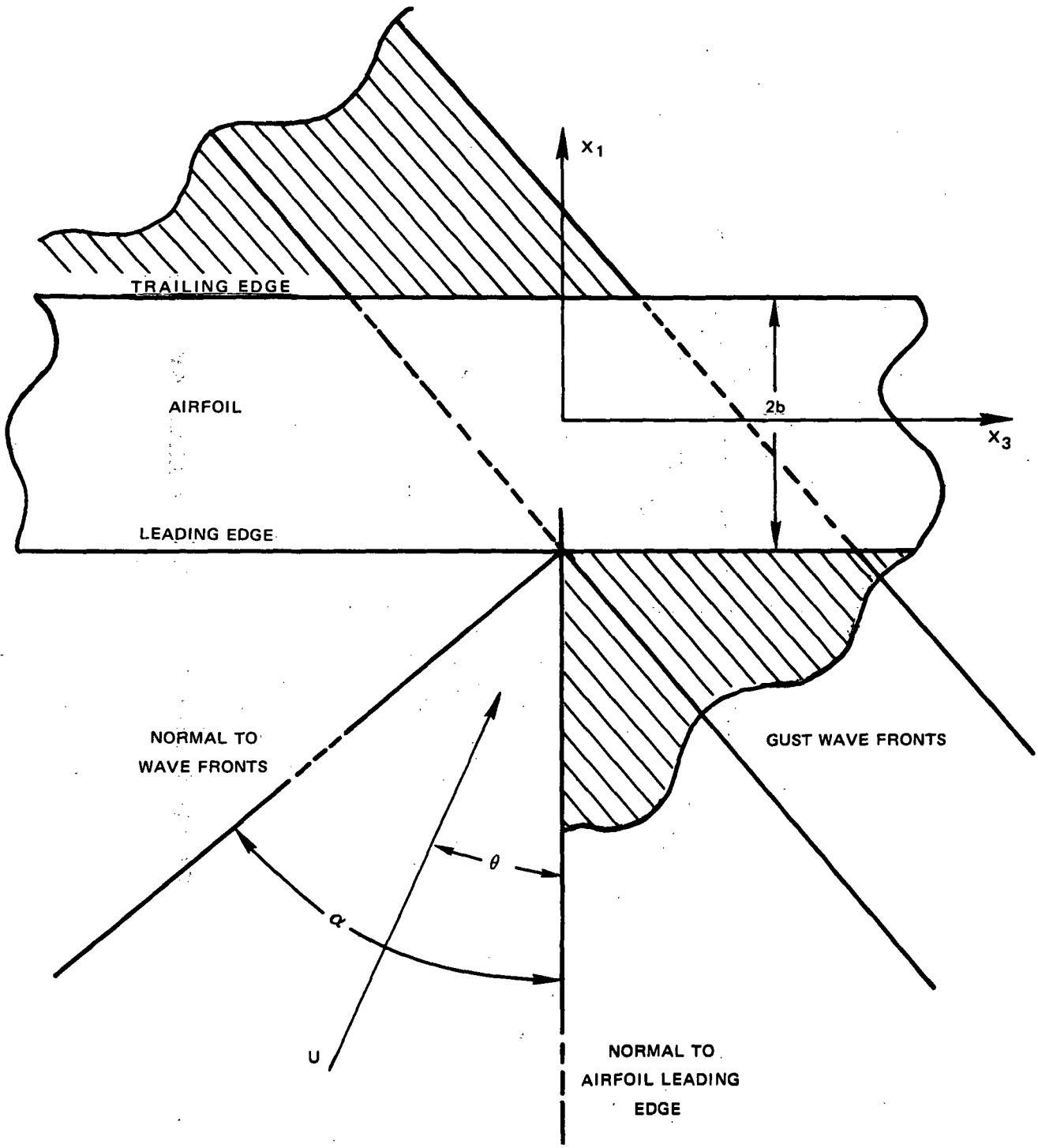


FIGURE 2. GEOMETRY OF THE ENCOUNTER

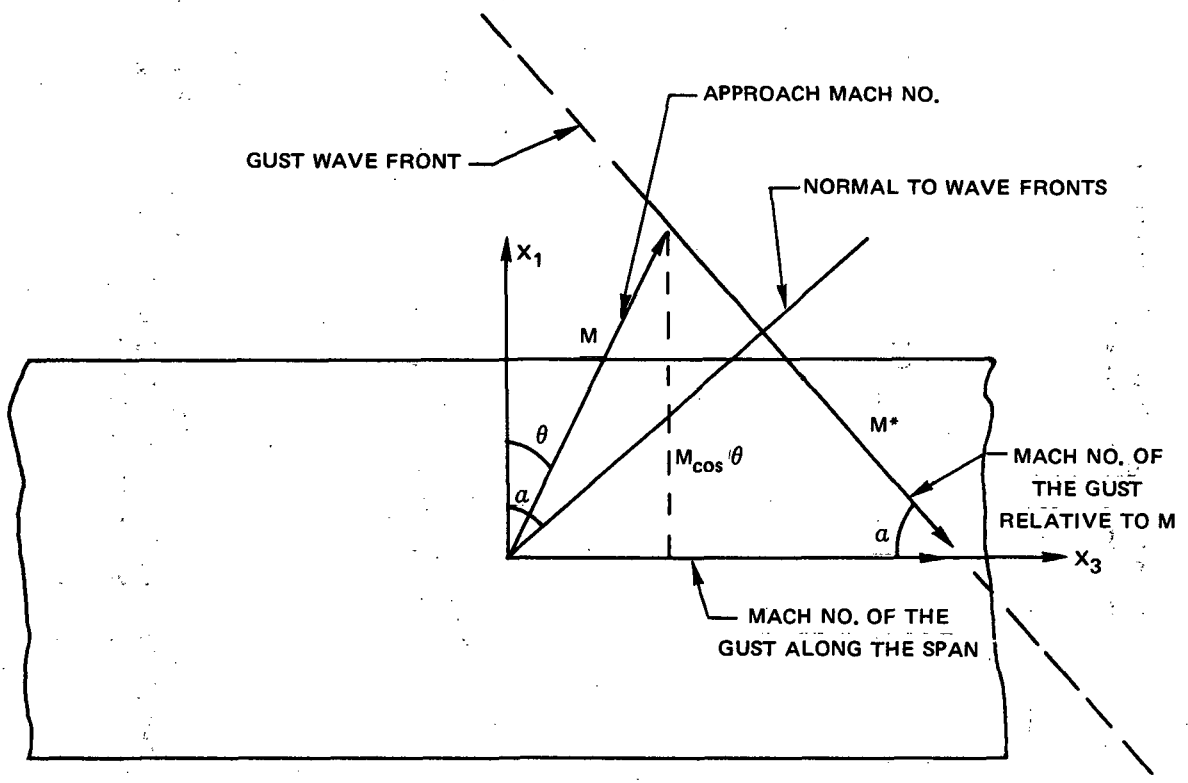


FIGURE 3. GEOMETRY DEFINING THE RELATIVE MACH NUMBER M^*

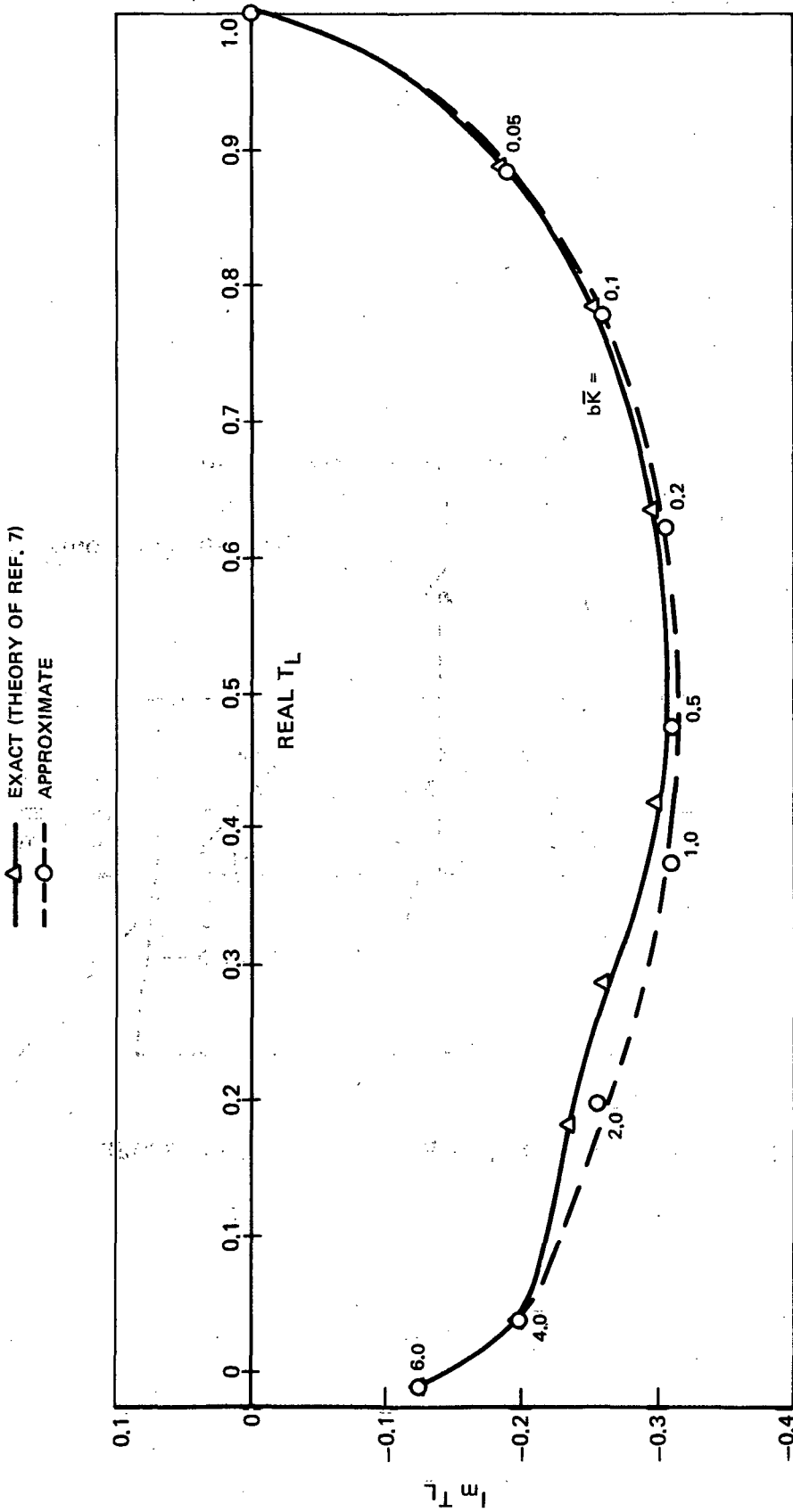




FIGURE 4. A COMPARISON BETWEEN EXACT AND APPROXIMATE EXPRESSIONS FOR THE LIFT TRANSFER FUNCTION FOR $\gamma > 0^\circ$ AND MACH NUMBER 0.3

 EXACT (THEORY OF REF. 7)
 APPROXIMATE

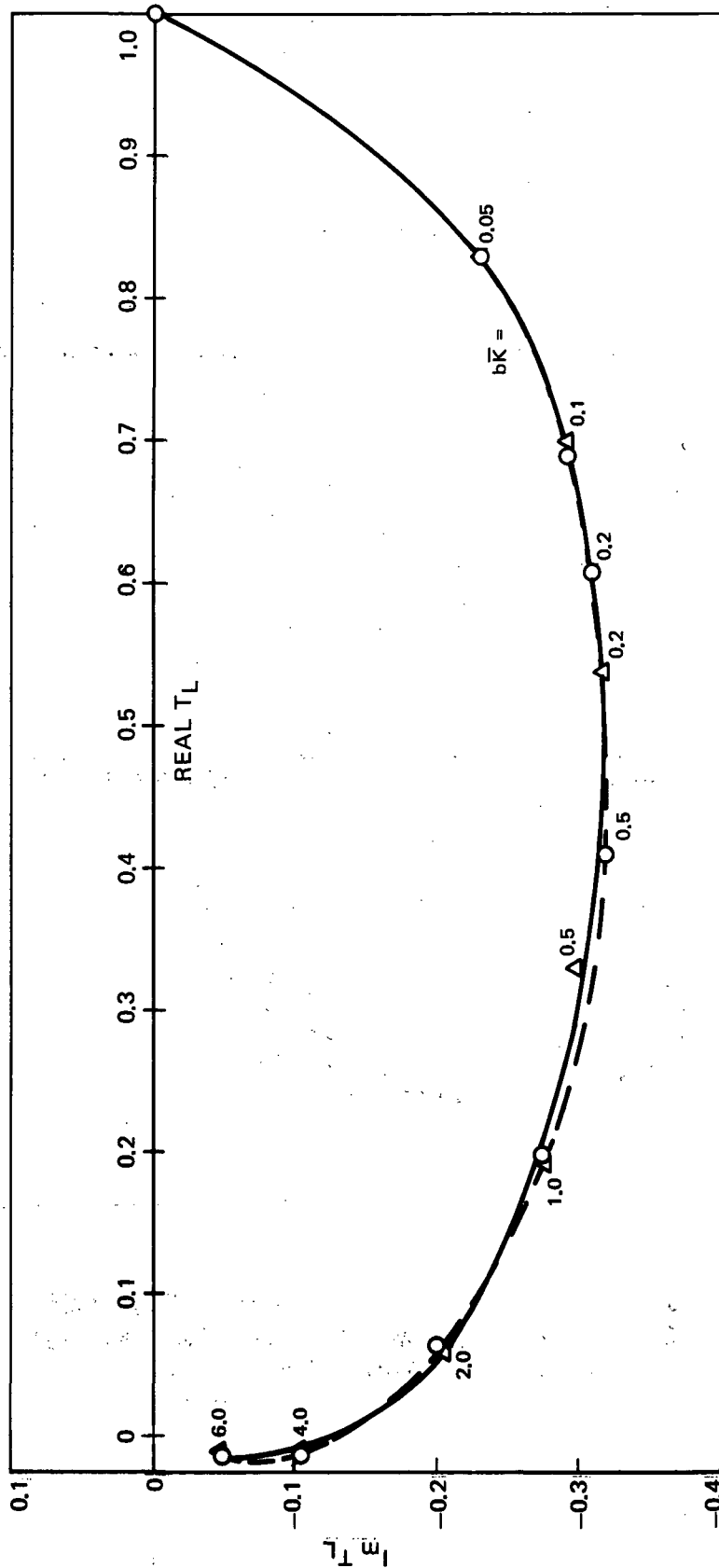


FIGURE 5. A COMPARISON BETWEEN EXACT AND APPROXIMATE
 EXPRESSIONS FOR THE LIFT TRANSFER FUNCTION
 FOR $\gamma > 0$ AND MACH NUMBER 0.6

—△— EXACT (THEORY OF REF. 7)
 - - - ○ - - - APPROXIMATE

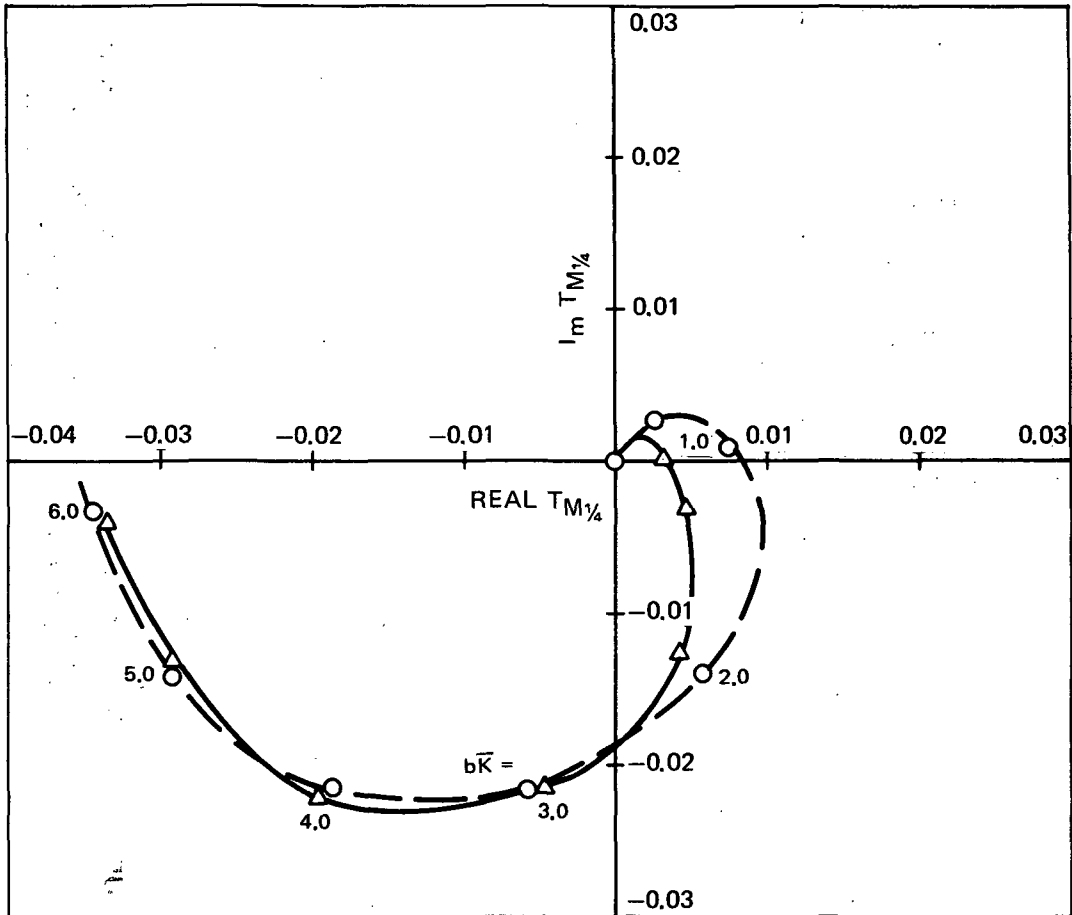


FIGURE 6. A COMPARISON BETWEEN EXACT AND APPROXIMATE EXPRESSIONS FOR THE MOMENT TRANSFER FUNCTION FOR $\gamma > 0$ AND MACH NUMBER 0.3

—△— EXACT (THEORY OF REF. 7)
 - -○- - APPROXIMATE

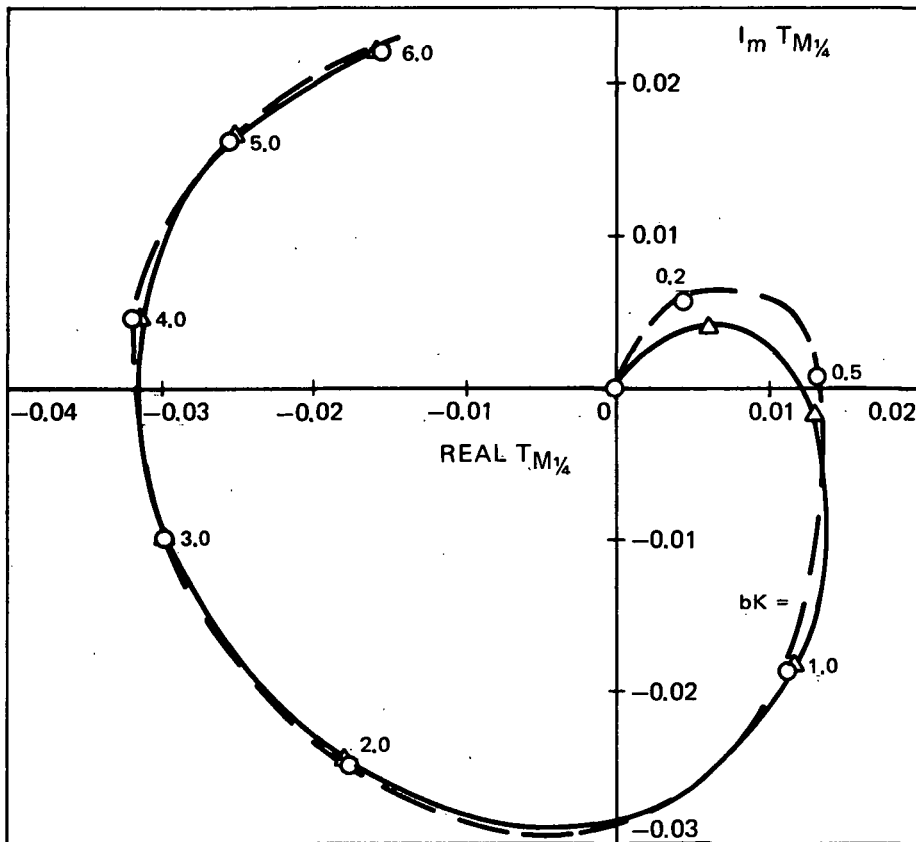


FIGURE 7. A COMPARISON BETWEEN EXACT AND APPROXIMATE EXPRESSIONS FOR THE MOMENT TRANSFER FUNCTION FOR $\gamma > 0$ AND MACH NUMBER 0.6

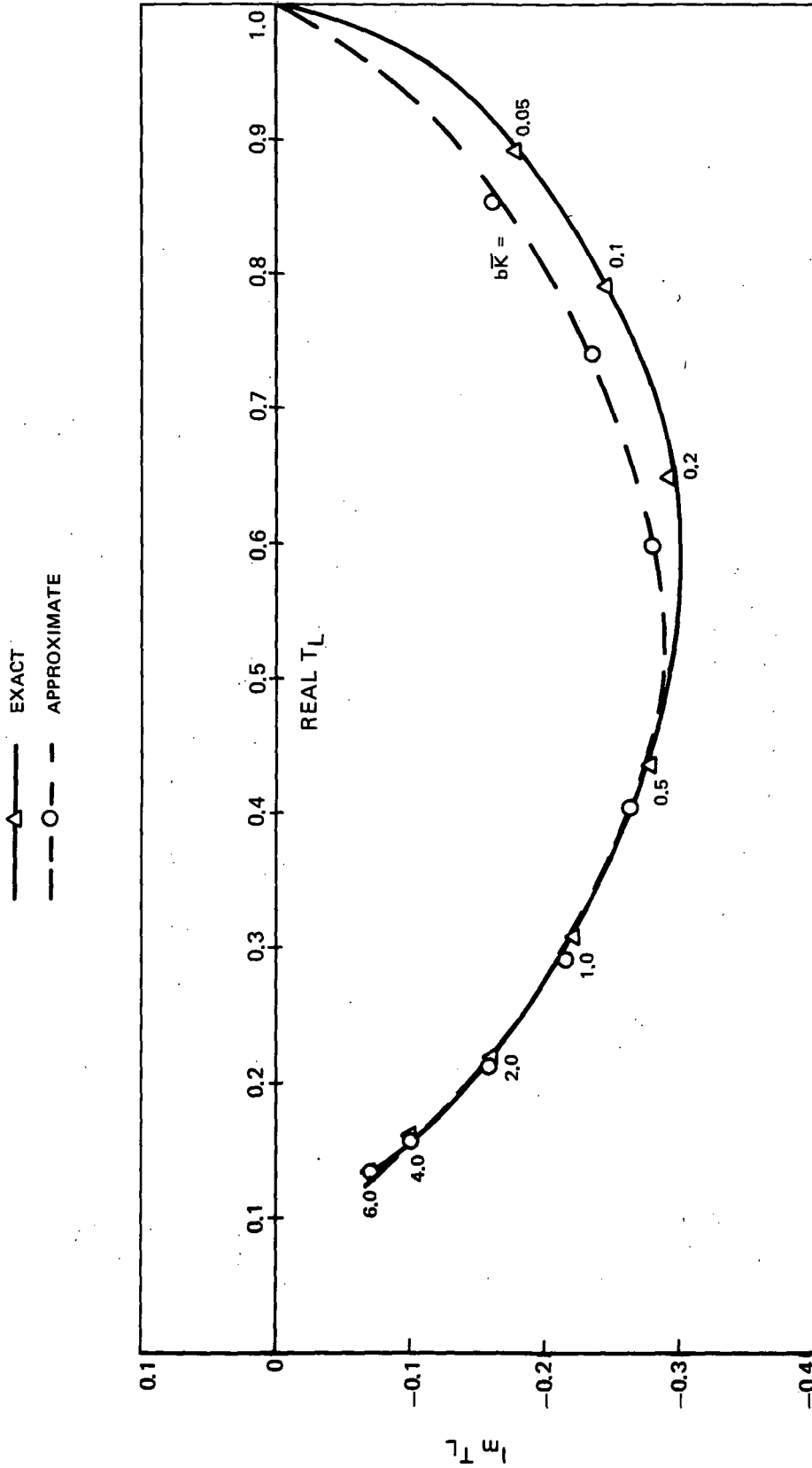


FIGURE 8. A COMPARISON BETWEEN EXACT AND APPROXIMATE EXPRESSIONS FOR THE LIFT TRANSFER FUNCTION FOR $\gamma = 0$ AND MACH NUMBER 0.3

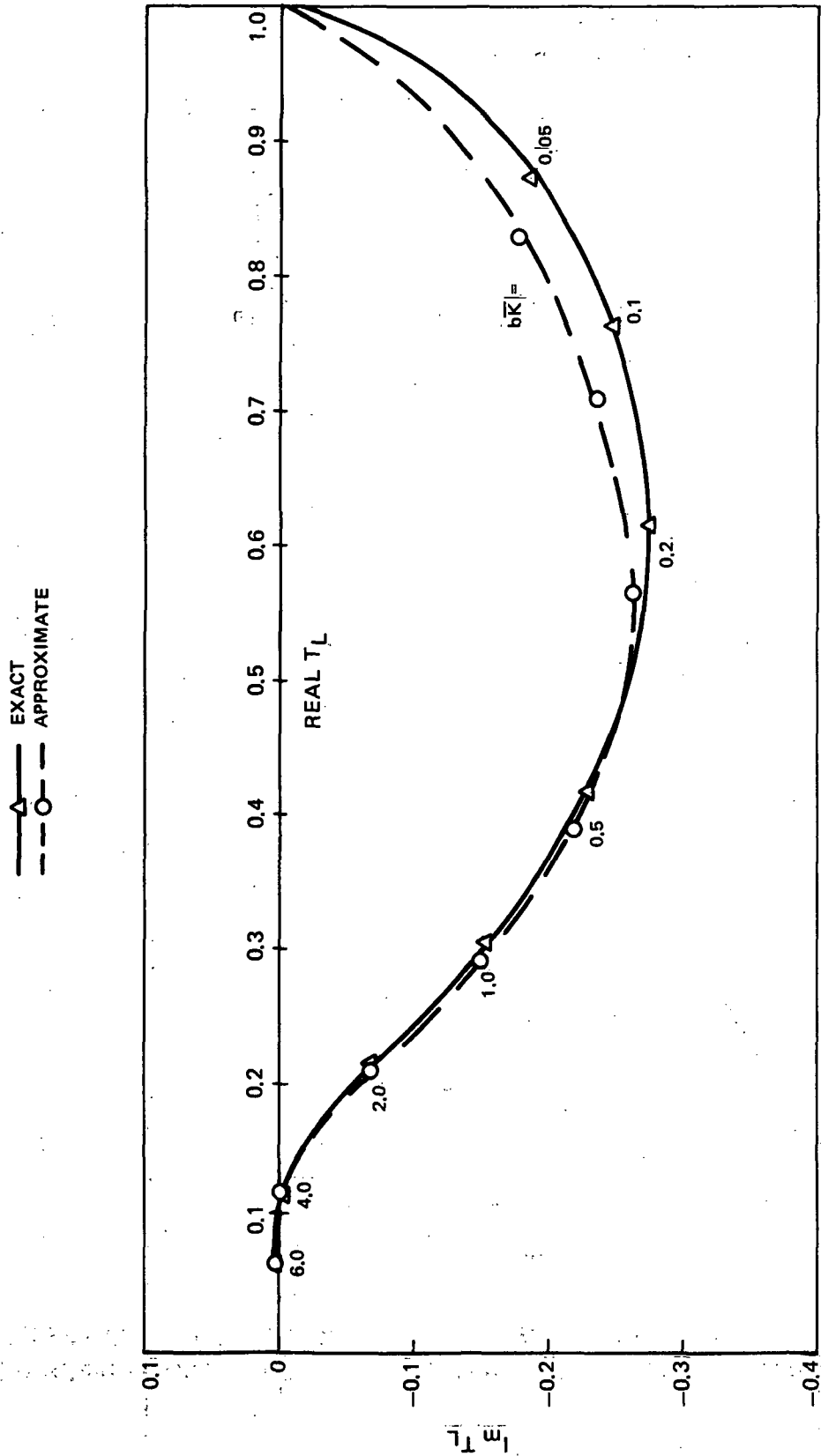


FIGURE 9. A COMPARISON BETWEEN EXACT AND APPROXIMATE EXPRESSIONS FOR THE LIFT TRANSFER FUNCTION FOR $\gamma = 0$ AND MACH NUMBER 0.6

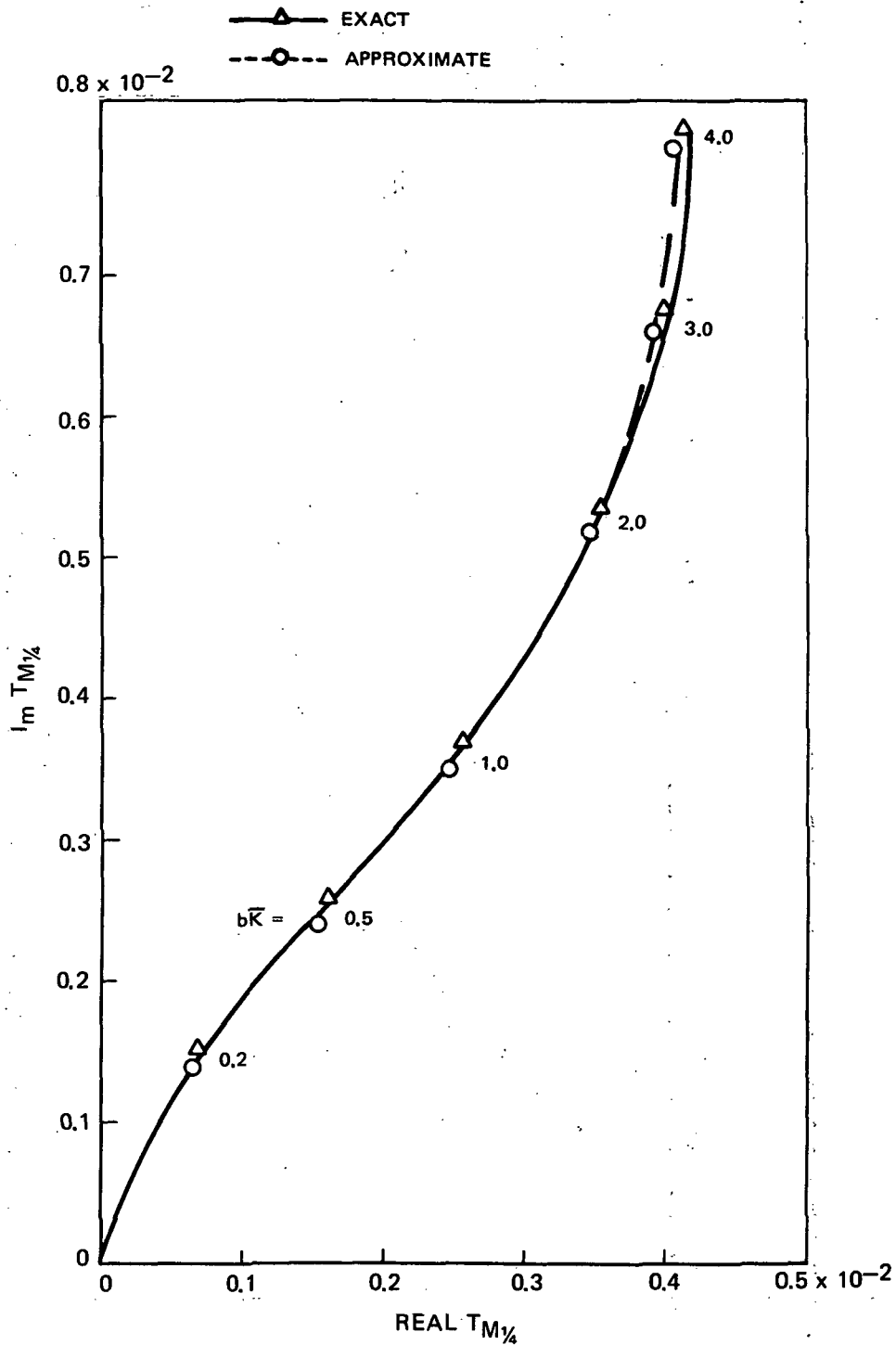


FIGURE 10. A COMPARISON BETWEEN EXACT AND APPROXIMATE EXPRESSION FOR THE MOMENT TRANSFER FUNCTION FOR $\gamma = 0$ AND MACH NUMBER 0.3

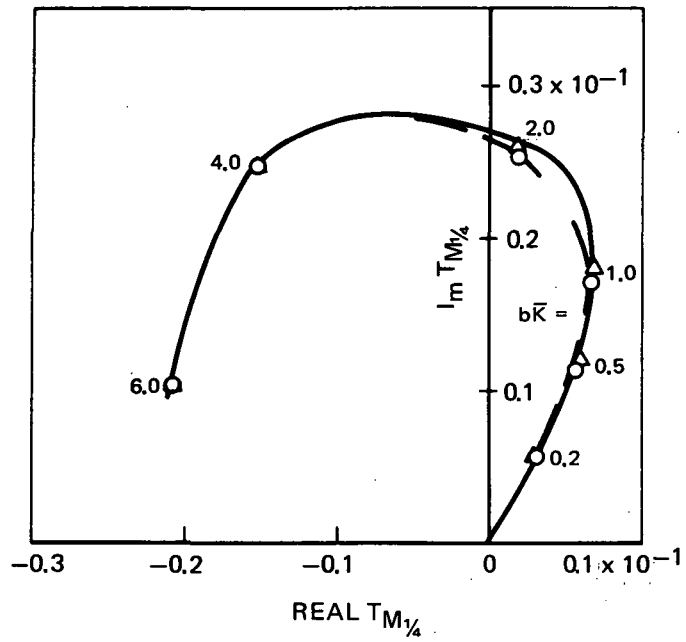


FIGURE 11. A COMPARISON BETWEEN EXACT AND APPROXIMATE EXPRESSIONS FOR THE MOMENT TRANSFER FUNCTION FOR $\gamma = 0$ AND MACH NUMBER 0.6

NOTE $I_m T_L = 0$

—————	EXACT (THEORY OF REF. 7)
- - - - -	APPROXIMATE (EQ. (34))
- - - - -	APPROXIMATE (EQ. (39))

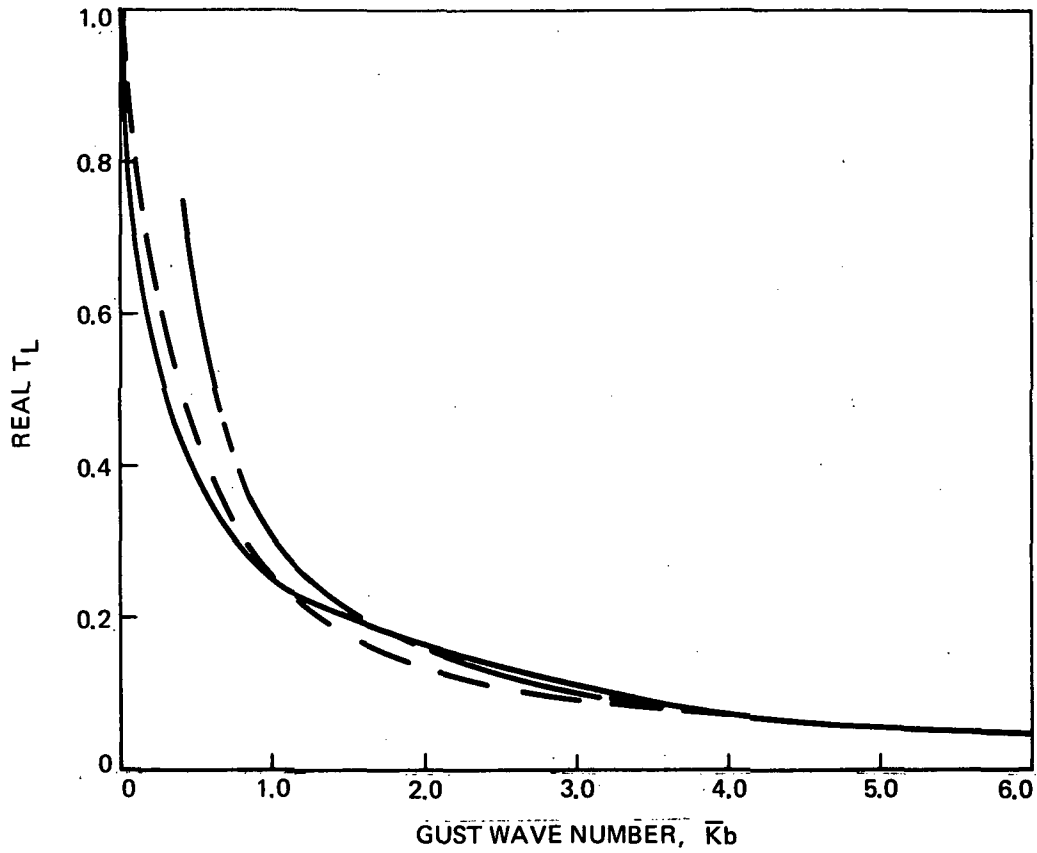


FIGURE 12. A COMPARISON BETWEEN EXACT AND APPROXIMATE EXPRESSION FOR THE LIFT TRANSFER FUNCTION FOR $\gamma^2 < 0$ AND MACH NUMBER 0.3

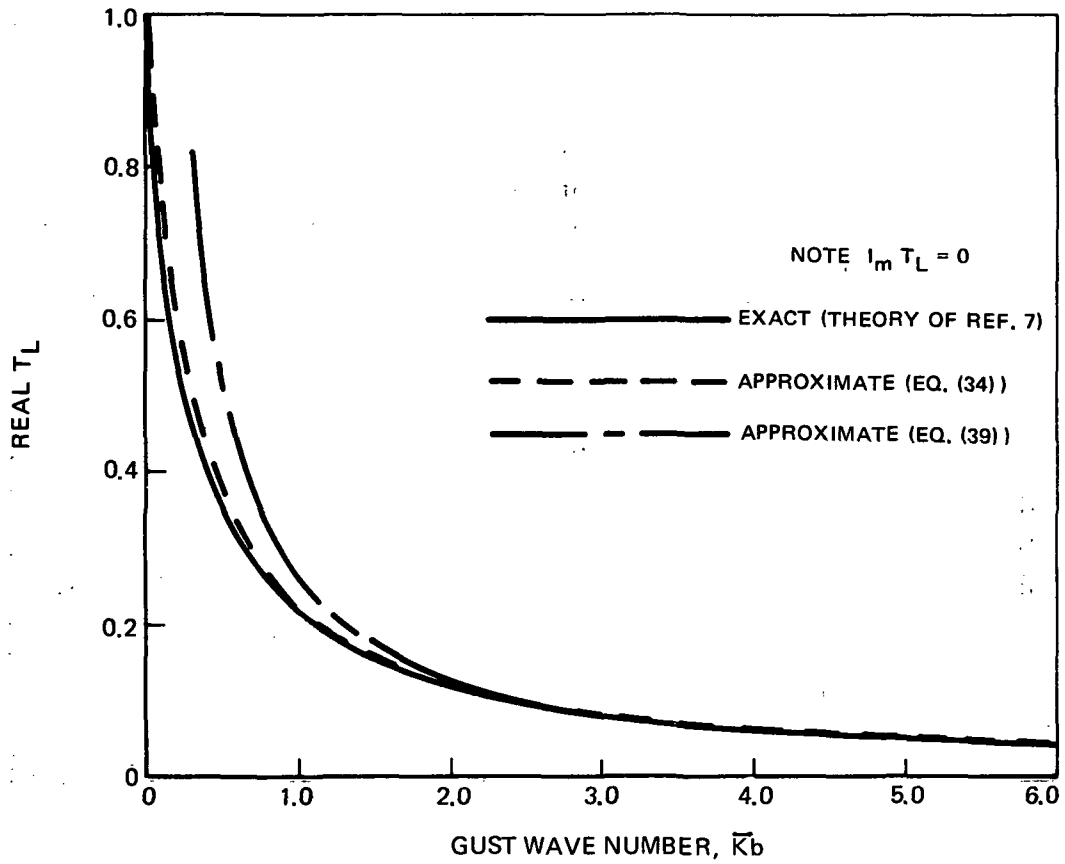


FIGURE 13. A COMPARISON BETWEEN EXACT AND APPROXIMATE EXPRESSION FOR THE LIFT TRANSFER FUNCTION FOR $\gamma^2 < 0$ AND MACH NUMBER 0.6

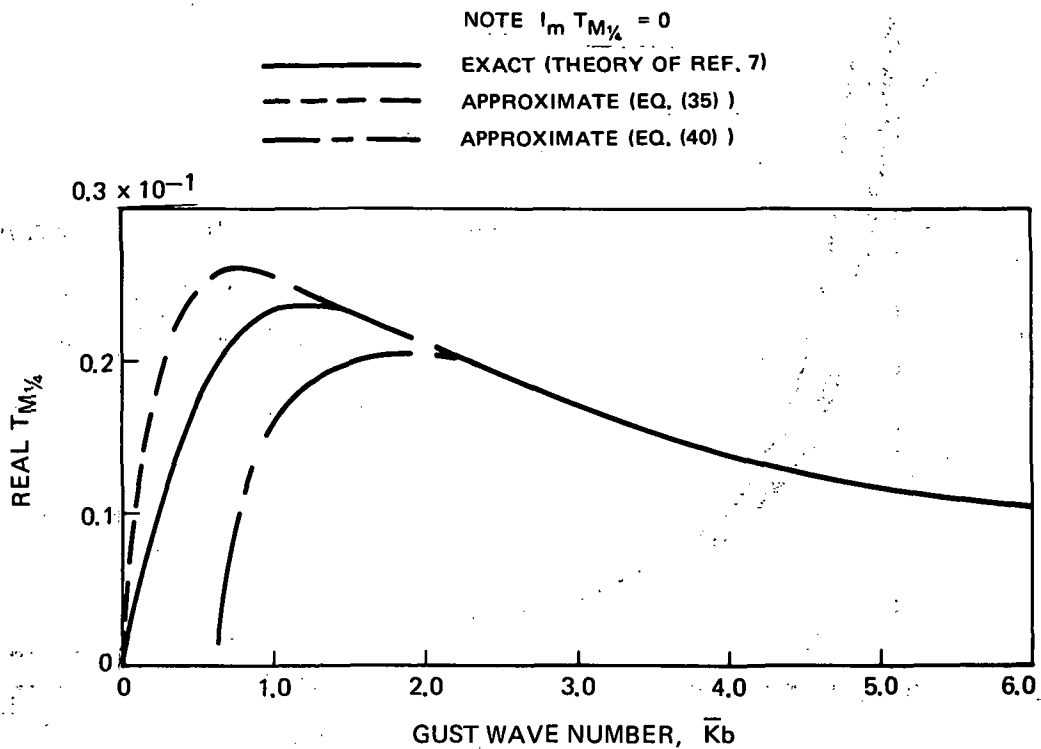


FIGURE 14. A COMPARISON BETWEEN EXACT AND APPROXIMATE EXPRESSIONS FOR THE MOMENT TRANSFER FUNCTION FOR $\gamma^2 < 0$ AND MACH NUMBER 0.3

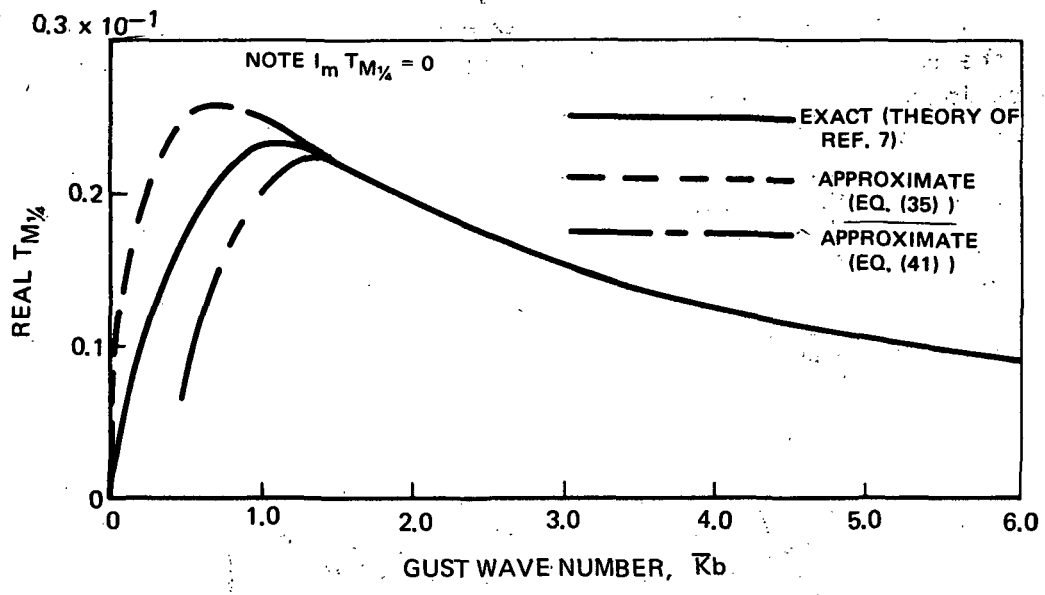


FIGURE 15. A COMPARISON BETWEEN EXACT AND APPROXIMATE EXPRESSIONS FOR THE MOMENT TRANSFER FUNCTION FOR $\gamma^2 < 0$ AND MACH NUMBER 0.6

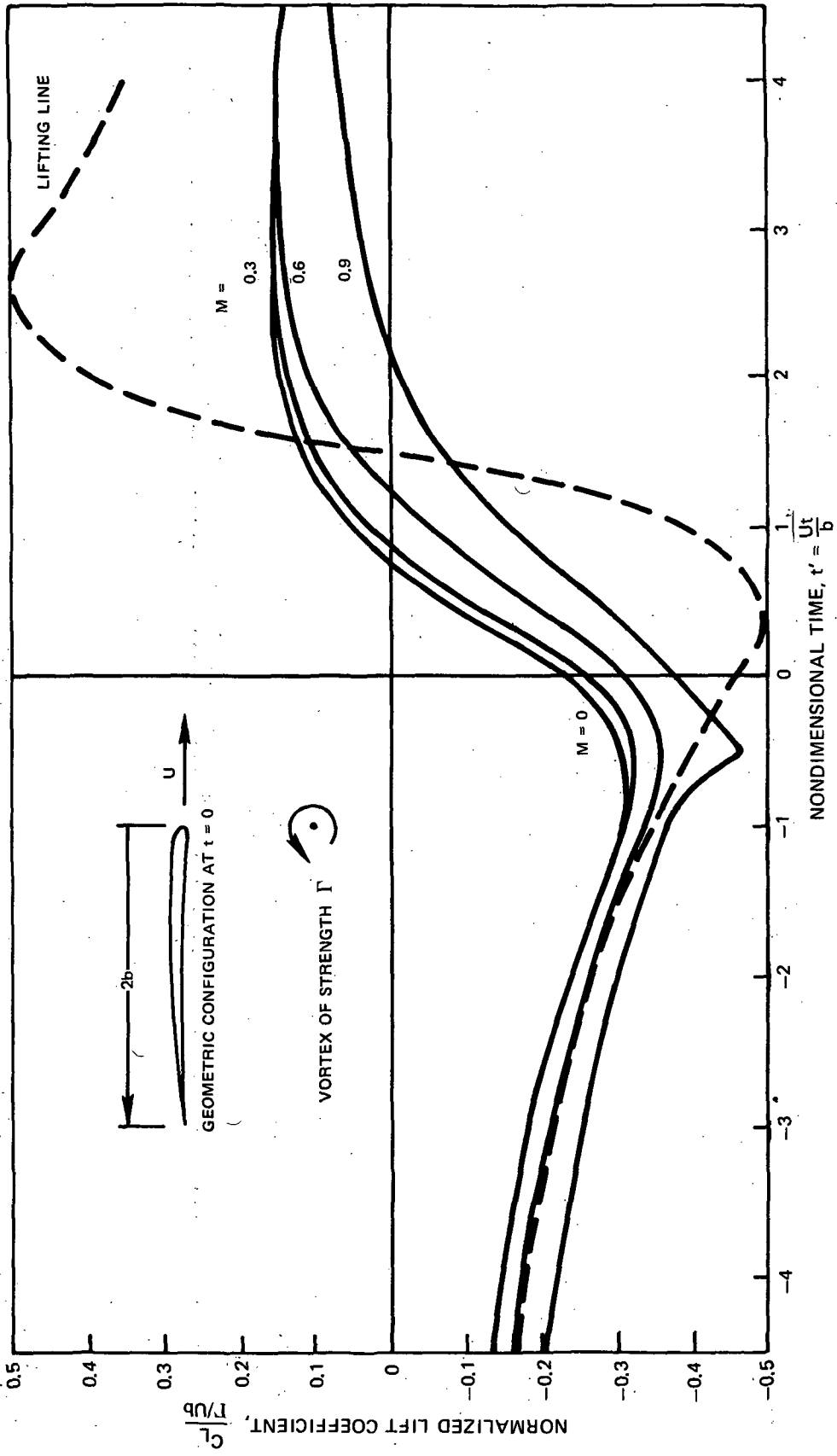


FIGURE 16. LIFT COEFFICIENT FOR A PARALLEL ENCOUNTER

MOMENT ABOUT QUARTER CHORD

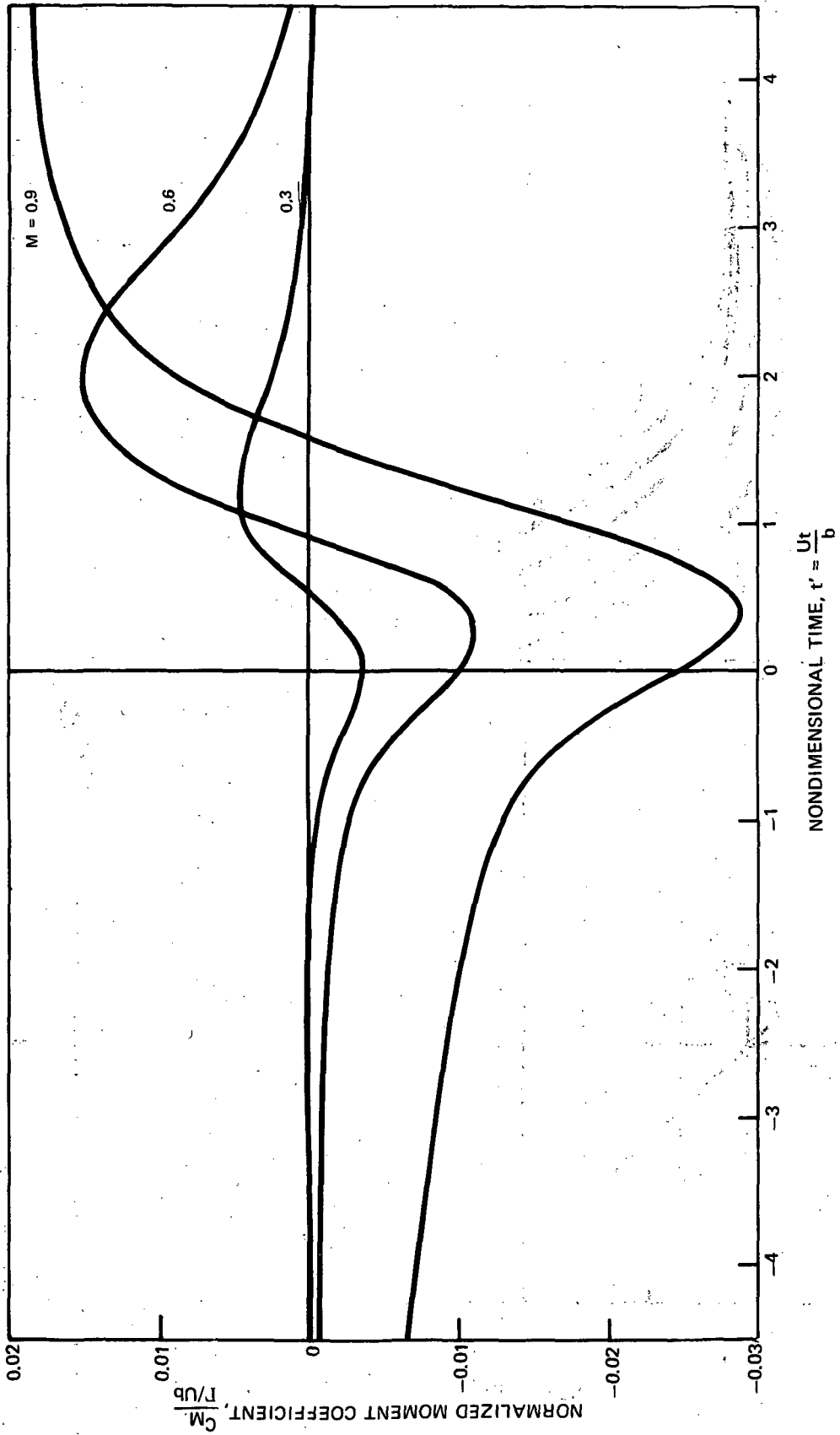


FIGURE 17. MOMENT COEFFICIENT FOR A PARALLEL ENCOUNTER

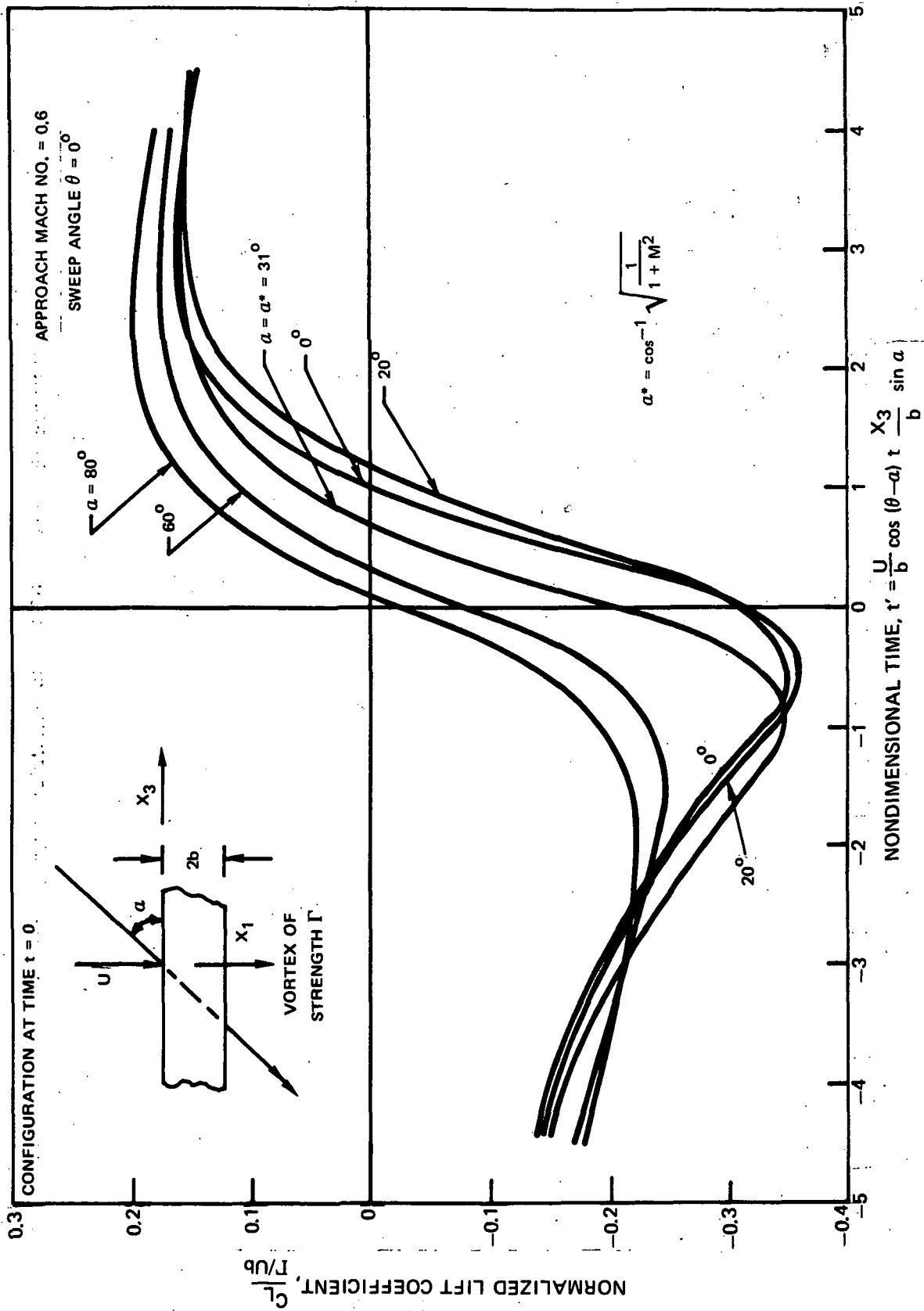


FIGURE 18. LIFT COEFFICIENT FOR AN OBLIQUE ENCOUNTER

APPROACH MACH NO. 0.6
MOMENT ABOUT QUARTER CHORD

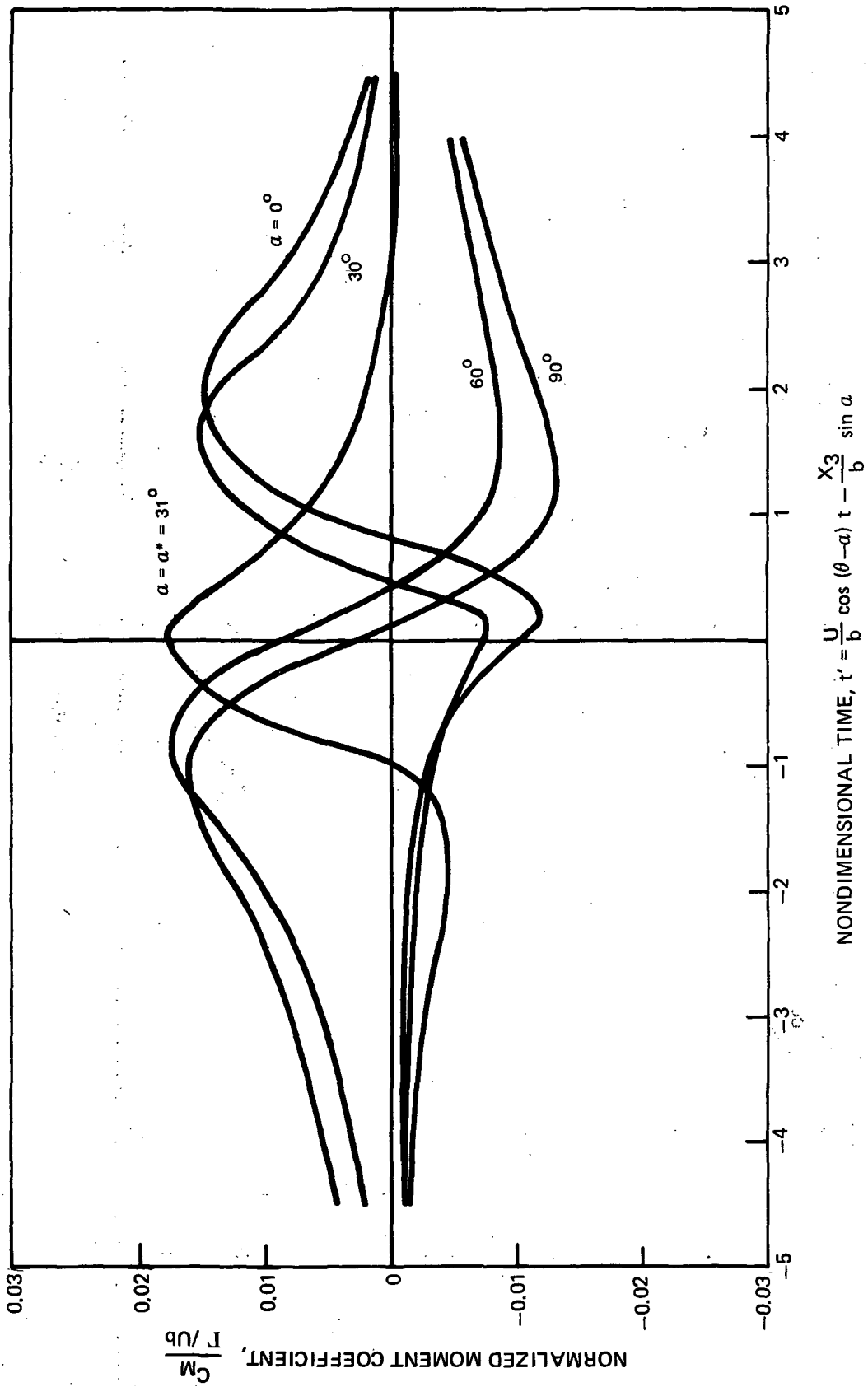


FIGURE 19. MOMENT COEFFICIENT FOR AN OBLIQUE ENCOUNTER

APPROACH MACH NO. = 0.6

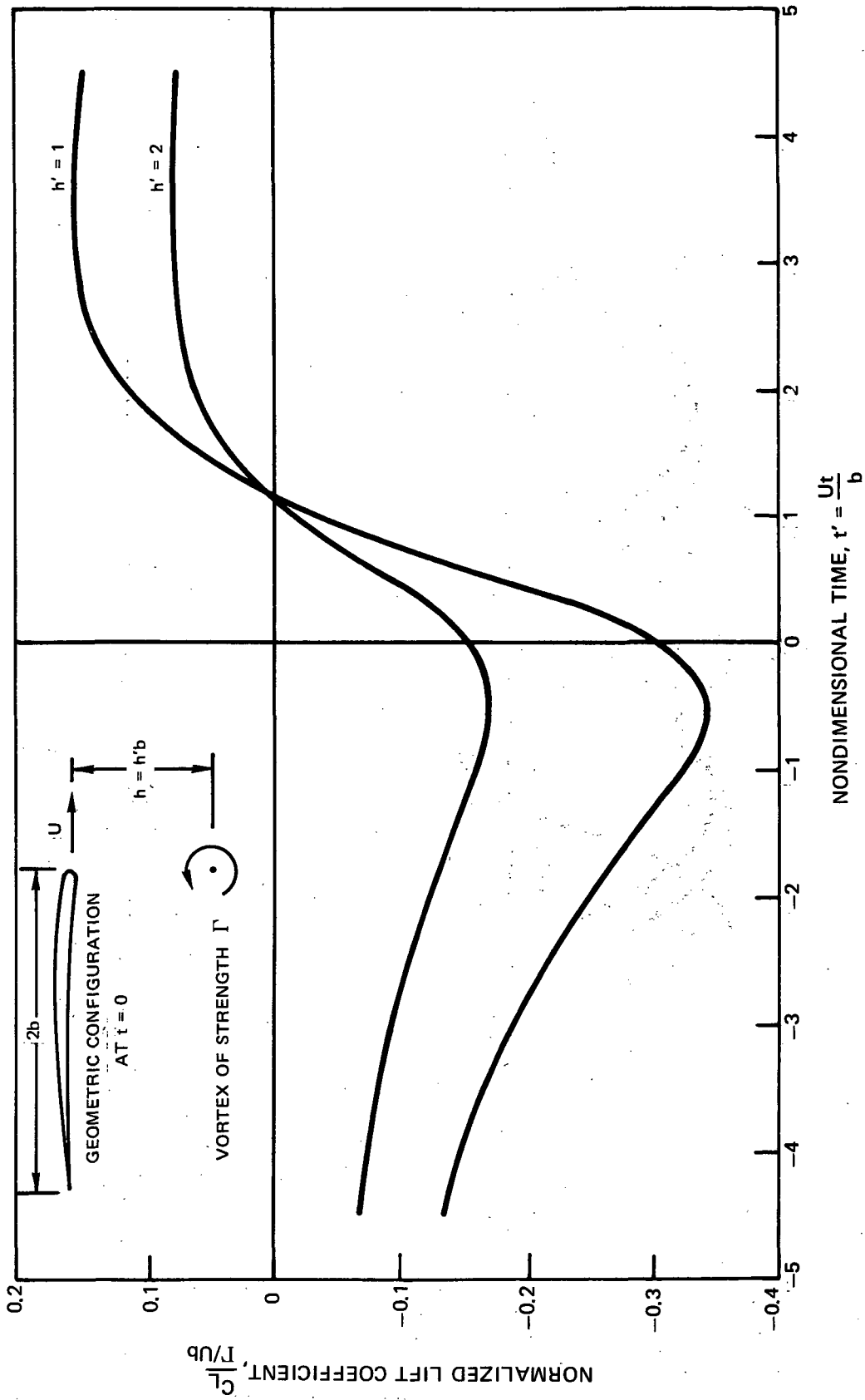


FIGURE 20. LIFT COEFFICIENT PER UNIT SPAN AS A FUNCTION OF TIME AND VORTEX VERTICAL DISPLACEMENT FOR A PARALLEL ENCOUNTER

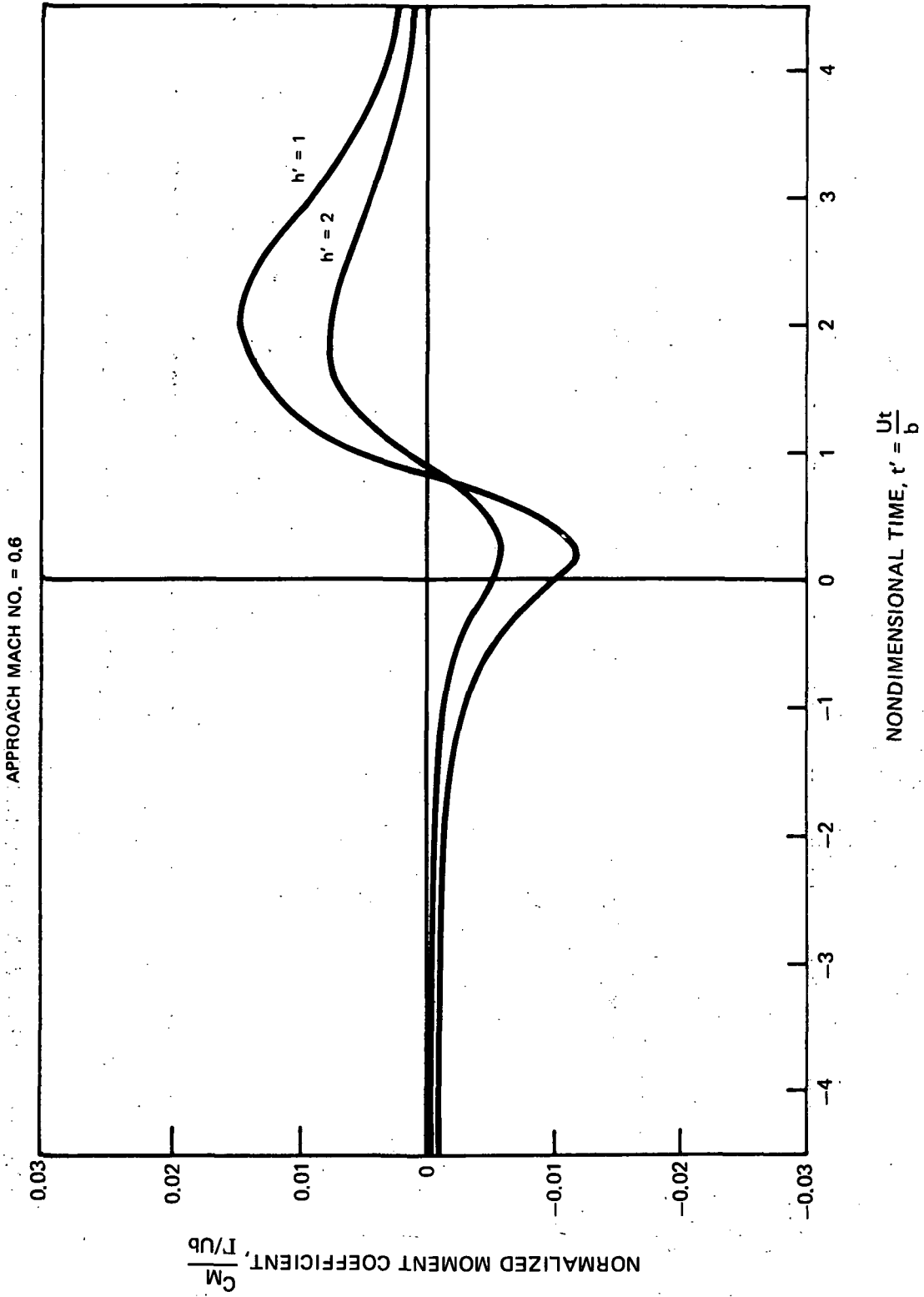


FIGURE 21. MOMENT COEFFICIENT PER UNIT SPAN ABOUT THE QUARTER-CHORD AS A FUNCTION OF TIME AND VORTEX VERTICAL DISPLACEMENT FOR A PARALLEL ENCOUNTER

— MINIMUM VALUES
 - - - MAXIMUM VALUES

APPROACH MACH NO. = 0.6

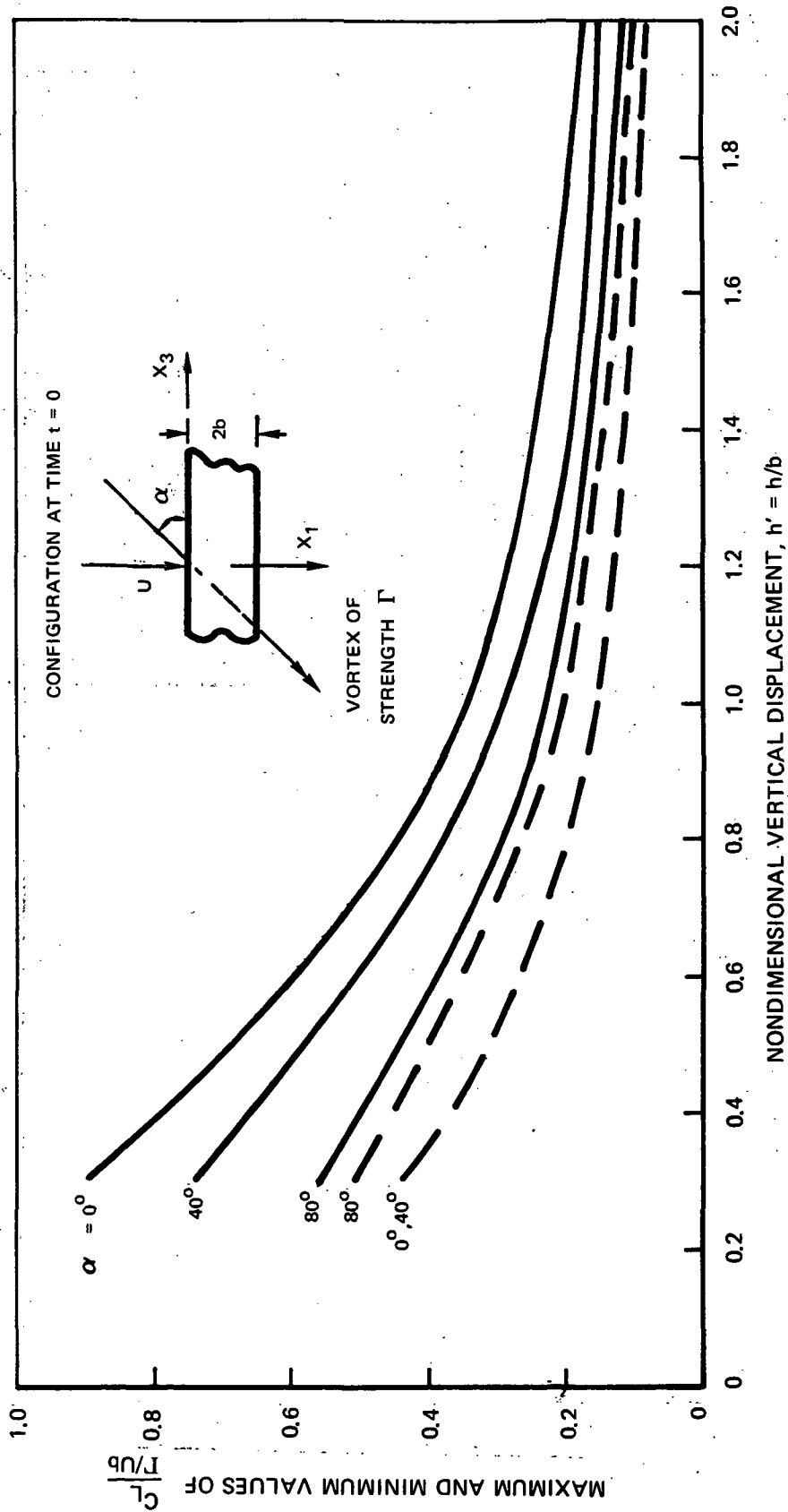


FIGURE 22. MAXIMUM AND MINIMUM VALUES OF THE LIFT COEFFICIENT PER UNIT SPAN

—— MINIMUM VALUES
- - - MAXIMUM VALUES

APPROACH MACH NO. = 0.6

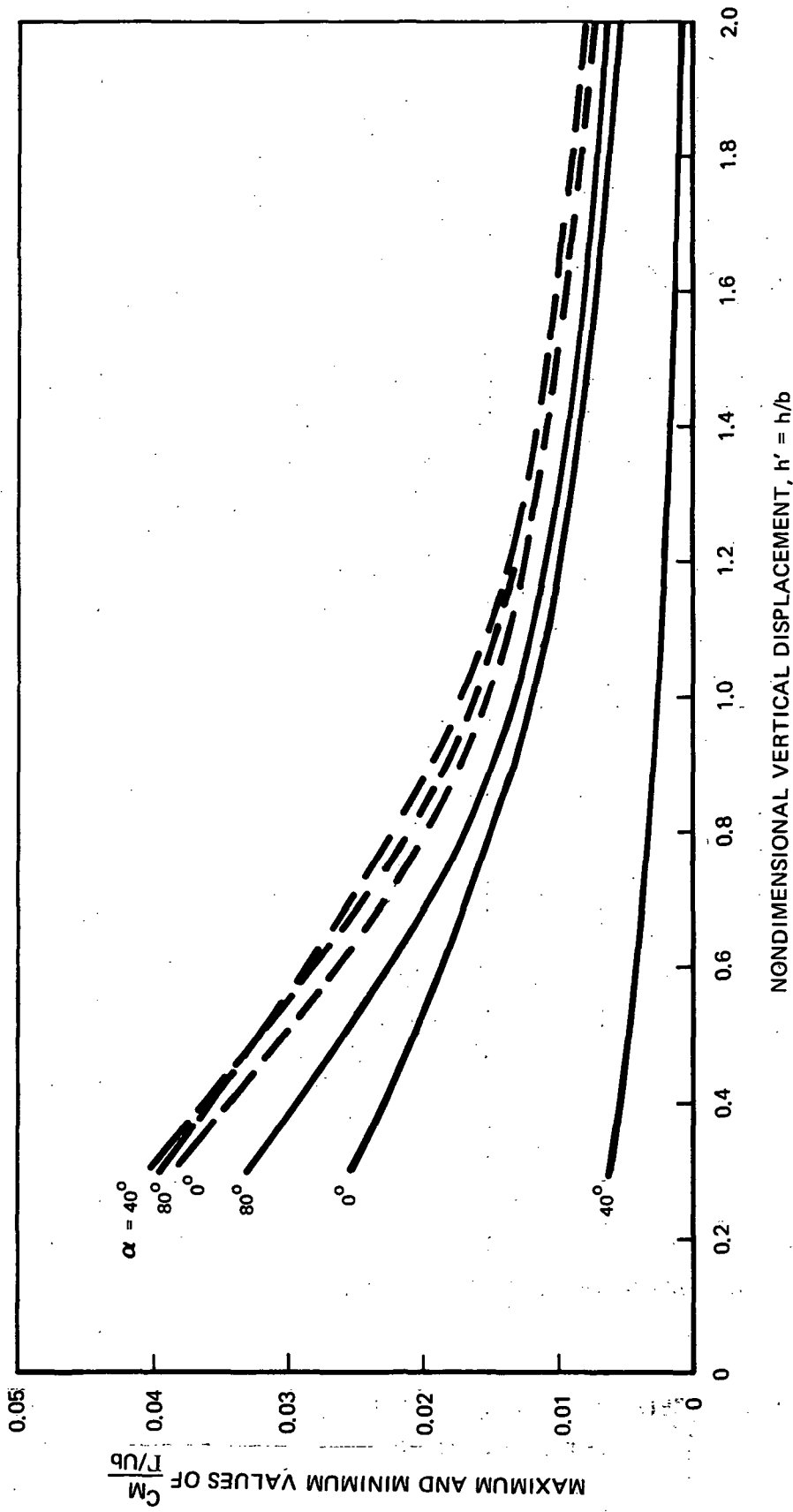


FIGURE 23. MAXIMUM AND MINIMUM VALUES OF THE MOMENT COEFFICIENT PER UNIT SPAN ABOUT THE QUARTER-CHORD

R_T - ROTOR RADIUS

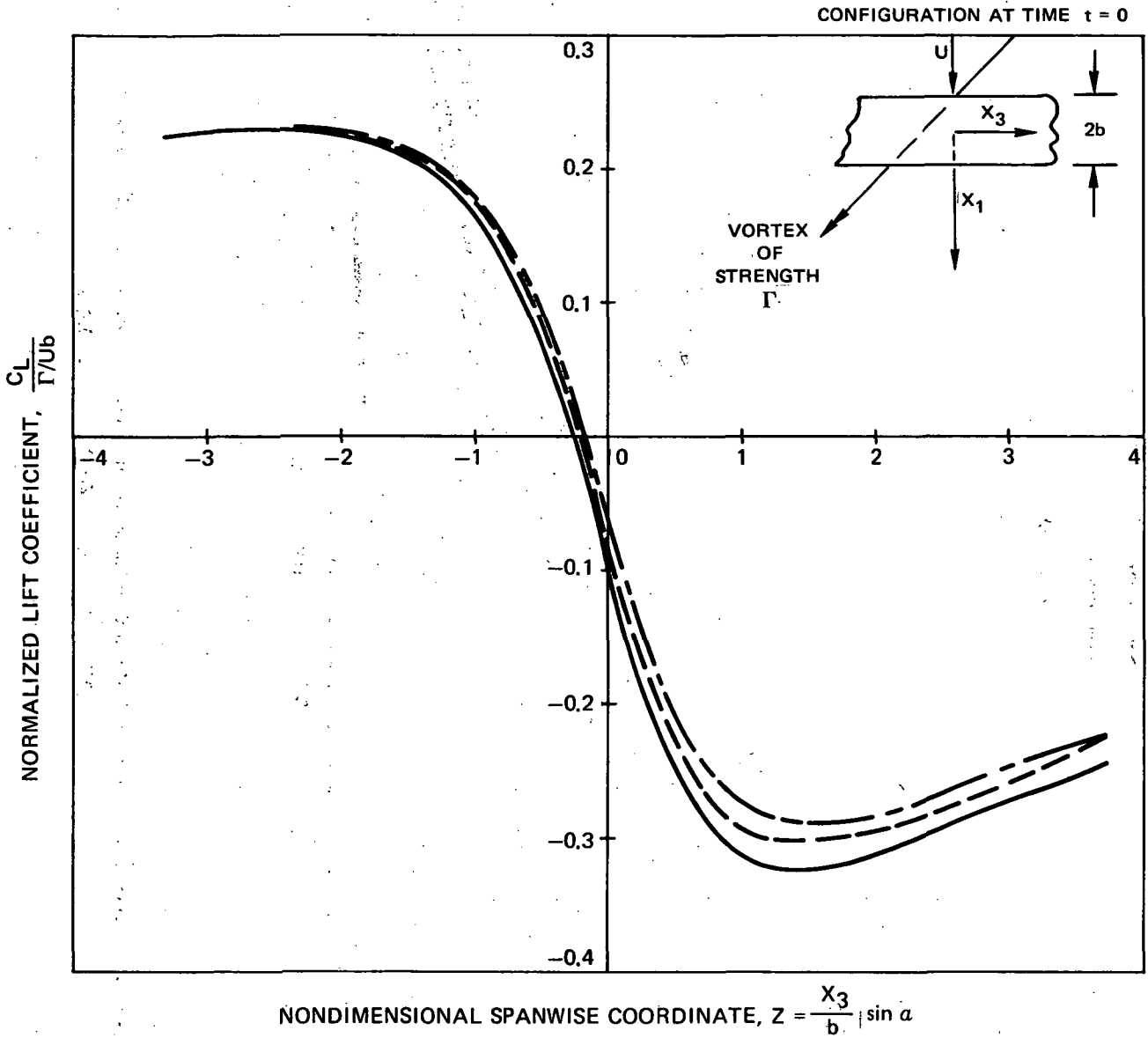
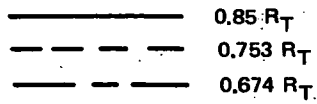
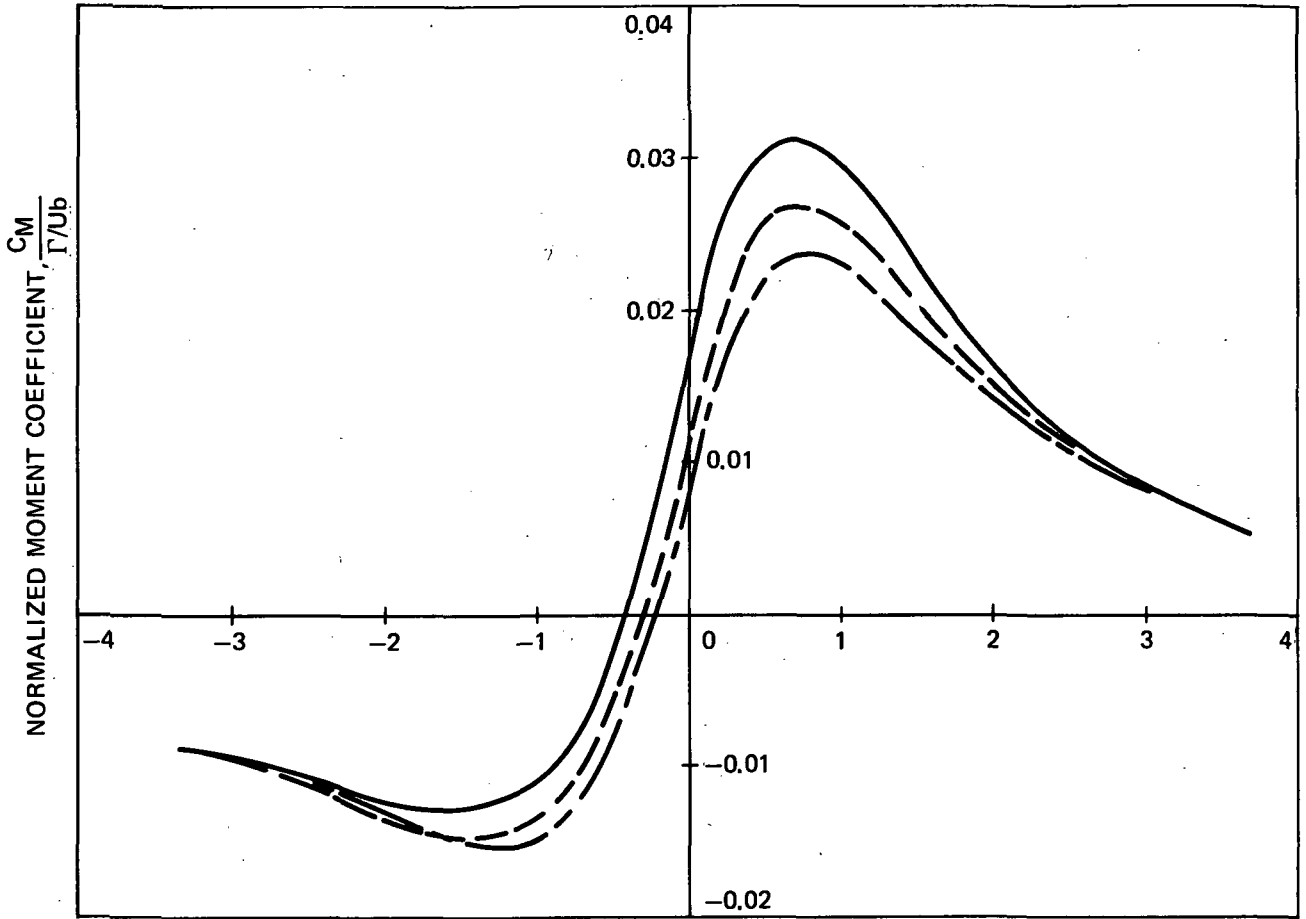


FIGURE 24. NORMALIZED LIFT DISTRIBUTION FOR SECOND-QUADRANT VORTEX ENCOUNTER OF A UH-1D ROTOR AT 90 KT

R_T - ROTOR RADIUS

- 0.85 R_T
- - - - 0.753 R_T
- · - · 0.674 R_T



NONDIMENSIONLESS SPANWISE COORDINATE, $Z = \frac{X_3}{b} \sin \alpha$

FIGURE 25. NORMALIZED MOMENT DISTRIBUTION FOR SECOND-QUADRANT VORTEX ENCOUNTER OF A UH-1D ROTOR AT 90 KT



POSTMASTER: If Undeliverable (Section 158
Postal Manual) Do Not Return

"The aeronautical and space activities of the United States shall be conducted so as to contribute . . . to the expansion of human knowledge of phenomena in the atmosphere and space. The Administration shall provide for the widest practicable and appropriate dissemination of information concerning its activities and the results thereof."

—NATIONAL AERONAUTICS AND SPACE ACT OF 1958

NASA SCIENTIFIC AND TECHNICAL PUBLICATIONS

TECHNICAL REPORTS: Scientific and technical information considered important, complete, and a lasting contribution to existing knowledge.

TECHNICAL NOTES: Information less broad in scope but nevertheless of importance as a contribution to existing knowledge.

TECHNICAL MEMORANDUMS: Information receiving limited distribution because of preliminary data, security classification, or other reasons. Also includes conference proceedings with either limited or unlimited distribution.

CONTRACTOR REPORTS: Scientific and technical information generated under a NASA contract or grant and considered an important contribution to existing knowledge.

TECHNICAL TRANSLATIONS: Information published in a foreign language considered to merit NASA distribution in English.

SPECIAL PUBLICATIONS: Information derived from or of value to NASA activities. Publications include final reports of major projects, monographs, data compilations, handbooks, sourcebooks, and special bibliographies.

TECHNOLOGY UTILIZATION PUBLICATIONS: Information on technology used by NASA that may be of particular interest in commercial and other non-aerospace applications. Publications include Tech Briefs, Technology Utilization Reports and Technology Surveys.

Details on the availability of these publications may be obtained from:

**SCIENTIFIC AND TECHNICAL INFORMATION OFFICE
NATIONAL AERONAUTICS AND SPACE ADMINISTRATION
Washington, D.C. 20546**